

**Development of Breakdown Probability Models for Rural Freeway Work Zones
Using Field Data and Simulation**

by

Nicholas Lee Jehn

A thesis submitted to the Graduate Faculty of
Auburn University
in partial fulfillment of the
requirements for the Degree of
Master of Science

Auburn, Alabama
May 5, 2018

Keywords: Freeway, Work Zone,
Capacity, Breakdown Probability, VISSIM

Copyright 2018 by Nicholas Lee Jehn

Approved by

Rod E. Turochy, Chair, James M. Hunnicutt Associate Professor in Traffic Engineering
Jeffrey J. LaMondia, Associate Professor of Civil Engineering
Huaguo Zhou, Associate Professor of Civil Engineering

ABSTRACT

The current state of the National Highway System often necessitates that agencies interrupt normal traffic operations for maintenance and capacity improvements. With nearly 9 million lane-miles of public roadway and an economy driven by the automobile, these interruptions are inevitable, but the significant safety and mobility impacts associated with queueing at freeway work zones are mitigable. The current methodology in the 6th edition of the *Highway Capacity Manual* is a vast improvement over historical work zone capacity guidance, but approaches the issue differently than research suggests agencies and practitioners should. Namely, a capacity defined by the mean queue discharge rate is deterministic and fails to account for the stochastic nature of traffic flow and breakdown. This thesis addressed these core issues by calibrating and validating a VISSIM model for a rural freeway work zone lane closure and exploring the probability of queue formation as a function of traffic volume, truck percentage, and lane closure side. The results were combined to form a capacity analysis tool that may be used by agencies and practitioners to make data-driven planning, design, and operations decisions at rural freeway work zones. The methodology applied herein may also be extended to freeway facilities exhibiting different geometric, traffic, and environmental characteristics.

ACKNOWLEDGEMENTS

It is my belief that who I have become and what I have accomplished is solely a product of the incredible people I have been blessed to call family, friends, coaches, teachers, classmates, and coworkers throughout my life. My journey from a small town in Kentucky to a master's degree at Auburn University would not have been possible without the love, support, friendship, and guidance that all of you have given me. This thesis is dedicated to you.

I would like to extend special thanks to my committee members, Dr. Huaguo Zhou and Dr. Jeffrey LaMondia. The enthusiasm and humor that you both bring to the classroom is unmatched and appreciated by all your students. Dr. Zhou, thank you for sharing your expertise in traffic simulation and for being my go-to faculty member for discussing college sports. Dr. LaMondia, thank you for providing me numerous opportunities to grow as a graduate student through your creative class projects and our collaboration on research papers. I am confident that students who take your courses receive a better background in statistics than at any other university in the country.

To my officemates in Ramsay 305 and 313—Veronica Ramirez, Travis Gajkowski, Raghu Baireddy, Jyothi Rani, Beijia Zhang, Dan Xu, Bo Zhang, Fernando Cordero, Chennan Xue, Md Atiquzzaman, and Mitch Fisher—I could not have shared a cubicle in a 93-year-old building with a better group of friends. Thank you for your company and for your help with research and class projects these last two years (whether during normal working hours or the

middle of the night). Lastly, I am especially appreciative of my fellow Gentlemen's Society of Civil Engineering (GSCE) colleagues—Michelle Knights, Dakota Basham, and Blake Whitman.

My advisor, Dr. Rod Turochy, and his family have impacted my life on many levels. First, I would like to thank Dr. Turochy for his mentorship and patience throughout my academic career at Auburn University. I would have never made it to graduation without long meetings in your office and your words of motivation through all my struggles. Second, I want to thank you and your family for teaching me how important it is to be humble, kind, and generous. You, Kathy, and your children embody these qualities, and I believe that you make a significant, positive impact on the lives of your students and the community. I am truly grateful to have met you three years ago and that you gave me the opportunity to attend Auburn University.

My most heartfelt gratitude belongs to my two amazing families. First, thank you to the Hardy family for treating me like your own and offering Megan and I your constant support. I love you and your daughter, and my life is better with you in it. To my parents, Jerry and Kathy Jehn, thank you for giving me life and raising me to be the man I have become. Though I may not always need your financial support, I cannot imagine walking through life without your love and advice. To my sisters, Natalie and Lindsay Jehn, thank you for continuing to be two of my best friends even while we live in different cities. Finally, thank you Megan Hardy for your unconditional love throughout this crazy journey that we're on together. I can't imagine a better life than the one I'm living with you, Ellie, and Meeko and I'm glad that you decided to fall off my front porch almost five years ago. I love you, I'm proud of you, and I can't wait to see what else we will accomplish together.

TABLE OF CONTENTS

ABSTRACT.....	ii
ACKNOWLEDGEMENTS.....	iii
LIST OF TABLES.....	viii
LIST OF FIGURES.....	xi
LIST OF ABBREVIATIONS.....	xiv
CHAPTER ONE: INTRODUCTION.....	1
1.1 BACKGROUND.....	1
1.2 PROBLEM STATEMENT.....	2
1.3 RESEARCH OBJECTIVES.....	4
1.4 ORGANIZATION OF THIS THESIS.....	5
CHAPTER TWO: LITERATURE REVIEW.....	7
2.1 INTRODUCTION.....	7
2.2 HISTORICAL MEASUREMENT AND DEFINITION OF FREEWAY CAPACITY ..	7
2.3 WORK ZONE CAPACITY IN THE HIGHWAY CAPACITY MANUAL.....	10
2.4 FACTORS AFFECTING FREEWAY WORK ZONE CAPACITY.....	11
2.4.1 Traffic Stream Characteristics.....	12
2.4.2 Work Zone Characteristics.....	14
2.5 BREAKDOWN PROBABILITY MODELS.....	16
2.5.1 Generating Breakdown Probability Models.....	17
2.5.2 Data Collection and Identification of Breakdown.....	19
2.6 FREEWAY WORK ZONE SIMULATION MODELS.....	21
2.6.1 Simulation Overview.....	22
2.6.2 Driving Behavior Parameters.....	24
2.6.3 Freeway Work Zone Simulation Case Studies.....	27
2.7 SUMMARY.....	34
CHAPTER THREE: METHODOLOGY.....	36
3.1 INTRODUCTION.....	36

3.2	SITE OVERVIEW AND DATA COLLECTION PLAN.....	36
3.3	DATA SCREENING AND PROCESSING	40
3.3.1	Vehicle Lengths	41
3.3.2	Vehicle Speeds.....	44
3.3.3	Exploration of Field Data.....	48
3.4	VISSIM MODEL DEVELOPMENT.....	52
3.4.1	Basic Network Coding.....	52
3.4.2	Volume Inputs and Traffic Stream Composition.....	54
3.4.3	Desired Speed Distributions	57
3.4.4	Modification of Key Truck Characteristics	58
3.4.5	Time Headway Distributions	62
3.5	CALIBRATION AND VALIDATION	67
3.5.1	Calibration Methodology	68
3.5.2	Calibration Results.....	71
3.5.3	Model Validation	76
3.6	EXPERIMENT DESIGN.....	78
3.6.1	Characterization of Typical Traffic Conditions.....	79
3.6.2	Experiment Input Parameters.....	83
3.7	SUMMARY	87
CHAPTER FOUR: ANALYSIS AND RESULTS.....		89
4.1	INTRODUCTION.....	89
4.2	AGGREGATION OF SIMULATED DATA	89
4.3	SURVIVAL ANALYSIS.....	92
4.3.1	Methodology	92
4.3.2	Curve Fitting.....	96
4.4	RESULTS.....	98
4.4.1	Effect of Explanatory Variables on Breakdown Probability	98
4.4.2	Calculation of Capacity-Based Passenger Car Equivalents.....	102
4.4.3	Development of a Freeway Work Zone Lane Closure Analysis Tool.....	105
4.5	SUMMARY	110
CHAPTER FIVE: CONCLUSIONS AND RECOMMENDATIONS		112
5.1	INTRODUCTION.....	112

5.2	CONCLUSIONS.....	113
5.3	RECOMMENDATIONS FOR FUTURE RESEARCH.....	115
	REFERENCES	117
	APPENDIX A: FIELD-COLLECTED DATA AND VISSIM INPUTS	127
	APPENDIX B: BREAKDOWN IDENTIFICATION ALGORITHMS AND WEIBULL DISTRIBUTION PARAMETERS	143

LIST OF TABLES

Table 2-1: Application of PLM to Highway Capacity Analysis (Source: Brilon et al. 2005).....	18
Table 2-2: VISSIM Car-Following Parameters (Adapted from Yeom et al. 2016).....	25
Table 2-3: Lane Use Balance Thresholds (Source: Yeom et al. 2016).....	31
Table 2-4: Regression Model for CC1 Estimation (Source: Yeom et al. 2016).....	31
Table 2-5: VISSIM Driving Behavior Parameter Guidance (Source: Yeom et al. 2016)	32
Table 3-1: Vehicle Classification Bounds	44
Table 3-2: Vehicle Speed Screening Results	45
Table 3-3: Vehicle Length Cutoff Values.....	46
Table 3-4: Summary of Lane-Specific Mean Free Flow Speeds	47
Table 3-5: Summary of Breakdown Events at Study Work Zone	49
Table 3-6: Example of Adjusted Truck Volumes.....	56
Table 3-7: Base VISSIM Model Vehicle Composition Input.....	57
Table 3-8: VISSIM Desired Speed Distributions	58
Table 3-9: Comparison of Truck Power and Weight in VISSIM.....	59
Table 3-10: VISSIM Input Desired Headway Distributions.....	67
Table 3-11: Calibration Objectives.....	69
Table 3-12: Calibration Parameter Ranges	71
Table 3-13: Calibrated Driving Behavior Parameters	73
Table 3-14: Calibration Summary (October 3 rd , 2016).....	75

Table 3-15: Validation Summary (October 6th, 2016).....	77
Table 3-16: Study Work Zone Volume Summary	80
Table 3-17: Final Volume and Truck Percentage Inputs	84
Table 3-18: Upstream Lane Distributions.....	86
Table 4-1: Example Breakdown Identification.....	91
Table 4-2: Survival Analysis Table (10% Trucks, 5-Minute Aggregation Interval, Left-Side Lane Closure).....	93
Table 4-3: PCE Calculation Summary (15-Minute Intervals)	103
Table 4-4: PCE Calculation Summary (5-Minute Intervals)	104
Table 4-5: Summary of Weibull Shape and Scale Parameters (Left-Side Closure, 15-Minute Intervals)	106
Table A-1: Sensor Vehicle Length Frequencies	128
Table A-2: Vehicle Length Summary (Passenger Cars).....	132
Table A-3: Vehicle Length Summary (Tractor-Trailers).....	132
Table A-4: Free Flow Speed Distribution (3.5 Miles Upstream)	133
Table A-5: Free Flow Speed Distribution (2.5 Miles Upstream)	133
Table A-6: Free Flow Speed Distribution (1.5 Miles Upstream)	133
Table A-7: Free Flow Speed Distribution (1/2 Mile Upstream).....	134
Table A-8: Free Flow Speed Distribution (Bottleneck).....	134
Table A-9: Field Volumes and VISSIM Input (October 3 rd , 2016).....	134
Table A-10: Field Volumes and Average Speeds at Bottleneck (October 3 rd , 2016).....	137
Table A-11: Field Volumes and VISSIM Input (October 6 th , 2016)	138
Table A-12: Field Volumes and Average Speeds at Bottleneck (October 6 th , 2016).....	140

Table A-13: Detailed Summary of Breakdown Events	142
Table A-14: Best-Fit Weibull Distribution Parameter Summary	148

LIST OF FIGURES

Figure 2-1: HCM 6th Edition Work Zone Capacity Model (Source: TRB 2016)	11
Figure 2-2: Sensitivity of Simulated Capacity to VISSIM Truck Characteristics (Source: Edara and Chatterjee 2010)	28
Figure 2-3: Lane Closure Network Setup for 2-1 Closure (Source: Edara and Chatterjee 2010)	29
Figure 2-4: VISSIM Network Setup for 2-1 Lane Closure (Source: Yeom et al. 2016)	30
Figure 2-5: Diagram of Simulated Network (Source: Heaslip et al. 2009)	33
Figure 2-6: Analytical Models by Lane Configuration (Source: Heaslip et al. 2009).....	34
Figure 3-1: Map of Study Work Zone (Traffic Data Source: ALDOT GIS).....	37
Figure 3-2: Traffic Sensor Deployment Scheme (drawing not to scale)	38
Figure 3-3: Vehicle Length Distributions for Sensors 101 and 102	41
Figure 3-4: Average Vehicle Length Frequency Distribution	43
Figure 3-5: Upstream Free Flow Speed Distributions	47
Figure 3-6: Flow vs. Density Curve (Left-Side Closure)	50
Figure 3-7: Flow vs. Density Curve (Right-Side Closure)	51
Figure 3-8: Diagram of VISSIM Network (drawing not to scale).....	53
Figure 3-9: Speed and Flow vs. Time on October 3 rd , 2016.....	55
Figure 3-10: CORSIM Vehicle Acceleration Curves (Source: FHWA)	60
Figure 3-11: VISSIM Default vs. Calibrated Truck Acceleration.....	61
Figure 3-12: Field Headway Distribution (Passenger Cars).....	65

Figure 3-13: Field Headway Distribution (Trucks)	65
Figure 3-14: Desired Safety Distance in VISSIM	65
Figure 3-15: Change in Headway Frequency (Passenger Cars)	66
Figure 3-16: Change in Headway Frequency (Trucks).....	66
Figure 3-17: Field, Default VISSIM, and Calibrated VISSIM Speed Profile Comparisons	74
Figure 3-18: QDR Distribution Comparison (October 3 rd , 2016).....	75
Figure 3-19: Field and Validated VISSIM Speed Profile Comparisons.....	76
Figure 3-20: QDR Distribution Comparison (October 6 th , 2016).....	78
Figure 3-21: Traffic Demand Profile (October 4 th , 2016)	82
Figure 3-22: Experiment Volume Input Scheme	85
Figure 4-1: Empirical Breakdown Probability Distribution (10% Trucks, 5-Minute Aggregation Interval, Left-Side Lane Closure)	94
Figure 4-2: Example Fitted Weibull Distribution (Source: TRB 2016)	95
Figure 4-3: Curve Fitting Example (10% Trucks, Left-Side Lane Closure, 5-Minute Aggregation Intervals)	97
Figure 4-4: Breakdown Probability vs. Lane Closure Side (5-Minute Intervals).....	100
Figure 4-5: Breakdown Probability vs. Lane Closure Side (15-Minute Intervals).....	100
Figure 4-6: Regression on Weibull Scale Parameter (15-Minute Intervals).....	107
Figure 4-7: Composite Breakdown Probability Model Verification (15-Minute Intervals).....	108
Figure 4-8: Beta Version of Rural Freeway Work Zone Capacity Analysis Tool.....	109
Figure A-1: VBA Code (1-Minute Breakdown Identification)	144
Figure A-2: VBA Code (5-Minute Breakdown Identification)	145
Figure A-3: VBA Code (15-Minute Breakdown Identification)	146

Figure A-4: VBA Code with Comments (15-Minute Breakdown Identification)..... 147

LIST OF ABBREVIATIONS

AADT	Annual Average Daily Traffic
ALDOT	Alabama Department of Transportation
BPM	Breakdown Probability Model
D Factor	Proportion of Traffic Occurring in Peak Direction During Peak Hour
DOT	Department of Transportation
FFS	Free Flow Speed
FHWA	Federal Highway Administration
HCM	Highway Capacity Manual
K Factor	Proportion of Traffic Occurring During Peak Hour
LCSI	Lane Closure Severity Index
LOS	Level of Service
MAPE	Mean Absolute Percentage Error
MOE	Measure of Effectiveness
mph	Miles Per Hour
NCHRP	National Cooperative Highway Research Program
NHS	National Highway System
NHTSA	National Highway Traffic Safety Administration
PBC	Pre-Breakdown Capacity
PCE	Passenger Car Equivalent
PCMS	Portable Changeable Message Sign
pcphpl	Passenger Cars Per Hour Per Lane
PHF	Peak Hour Factor
PLM	Product-Limit Method
QDR	Queue Discharge Rate

RMSNE	Root Mean Square Normalized Error
SFI	Sustained Flow Index
SRF	Safety Distance Reduction Factor
STRIDE	Southeastern Transportation Research, Innovation, Development, and Education Center
TDHV	Truck Design Hour Volume
TRB	Transportation Research Board
TTC	Temporary Traffic Control
TTI	Texas A&M Transportation Institute
U.S.	United States
VMT	Vehicle Miles Traveled
vph	Vehicles Per Hour
vphpl	Vehicles Per Hour Per Lane
WIM	Weigh-in-Motion

CHAPTER ONE: INTRODUCTION

1.1 BACKGROUND

As of 2015, it is estimated that there are 8.8 million lane-miles of public roadway in the United States. This constitutes only an 11% increase from the approximate 7.9 million lane-miles in 1980, whereas the number of vehicle miles traveled (VMT) has increased by 104% during the same 35-year period (Federal Highway Administration 2016). The Texas A&M Transportation Institute (TTI) recently partnered with INRIX to publish comprehensive nationwide congestion data showing the consequences of this trend. In 2014, 160 billion dollars and 3.1 billion gallons of fuel were lost to travel delay experienced by road users, who spent an average of 42 additional hours in traffic (Schrank et al. 2015). Increased travel and congestion also place an immense responsibility on state and local agencies, who have been forced to shift focus to the maintenance, rehabilitation, and expansion of the nation's crumbling infrastructure. During the 10-year period from 2002 to 2012 alone, the percentage of Federal-aid highways with an acceptable pavement ride quality decreased from 87.4% to 80.3% (Federal Highway Administration 2015). Thus, it is apparent that both congestion and roadway degradation are increasing faster than agencies can respond.

Accordingly, much of the National Highway System (NHS) is under construction each year. A survey of work zone activity during the summers of 2001 and 2002 found this to be the case for 20-27% of all public roadway mileage (Federal Highway Administration 2017). Given the trends discussed earlier, it would not be surprising if even more of the nation's highways

were under construction during the peak season today. As such, it is concerning that work zones are responsible for approximately 24% of non-recurring congestion, a category including incidents, weather, and special events that accounts for 40% of all the delay discussed previously (Federal Highway Administration 2017). Although most non-recurring congestion is unplanned and uncontrollable, agencies can strive to design and operate work zones in a fashion that minimizes mobility implications. Of particular concern are freeway work zones, as such facilities carry 25.1% of all traffic while accounting for only 1.3% of all lane-miles on the NHS (Federal Highway Administration 2016). Fortunately, this disparity makes even small congestion mitigation efforts impactful.

1.2 PROBLEM STATEMENT

Despite compelling evidence supporting careful attention to freeway work zone design and operations, agency decision making practices are often not data driven. For example, a survey of state Departments of Transportation (DOTs) in 2016 found that traffic control strategies at freeway work zones were chosen based on experience alone by 40% of agencies (Sisiopiku and Ramadan 2016). Decision variables affecting the choice of daytime versus nighttime work have been relatively consistent, as several surveys have cited high daytime traffic, safety, traffic control, and road user costs as the most influential scheduling factors (Hancher and Taylor 2001; Park et al. 2002; Rebholz et al. 2004). However, data suggests that nighttime and off-peak operations will not always optimize safety and mobility. In 2014, 41% of all congestion occurred during off-peak hours, so shifting operations to these time periods does not always eliminate mobility issues (Schrank et al. 2015). Furthermore, drivers are more likely to expect free-flowing conditions during off-peak and overnight hours, so crash risk and severity are both increased despite decreased exposure. In 2015, only 15.3% of all crashes occurred

between the hours of 9PM and 6AM, but this time period accounted for 32.8% of fatal work zone crashes (NHTSA 2015, 2016a).

Even when off-peak or nighttime operations improve safety and mobility for road users, they do so at the expense of decreased worker safety and productivity and increased construction costs. Several research efforts have performed sensitivity analyses and developed optimization models to strike a balance between these variables (Abdelmohsen and El-Rayes 2016; Jiang and Adeli 2003; Tang and Chien 2008). While the results of these studies show that work zone design and operations can be optimized to best serve road users and decrease construction costs, the results do not provide guidance applicable on a case-by-case basis. Such guidance requires a more precise measurement of freeway work zone capacity, queueing, and delay through field data or simulation. In any case, there is compelling evidence to support that work zone scheduling decisions should be better informed than they often are.

As will be discussed in the next chapter, the measurement and definition of freeway work zone capacity has been a topic of debate for several decades, leaving agencies with little formal guidance on predicting the behavior of traffic flow at given volumes for various work zone configurations. Recently, however, well-calibrated microsimulation models have shown promise as a work zone traffic analysis tool. Although these studies have provided guidance to practitioners on developing site-specific microsimulation models, many agencies may not wish to invest the time and resources required to carry out such analyses. Consequently, deterministic tools are still widely used in making freeway work zone design and operations decisions, even though traffic flow and breakdown are stochastic phenomena. This thesis aims to address these shortcomings by developing a freeway work zone traffic analysis tool based on probabilistic capacity estimates to support agency decision making.

Lastly, though urban freeway facilities carry approximately 70% of all interstate traffic in the United States, they compose less than half of the total lane mileage for this functional classification (Federal Highway Administration 2016). Despite the lack of traffic exposure, rural freeway facilities also exhibit a fatality rate 1.7 times higher than their urban counterparts, placing increased importance on their design and operation (NHTSA 2016b; NHTSA 2015). Therefore, the primary focus of this thesis was on developing guidance for rural freeway work zones, although the methodologies herein may be extended to urban facilities as part of future research.

1.3 RESEARCH OBJECTIVES

This thesis is intended to support ongoing research related to a project funded by the Southeastern Transportation Research, Innovation, Development, and Education Center (STRIDE). The focus of the larger parent project is to complete a series of tasks that will aid transportation agencies in the planning, design, and operations of freeway work zones through microsimulation and field data collection. One such task involves the quantification of queuing and delay as a function of traffic demand and other explanatory variables so that agencies can determine the impact of scheduling lane closures by time of day and day of the week. While this research was not meant to be comprehensive, the following objectives were sought:

1. Develop, calibrate, and assess the validity of a microscopic simulation model for a 2-1 (two-lanes-to-one) rural freeway work zone lane closure
2. Use microsimulation outputs to construct breakdown probability models for rural freeway work zones with varying demand volume, truck percentage, and lane closure side to determine the effect of these variables on the likelihood of queue formation

3. Provide a framework for the continuation of the parent STRIDE project so that models may be developed for other lane closure configurations commonly experienced on rural and urban freeway facilities

Each of the objectives above center around the fundamental idea that demand-based work zone planning, design, and operations decisions should be based on stochastic estimates of capacity, rather than deterministic pre-breakdown or queue discharge flow rates. As Chapter Two will discuss, such an assertion agrees with the state of the art in capacity measurement and allows for agencies to make defensible, data-driven decisions, rather than experience-based assumptions. Furthermore, it focuses on the prevention of queueing, rather than just queue mitigation. While queueing and delay are not unavoidable at every site, they should be eliminated when possible and minimized when inevitable.

1.4 ORGANIZATION OF THIS THESIS

The remainder of this thesis is organized as follows. First, Chapter Two reviews pertinent literature related to the measurement and definition of freeway capacity and its extension to work zones. Here, the application of breakdown probability models as a stochastic alternative to traditionally deterministic methods of defining freeway capacity are discussed in greater detail, as such methodology would ultimately be used in later chapters. Finally, case studies of freeway work zone simulation are explored. In Chapter Three, collection and screening of field data used to inform VISSIM model development, calibration, and validation are outlined. The chapter concludes by detailing the partial factorial experiment design utilized to obtain simulated data from VISSIM. Next, Chapter Four describes the aggregation and analysis of simulated data gathered from VISSIM and its ultimate compilation as a lane closure analysis tool for rural freeway work zones. Lastly, Chapter Five provides conclusions from this work and

recommendations for future research. Specifically, extension of the research presented herein through additional field data collection and expansion of the associated capacity analysis tool is proposed.

CHAPTER TWO: LITERATURE REVIEW

2.1 INTRODUCTION

This chapter synthesizes relevant literature on the topic of measuring and predicting freeway work zone capacity using field data and simulation. First, historical context will be given regarding past and current freeway work zone capacity methodology in the *Highway Capacity Manual* (HCM) and the research that has led to the state of the practice. Second, factors that have been found to influence freeway work zone capacity will be discussed to demonstrate where further research is necessary. The process by which breakdown probability models may be developed to estimate capacity from mathematical distributions will then be explored. Finally, case studies will be summarized in which microsimulation models have been created and calibrated to measure freeway work zone capacity under various conditions.

2.2 HISTORICAL MEASUREMENT AND DEFINITION OF FREEWAY CAPACITY

The 6th edition of the HCM defines capacity as “the maximum sustainable hourly flow rate at which persons or vehicles reasonably can be expected to traverse a point or a uniform section of a lane or roadway during a given time period under prevailing roadway, environmental, traffic, and control conditions” (Transportation Research Board 2016). Although this definition has long remained unchanged, debate on the measurement of capacity at freeway facilities began in the 1960s, when several authors documented a discontinuity between capacity under stable flow and that under unstable flow (Drake et al. 1967; Edie 1961). Roess and Prassas synopsise nearly five

decades of research on this topic, during which most researchers agreed the maximum throughput of a freeway facility drops after the transition from non-congested to congested conditions, but no consensus was drawn on how to define freeway capacity in the presence of bottlenecks such as work zones (Roess and Prassas 2016). This point of conflict has more commonly been referred to as “the two-capacity phenomenon” and has led to inconsistencies in practice, as documented in a more recent study (Yeom et al. 2015). Specifically, Yeom et al. argued that if capacity is to be defined as a “sustainable” flow rate, the queue discharge rate after breakdown may be a more appropriate measure than pre-breakdown capacity.

In a similar way, there has been a growing body of research since the mid-1990s that suggests freeway capacity cannot be defined as a single value, but rather should be represented by a probability distribution (Brilon et al. 2005; Elefteriadou et al. 1995; Lorenz and Elefteriadou 2001; Minderhoud et al. 1997; Persaud et al. 1998). This concept was backed by Lorenz et al., among others, with field data providing evidence that breakdown is not a deterministic event, but is stochastic in nature and can vary by several hundred vehicles per hour under identical prevailing conditions (Lorenz and Elefteriadou 2001). Thus, if capacity is to be identified by the onset of breakdown, both capacity and breakdown should be considered random variables and estimated using mathematical distribution functions.

In the early 2000s, TRB’s Highway Capacity and Quality of Service Committee appointed a task force to provide clarity on these issues, and their findings were presented in 2006 in Yokohoma, Japan (Elefteriadou et al. 2006). Elefteriadou built on these findings and summarized the “state of the art in capacity measurement” in her book, *An Introduction to Traffic Flow Theory* (Elefteriadou 2014), where the following conclusions were drawn:

1. Breakdown is probabilistic and its occurrence does not necessarily coincide with the highest observed flow rate.
2. Capacity is a random variable and will vary by several hundred vehicles per hour per lane, even under identical prevailing conditions.
3. There are multiple time periods of interest during which flow measurements may be taken to define capacity: well in advance of breakdown, just prior to breakdown, and during congested conditions after breakdown.
4. Regardless of whether the pre-breakdown capacity (PBC) or queue discharge rate (QDR) is chosen to measure capacity, single values should be estimated from distributions obtained over many breakdown events.

Despite these discoveries, the stochastic nature of freeway work zone capacity has yet to be formalized in the core HCM methodology, though Chapter 26 of the 6th edition demonstrates such a methodology for recurring bottlenecks (Transportation Research Board 2016). Most recently, a few studies have recommended that probabilistic methods be applied to describe work zone capacity, but work in this area is limited to date (Heiden and Geistefeldt 2016; Weng and Yan 2016; Weng and Yang 2014). As such, measurement of capacity at freeway work zones remains ambiguous and practice varies among agencies. Studies conducted by the Indiana and Missouri Departments of Transportation suggest that PBC may be appropriate when practitioners wish to avoid congestion altogether, while QDR may be more meaningful when congestion is expected but queue mitigation is desired (Bham et al. 2011; Jiang 1999). Nonetheless, recent studies have finally established a numerical connection between PBC and QDR by synthesizing freeway work zone capacity values in literature and from field data (Hu et al. 2012; Yeom et al. 2015), the results of which will be discussed next.

2.3 WORK ZONE CAPACITY IN THE HIGHWAY CAPACITY MANUAL

Given that freeway work zones often involve lane closures that function as bottlenecks, the issues discussed above are paramount in determining capacity at such locations. Both HCM 2000 and HCM 2010 presented short-term work zone capacity methodology based on studies conducted in Texas from 1987 to 1991 (Krammes and Lopez 1994). These studies were limited not only in the sense that they contained data from a single state, but that they only considered four variables: intensity of work activity, presence of ramps, presence of heavy vehicles, and number of open lanes through the work zone. Furthermore, the adjustments for work intensity and presence of on-ramps were to be done manually using engineering judgement, with little numerical guidance given. For long-term work zones, a table of average values under various lane closure configurations in several states was given and practitioners were advised to adjust these based on local experience (Chatterjee et al. 2009).

It wasn't until the recent publishing of the 6th edition of the HCM that formal, detailed guidance was given on determining work zone capacity. Yeom et al. built on a past study conducted by several of the co-authors (Hu et al. 2012) to perform an extensive literature search, establish a relationship between QDR and PBC, and provide a regression model for estimating work zone capacity under various conditions (Yeom et al. 2015). The model currently included in the 6th edition of the HCM is given in Figure 2-1 and was created from 90 archival literature sources and 12 field-collected datasets.

Most significant to note is that work zone capacity has now been formally defined in terms of the average queue discharge rate occurring after breakdown, rather than by the maximum pre-breakdown flow rate. The language in the 6th edition of HCM and that of the

authors of the works associated with NCHRP Project 03-107, the basis for the work zone capacity methodology update, still note the importance of PBC. In fact, wording within the HCM implies that freeway capacity should still be defined by the maximum flow prior to breakdown. However, as noted by Yeom et al., QDR is much easier to measure than PBC and provides a more practical means of obtaining freeway work zone capacity (Yeom et al. 2015). Thus, it was ultimately proposed that freeway work zone capacity be estimated in terms of QDR, then converted to PBC if desired by using a default conversion factor of +13.4% or one obtained from local data.

$$\text{average QDR} = 2,093 - 154 \times f_{\text{LCST}} - 194 \times f_{\text{barrier}} - 179 \times f_{\text{area}} \\ + 9 \times f_{\text{lateral}_{12}} - 59 \times f_{\text{day_night}}$$

where

$$f_{\text{LCST}} = \frac{1}{\text{number of open lanes} \times \text{open ratio}}$$

average QDR = average queue discharge flow rate (pcphpl);

f_{barrier} = 0: concrete, 1: cone or drum;

f_{area} = 0: urban, 1: rural;

$f_{\text{lateral}_{12}}$ = lateral distance—12 (minimum -11.9, maximum 0) (ft); and

$f_{\text{day_night}}$ = 0: day, 1: night.

Figure 2-1: HCM 6th Edition Work Zone Capacity Model (Source: TRB 2016)

2.4 FACTORS AFFECTING FREEWAY WORK ZONE CAPACITY

Current understanding of freeway work zone capacity is primarily based on field-collected data in various states, where the effect of several traffic stream, environmental, roadway, and work zone characteristics on throughput have been studied. Weng and Meng performed an extensive

literature search in a 2013 study, where the following factors were found to influence work zone capacity in past research (Weng and Meng 2013):

1. Traffic Stream Characteristics: heavy vehicle percentage, driver composition
2. Environmental Characteristics: time of day, weather, locale
3. Roadway Characteristics: roadway functional classification, grade, presence of on-ramps
4. Work Zone Characteristics: number of open and closed lanes, lane closure side, work zone length, work intensity, work zone duration, work zone speed limit

However, the significance and relative effect of many traffic- and work zone-related factors have been debated in the literature, as will be discussed next.

2.4.1 Traffic Stream Characteristics

It is well understood that heavy vehicles, which differ in size and performance from passenger cars, influence capacity. For this reason, HCM methodologies include passenger car equivalency factors (PCEs) to facilitate comparison of estimated capacity values when the percentage of trucks in the traffic stream varies. However, the extent to which trucks affect freeway capacity in the presence of a work zone lane closure is complex and has been explored by several researchers. A study involving multiple reconstruction zones in Ontario, Canada in 2002 focused entirely on developing PCEs for congested freeways and noted that the effect of heavy vehicles is magnified during queue discharge flow (Al-Kaisy et al. 2002). Consequently, the researchers suggested that higher PCE values be applied during such conditions, where the specific factor is dependent on terrain. Later, Sarasua et al. used field-measured vehicle headways on freeways in South Carolina to calculate PCEs and found an average value of 1.93, which is significantly more than the value of 1.5 given in the 2010 HCM for level terrain (Sarasua et al. 2004). In

phase two of the same study, however, the authors found that different PCEs should be used at different speeds and that these values do in fact increase during congested conditions (Sarasua et al. 2006).

Heavy vehicles have generally been found to decrease freeway work zone capacity, but whether this decrease is significant relative to decreases observed for basic freeway segments has been debated. A 2007 report for the Florida Department of Transportation developed microsimulation models to estimate freeway work zone capacity given 0%, 10%, and 20% trucks and found a strong, negative linear relationship with increasing heavy vehicle percentage (Elefteriadou et al. 2007). However, these findings were reported in vehicles per hour per lane (vphpl), rather than passenger cars per hour per lane (pcphpl), so the results are not surprising nor simply comparable. Additionally, only three truck percentages were modeled, whereas including several smaller increments may have provided a more accurate relationship. An earlier study conducted for freeway work zones in Indiana found that a decrease in capacity of approximately 4 vphpl occurs for each 1% increase in trucks, but that this trend was not significantly different than that found for non-work zone segments (Venugopal and Tarko 2001).

In addition to vehicle composition, the effect of driver population on capacity has been heavily studied. Al-Kaisy et al. researched this topic for various freeway work zones in Ontario, Canada and found that capacity is highest during peak hours and at long-term construction sites, when the traffic stream is composed mostly of commuters or those who are familiar with the ongoing work (Al-Kaisy and Hall 2001). The authors suggested a 7% capacity reduction during off-peak hours and a 16% reduction on weekends to account for these effects. An earlier study in North Carolina agreed with this notion and found that urban work zone sites had higher capacities, possibly due to increased driver familiarity (Dixon et al. 1996). Regardless of driver

population, research has shown that driving behavior in work zones is different from that outside of work zones due to frictional effects found in the changed driving environment (Yeom et al. 2015, 2016). These effects are particularly important when microsimulation is used to model work zone capacity, as will be discussed later.

2.4.2 Work Zone Characteristics

Although the temporal, behavioral, and traffic-related factors discussed previously have been shown to be significant, the geometric and environmental features of a specific work zone have the greatest impact on its capacity. Of these factors, the lane closure configuration has been given the most attention in literature and been shown to have the strongest influence. Several state-specific field data collection efforts from the mid-1990s through mid-2000s developed regression models to estimate work zone capacity and included the number of closed lanes as an input variable (Al-Kaisy and Hall 2003; Dixon et al. 1996; Kim and Lovell 2001; Sarasua et al. 2006, 2004). More recently, however, Yeom et al. have found that the lane closure severity index (LCSI) included in the 6th edition of HCM is a more distinguishing method of defining the work zone lane closure configuration (Yeom et al. 2015).

The LCSI is calculated using the inverse of the product of the number of open lanes and the ratio of open to closed lanes and allows for the effects of work on the shoulder or median that may not include a lane closure to be modeled. Moreover, this method differentiates lane closure configurations with the same ratio of open to closed lanes, such as 4-2 and 2-1 closures. Here, 4-2 and 2-1 lane closures refer to four-lane and two-lane freeway segments reduced to two and one open lane(s), respectively. Regardless, past studies agree that the per-lane work zone capacity decreases as the number of open and closed lanes decrease and increase, respectively. For instance, several authors have documented stark differences in per-lane capacity between 2-1, 3-

1, and 3-2 lane closures, where a 3-2 closure has the highest capacity and 3-1 the lowest (Sarasua et al. 2006; Yeom et al. 2015).

While the effect of lane closure configuration on work zone capacity is well-documented and agreed upon, the influence of lane closure side and length is less clear. Al-Kaisy et al. found that right-side lane closures resulted in approximately 6% higher capacities than left-side lane closures, but could not explain this phenomenon (Al-Kaisy and Hall 2003). On the contrary, Weng and Yan studied the relative effect of several factors on work zone capacity using archival literature sources and found that right-side lane closures will decrease capacity by approximately 2.7% relative to left-side lane closures (Weng and Yan 2016). Others found lane closure side to be insignificant, but acknowledged that this variable should be examined in future research (Heaslip et al. 2009; Kim and Lovell 2001).

Likewise, studies on the significance of lane closure length have been largely inconclusive. Data from South Carolina and Maryland freeway work zones found this variable to be insignificant, but noted that insufficient sample size was an issue (Kim and Lovell 2001; Sarasua et al. 2004). Earlier research for North Carolina freeways, however, observed that the size of the activity area (i.e., length of the lane closure) is a driving factor in determining the magnitude of the drop in throughput under queue discharge flow as compared to pre-breakdown conditions (Dixon et al. 1996). This observation is thought to be explained by vehicles maintaining larger headways during congested conditions, especially in the presence of trucks, as discussed earlier (Al-Kaisy et al. 2002). Length and relative position of the advance warning area has been studied by others but without significant results (Elefteriadou et al. 2007; Heaslip et al. 2009).

Finally, work intensity has been shown to have a strong negative effect on work zone capacity, but there has been no consistency in how to measure or model this variable. To date, this variable has mostly been represented in deterministic equations for estimating capacity where the user must specify an adjustment using engineering judgement. Typically, this value has been suggested as +/- 10% of the base capacity of the work zone in question (Dixon et al. 1996; Sarasua et al. 2004). Thus, it is impractical to attempt to measure this variable's effect in most cases, as work intensity is typically described qualitatively as "light", "moderate", or "heavy". More recently, Heaslip et al. used the rubbernecking factor in CORSIM to attempt to capture the impact of work intensity on capacity more precisely (Heaslip et al. 2009). However, field data was not available to calibrate this factor, so the researchers relied on previous literature findings that indicated a 7% reduction in capacity when work activity was ongoing (Al-Kaisy and Hall 2003). The final model results indicated that rubbernecking factors of 0% and 5.6% should be used when work activity is not present and present, respectively.

2.5 BREAKDOWN PROBABILITY MODELS

Past research dedicated to determining which factors influence freeway work zone capacity have played a vital role in shaping the methodology found in the HCM and improving the way that agencies design and operate their work zones. However, nearly every study to date has taken a deterministic approach to estimating freeway work zone capacity, despite recent findings that indicate probabilistic methods may be more appropriate. Therefore, defining freeway work zone capacity by the maximum achievable flow rate prior to breakdown warrants further investigation. Given that instantaneous conditions within a freeway work zone are stochastic, such capacity may be best described by breakdown probability models (BPMs). To date, these models have

mostly been applied to metered freeway ramp merge junctions, but the methodology presented is applicable to any freeway bottleneck.

2.5.1 *Generating Breakdown Probability Models*

It is widely accepted that the development of BPMs requires the use of the product limit method (PLM) developed by Kaplan and Meier (Kaplan and Meier 1958). This methodology was first developed to describe the statistical properties of the lifetime of mechanical parts or human life, but has a similar application in capacity estimation. This relationship is shown in Table 2-1, where breakdown can be described as the “failure” or “death” of a highway facility (Brilon et al. 2005). Earlier, it was mentioned that the maximum flow rate is not always synonymous with the breakdown flow rate. This phenomenon leads to incomplete observations referred to as right-censored data, because the upper end of the mathematical probability distribution is unattainable when the highest flow rates do not always result in breakdown. Consequently, the breakdown probability distribution appears truncated, but an incomplete empirical distribution can be obtained using Equation 2-1 because the PLM is non-parametric.

$$\hat{S}(t) = \prod_{j:t_j < t} \frac{n_j - d_j}{n_j} \tag{2-1}$$

$\hat{S}(t)$ = estimated survival function

n_j = number of individuals with lifetime $T \geq t_j$

d_j = number of deaths at time t_j

Table 2-1: Application of PLM to Highway Capacity Analysis (Source: Brilon et al. 2005)

	Analysis of Lifetime Data	Highway Capacity Analysis
Lifetime Parameter	Time, t	Volume, q
Failure Event	Death at time t	Breakdown at volume q
Lifetime Variable	Lifetime, T	Capacity, C
Censoring	Lifetime, T , longer than duration of experiment	Capacity, C , greater than traffic demand
Survival Function	$S(t) = 1 - F(t)$	$S(q) = 1 - F(q)$
Probability Density Function	$f(t)$	$f(q)$
Cumulative Distribution Function	$F(t)$	$F(q)$

After using the PLM to obtain an initial probability distribution, it is recommended that the best-fit mathematical distribution be estimated to extrapolate the data (Kondyli et al. 2013). Studies of California and German freeway work zones found that the Weibull distribution was most appropriate after using maximum likelihood estimation to compare several candidate distributions (Brilon et al. 2005; Chow et al. 2009). Others have contended, however, that the lognormal or shifted lognormal distribution may also be suitable (Jia et al. 2010; Kondyli et al. 2013; Weng and Yan 2016). It should be noted that the most recent of these three studies was conducted for freeway work zones, but generated capacity distributions from archival literature rather than sequential field data. Nonetheless, the slight disagreement in the literature and site-specific variation suggests that several mathematical distributions should be considered. Elefteriadou et al. stressed this point in early research related to BPMs, where the authors also found that several hundred breakdown events may be necessary to validate such models. For example, to estimate the point corresponding to a 50% chance of breakdown with 95% confidence, it was determined that a minimum of 384 breakdown events should be observed (Elefteriadou et al. 1995). As such, developing BPMs for freeway work zones, even long-term, is likely only attainable using simulation.

2.5.2 Data Collection and Identification of Breakdown

Correctly identifying the onset of breakdown and return to uncongested conditions is critical in developing meaningful BPMs. This process requires: (1) appropriate placement of data collection sensors, (2) proper choice of data observation and aggregation intervals, and (3) the combination of speed, occupancy, and volume algorithms to define breakdown and recovery periods.

BPMs have various practical applications, so the placement of data sensors has varied somewhat in literature. The bottlenecks in one study of United States and Canadian freeways were defined by several closely-spaced ramp merging segments, so the authors placed multiple sensors just upstream and downstream of each bottleneck location in order to verify which ramp was the cause of each breakdown event (Kondyli et al. 2013). This placement strategy was crucial, as literature agrees that the onset of breakdown should be defined by observations made close to the bottleneck in question and not influenced by conditions downstream of the data collection point (Brilon et al. 2005; Elefteriadou et al. 1995; Jia et al. 2010; Kondyli et al. 2013). In the absence of on-ramps or other downstream influencing factors, most agree that the ideal sensor is one placed just downstream of the bottleneck in question (Jia et al. 2010; Lorenz and Elefteriadou 2001), although a study of German freeways contended that sensors should be placed just upstream of the bottleneck to avoid influence of conditions within the bottleneck (Brilon et al. 2005).

The choice of data aggregation periods is also important, as different probability distributions can be obtained from the same data when these intervals are changed. Lorenz et al. studied this concept for 1-, 5-, and 15-minute aggregation intervals and found that shorter intervals result in lower breakdown probability rates for a given flow rate, and vice versa. This

phenomenon was explained by the fact that brief fluctuations in flow rates, even to above 2,000 vphpl, can be absorbed by the traffic stream over brief time periods. However, as the aggregation interval increases, an average flow rate of 2,000 vphpl would indicate sustained periods of high volume that are more likely to lead to congestion (Lorenz and Elefteriadou 2001). Later work by Kondyli et al. argued strongly for the use of 1-minute intervals to capture abrupt oscillations in traffic (Kondyli et al. 2013), while others concluded that 5-minute intervals provided the best compromise between accounting for brief spikes in volume and smoothing the data (Brilon et al. 2005; Persaud et al. 1998). Given that data availability and study objectives will vary, it seems that any choice is defensible so long as the researcher clearly defines which time interval was used.

While the breakdown mechanism can typically be identified from visual observation of the fundamental diagram of traffic flow or speed versus time plots, algorithms have generally been used to systematically pinpoint congested conditions. In the literature, these algorithms have involved combinations of speed, occupancy, and volume thresholds. Brilon et al. applied a constant speed threshold of 70 km/hr (43 mph) and classified all flow measurements that coincided with speeds equal to or less than this threshold as congested flow (Brilon et al. 2005). However, the study was conducted for German freeways, which the authors noted was a caveat of the research, as different speed values would likely apply in other countries. Others found that breakdown should be defined by both speed and density to avoid identifying congestion from anomalous free flow conditions (Chow et al. 2009; Jia et al. 2010). Jia et al. designated critical speed and density thresholds based on conditions where speeds were below 55 mph and densities above the level of service *D* threshold, or 26 passenger cars per mile per lane.

Modern studies have shown, however, that speed thresholds sustained over specified time periods may be most appropriate. The 6th edition of the HCM defines the onset of breakdown as a sudden speed drop at least 25% below the free flow speed (FFS) sustained for at least 15 minutes (Transportation Research Board 2016). Conversely, the recovery period is defined as a return to speeds within 10% of FFS for at least 15 minutes. Work by Elefteriadou et al. applied a 90 km/hr (56 mph) threshold to Canadian freeways, but required that these speeds be maintained for a period of at least five minutes. Similarly, the authors stated that the return of stable traffic conditions should be signified by speeds above this value maintained for at least five minutes (Elefteriadou et al. 1995).

Later, several of the co-authors contributed to a study in which selection of these thresholds was examined in more detail. The findings suggested that breakdown identification algorithms should be based only on speed when sequential speed data is available because this method results in less variance among breakdown volumes. Their specific recommendations were to use a speed drop threshold of 16 km/hr (10 mph), where the reduced speed is sustained for at least five minutes, and a breakdown recovery time period of 10 minutes (Kondyli et al. 2013). The first of these two requirements prevents false identification of brief drops in speed and spikes in traffic flow that are ultimately absorbed, while the second ensures that multiple breakdown events are not identified from a single period of congestion. Accordingly, a similar set of speed-based breakdown identification algorithms will later be applied in this thesis.

2.6 FREEWAY WORK ZONE SIMULATION MODELS

The freeway work zone capacity methodology presented in the 6th edition of the HCM is substantially improved from that in previous editions, but is still limited by the fact that it is a

macroscopic model and cannot account for complex work zone configurations unique to specific sites. Capacities estimated from this model and those from past editions of the HCM are often used as input parameters in other deterministic work zone software such as QUEWZ and QuickZone to predict queueing, delay, and road user costs associated with various scheduling and traffic control strategies. QUEWZ, developed in 1998 by the Texas A&M Transportation Institute, and QuickZone, developed in 2001 by FHWA, have been heavily used of late, but have been shown by some studies to provide inconsistent and often inaccurate estimates of these parameters (Benekohal et al. 2003; Ramezani and Benekohal 2012). Furthermore, although field data collection and empirical capacity measurement are the most accurate means of depicting real traffic conditions, these efforts are often costly and difficult to obtain sufficiently large sample sizes from. Likewise, it has been shown previously that the development of BPMs for freeway work zones is likely not feasible using field data. Fortunately, the emergence of microsimulation software such as CORSIM and VISSIM has provided a means to more accurately and economically deal with such complexity as computing power has increased in recent years.

2.6.1 Simulation Overview

Simulation is a valuable traffic analysis tool with wide-ranging applications, not just in work zones. The discussion to follow is based on principles outlined in Elefteriadou's *An Introduction to Traffic Flow Theory* and the FHWA Traffic Analysis Toolbox regarding the use of traffic analysis tools and simulation models (Dowling et al. 2004; Elefteriadou 2014).

At the most basic level, traffic analysis software can be divided into four categories. From most generalized to most complex, these are: sketch-planning, macroscopic, mesoscopic,

and microscopic. Sketch-planning or analytical tools include software such as QUEWZ-98, QuickZone, FREVAL-WZ, or any spreadsheet created to calculate various performance measures. These deterministic tools primarily have high-level planning applications and should be used in situations where agencies wish to guide work zone design and operations decisions while spending the least time or money. However, these advantages are coupled with the disadvantage that randomness associated with individual driving behavior and other factors within work zones are unaccounted for. Thus, it is not surprising that studies have found these tools to be inaccurate in the past (Benekohal et al. 2003; Ramezani and Benekohal 2012). Although QUEWZ-98 and QuickZone apply now-outdated HCM methodology to determine various performance measures in work zones, FREEVAL-WZ applies the 6th edition methodology and can model more complexity than the other two programs (Trask et al. 2015). Nonetheless, its effectiveness as an analysis tool has yet to be fully explored.

Macroscopic models replicate the movement of platoons of vehicles without analyzing individual vehicle movement. These simulation models are based solely on deterministic relationships between flow, speed, and density and include software such as the TRANSYT-7F package included with the *Highway Capacity Software* from McTrans. While these models may be useful in optimizing flow of the traffic stream and provide slightly more detail than the analytical tools mentioned previously, they are still generalized and ignore the stochasticity of work zone environments.

Mesoscopic simulation models are a hybrid of macroscopic and microscopic models. While they still only model platoons of vehicles, these models employ equations to indicate how different platoons interact. One such example of mesoscopic software is DYNASMART-P, another software package developed by McTrans in 2007 that can model the dynamic evolution

of traffic flows as individual drivers make decisions about their best route. Such a tool may be useful for regional work zone management, but not as valuable for individual work zones.

Finally, microscopic simulation models imitate the movement of every vehicle in the network by accounting for how drivers respond to the surrounding roadway environment. Unlike the deterministic software discussed earlier, microsimulation tools are stochastic, meaning that each model run will produce a unique result. These characteristics make microsimulation the most valuable tool available for estimating freeway work zone capacity. Popular commercially available microsimulation software used by practitioners include CORSIM and VISSIM, developed by FHWA and the PTV Group, respectively. Each of these software packages follow three main algorithms to define the randomness of driving behavior: car-following, lane-changing, and gap acceptance. Recently, several studies have examined the effect of modifying these parameters on simulated work zone capacity and provided guidance for practitioners.

2.6.2 Driving Behavior Parameters

Although microsimulation is a powerful traffic analysis tool, the validity of any developed model is dependent on a strong calibration effort. Simulation models must be adjusted so that they can replicate field conditions before any hypothetical scenarios can be examined. The authors responsible for the work zone capacity methodology update mentioned earlier have already published work that supplements the analytical model in the 6th edition of HCM with guidance on developing simulation models in VISSIM (Yeom et al. 2016), following suit with several other previous studies (Chatterjee et al. 2009; Chitturi and Benekohal 2008; Edara and Chatterjee 2010; Kan et al. 2014; Lownes and Machemehl 2006). While CORSIM has been applied in past freeway work zone capacity studies (Heaslip et al. 2009; Ramadan and Sisiopiku 2016), VISSIM

was the chosen analysis tool for this thesis and will be the focus of the literature discussion to come.

The most heavily studied driving behavior parameters are those that pertain to car-following algorithms. These algorithms estimate the trajectory of a following vehicle given the behavior and position of a lead vehicle. Table 2-2 lists the 10 car-following parameters in VISSIM, which are based on the Wiedemann 99 car-following model (PTV Group 2017).

Table 2-2: VISSIM Car-Following Parameters (Adapted from Yeom et al. 2016)

Parameter	Description	Default Value
CC0	standstill distance between two vehicles	4.92 ft
CC1	desired headway time between lead and trailing vehicles	0.9 s
CC2	maximum additional distance over desired safety distance	13.12 ft
CC3	time in seconds to start of the deceleration process	-8.0 s
CC4	negative speed variations during the following process	-0.35 ft/s
CC5	positive speed variations during the following process	0.35 ft/s
CC6	influence of distance on speed oscillation	11.44
CC7	oscillation during acceleration	0.82 ft/s ²
CC8	desired acceleration from standstill	11.48 ft/s ²
CC9	desired acceleration at 50 mph	4.92 ft/s ²

The first three parameters are all related to determining the safety distance at which vehicles will follow each other and have been found to be the most influential in determining capacity. This relationship is described by Equation 2-2 (Edara and Chatterjee 2010).

$$\text{safety distance} = CC0 + CC1 * v + CC2 \quad (2-2)$$

where v = velocity (ft/s)

Related to this safety distance are two primary lane-changing and gap acceptance parameters, the lane-changing distance and safety distance reduction factor (SRF), respectively.

Previously known as the “look-back distance”, the lane-changing distance parameter in VISSIM specifies the distance upstream of a necessary lane change (e.g. lane closure) that a driver will begin to look for opportunities to merge. This is the first of three conditions required for a vehicle to change lanes in VISSIM: (1) a desire to change lanes, (2) favorable driving conditions in the neighboring lane(s), and (3) gap availability (Edara and Chatterjee 2010). The latter two conditions are defined by the safety distance mentioned before and any adjustment to this distance defined by the SRF. This factor reduces the safety distance during the lane-changing process and essentially specifies the aggressiveness of drivers during such maneuvers. For example, if the safety distance is computed as 72 feet and the SRF is 0.6, the required gap would be only 43 feet (Edara and Chatterjee 2010).

In a non-work zone study of congested freeway segments in California, Gomes et al. also modified the emergency stop distance and waiting time before diffusion, two parameters that help to prevent unusual driving behavior during congested conditions. For example, the authors found that the initial model of one freeway merge junction consisted of stopped traffic in the rightmost lane with nearly free flowing conditions in the left lane. This phenomenon was explained by vehicles getting “stuck” while trying to merge and was corrected by decreasing the waiting time before diffusion. However, it was advised that these values be modified with caution so that queued vehicles which researchers do not desire to evaporate from the network are retained (Gomes et al. 2004). Other studies found that this issue was a result of unbalanced lane use upstream, and verified that lane use balance thresholds were satisfied prior to validating a particular simulation run (Chatterjee et al. 2009; Yeom et al. 2016). Multiple case studies will be examined in the next section that address these topics in more detail.

2.6.3 Freeway Work Zone Simulation Case Studies

The following section discusses case studies that have shaped the simulation methodology used in this thesis. The focus of recent work zone simulation research has been on the calibration effort, as the authors of those studies intended for practitioners to use the results to develop localized simulation models. Consequently, two of the studies presented were carried out to provide guidance on modifying driving behavior parameters and other elements of the simulation environment in VISSIM to replicate field-measured capacities. The third study was conducted using CORSIM, but proceeded beyond calibration to investigate the effect of several factors on work zone capacity.

Calibration Case Study #1

In 2010, Edara and Chatterjee used data from Ohio work zones to evaluate default truck characteristics in VISSIM and develop regression models for determining driving behavior parameters based on the capacity, truck percentage, lane configuration, and upstream lane distribution of a given freeway work zone (Edara and Chatterjee 2010). The authors noted that the default length of a truck in VISSIM is 33.5 feet, but approximately 65% of truck-miles in the United States are driven by Class 9 tractor-trailers 73.5 feet in length (Harwood et al. 2003). As such, they recommend that any future studies consider a distribution of truck length based on local field data and power and weight specifications that are consistent with such trucks. Figure 2-2 shows the discrepancy in simulated capacity for a 2-1 lane closure when the default VISSIM truck characteristics were used versus adjusted values.

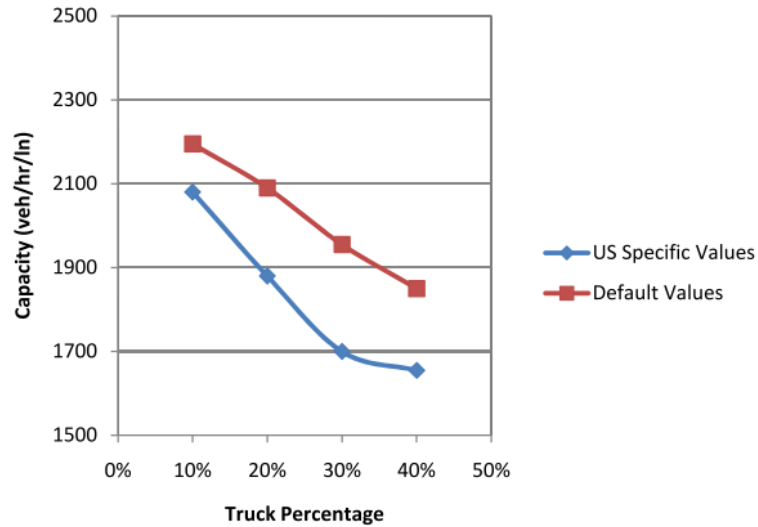


Figure 2-2: Sensitivity of Simulated Capacity to VISSIM Truck Characteristics (Source: Edara and Chatterjee 2010)

After using pilot simulation runs to guide modification of default truck characteristics, the authors performed a sensitivity analysis to determine the effect of select driving behavior parameters on simulated capacity. Based on past research (Chatterjee et al. 2009), the car-following, lane-changing, and gap acceptance variables ultimately examined were CC1, CC2, and SRF. Variations in lane-changing distance were not studied, but a value of 2500 feet was selected to mimic the expected location of a “___ LANE CLOSED ½ MILE” sign in the field. As shown in Figure 2-3, capacity was measured as the QDR just downstream of the bottleneck, while data collection points were placed at four locations to verify lane use balance upstream of the closure point. A total of 900 scenarios were simulated between 2-1, 3-2, and 3-1 lane closure configurations; however, only those which produced reasonable upstream lane balance consistent with field data were retained.

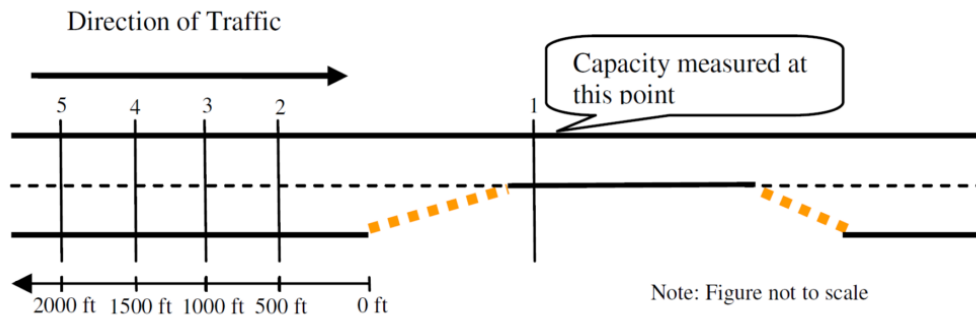


Figure 2-3: Lane Closure Network Setup for 2-1 Closure (Source: Edara and Chatterjee 2010)

The results of the study were three sets of regression equations, one for each lane closure configuration, that provide guidance for selecting the values of $CC1$, $CC2$, and SRF based on the field-measured capacity (Q_C), truck percentage (P_T), and lane distribution 1000 feet upstream of the lane closure (P_{CL}). An example of these for a 2-1 closure is given in Equation 2-3 and is intended to provide practitioners with values of driving behavior parameters that are consistent with conditions in freeway work zones. It should be noted, however, that other research has found that these are not the only driving behavior parameters in VISSIM that affect capacity significantly (Chitturi and Benekohal 2008; Gomes et al. 2004; Kan et al. 2014; Lownes and Machemehl 2006; Woody 2006). Furthermore, while this guidance may serve as a good starting point, the total calibration effort will likely require more fine-tuning after adjusting the parameters studied here.

$$CC1 = 2.974 - 0.0009 * Q_C + 0.0267 * P_T + 0.0022 * P_{CL} - 0.000029 * Q_C * P_T \quad (2-3)$$

$$CC2 = 82.39 - 0.0266 * Q_C + 0.208 * P_T - 0.302 * P_{CL} - 0.00009 * Q_C * P_T$$

$$SRF = 0.656 - 0.0002 * Q_C + 0.0057 * P_T + 0.0078 * P_{CL} - 0.000009 * Q_C * P_T$$

Calibration Case Study #2

A subsequent study conducted in 2016 by Yeom et al. used nationwide field data from their NCHRP 03-107 research to perform a sensitivity analysis on a similar set of driving behavior parameters (Yeom et al. 2016). However, the authors neglected trucks and instead focused solely on the modification of CC0, CC1, CC2, CC4, CC5, CC8, SRF, and lane-changing distance. A diagram of their network setup is given in Figure 2-5, where several key items should be noted. First, data collection points were placed 1000 feet upstream and 100 feet downstream of the lane closure point to allow for lane use balance verification and measurement of QDR, respectively. To ensure that the frictional effects within the work zone were accurately modeled, a reduced speed area and desired speed decision point were placed at the beginning of the lane closure. The former has a “look ahead” function that allows vehicles to begin slowing down prior to reaching the speed decision point. Speed distributions within and outside of the work zone were based on field data.

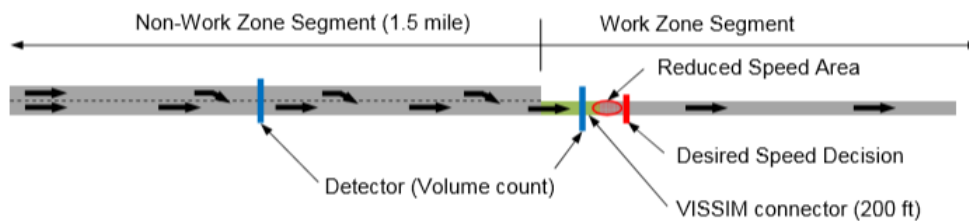


Figure 2-4: VISSIM Network Setup for 2-1 Lane Closure (Source: Yeom et al. 2016)

Given that capacity was to be measured as the average QDR, the network was coded with a demand of 2,000 vphpl to ensure that congested conditions would develop. Like the previous case study (Edara and Chatterjee 2010), lane use balance verification was critical in retaining realistic results; however, the researchers could not find sufficient guidance in the literature on

appropriate lane use upstream of a work zone with a lane closure, so they used the thresholds given in Table 2-3 based on a late, or “zipper”, merge strategy.

Table 2-3: Lane Use Balance Thresholds (Source: Yeom et al. 2016)

Number of Lanes in Upstream Segment	Minimum	Expected Even Ratio	Maximum	Unconditional Minimum
2	0.35	0.5	0.65	N/A
3	0.23	0.33	0.43	0.15
4	0.18	0.25	0.33	0.05

A total of 8,478 experiments were planned by varying each of the parameters listed in Table 2-2 from 100 to 700 percent of their default values. The complete calibration effort included verification of lane use balance and cross-checking of simulated capacity against predicted capacity from the model in the 6th edition of the HCM. Only model runs that produced results within the thresholds in Table 2-3 and the minimum and maximum values predicted by the HCM model were retained. Ultimately, only CC1 and CC2 produced valid results under all the tested lane configurations, so it was recommended that the remaining parameters be held at their default value apart from lane-changing distance. Regression equations for determining CC1 while holding CC2 constant are given in Table 2-4, and generic guidance for driving behavior parameter settings is given in Table 2-5.

Table 2-4: Regression Model for CC1 Estimation (Source: Yeom et al. 2016)

Lane Configuration	LCSI	CC2 (ft)	CC1 (s) Estimation Regression Model	R ² Value
4 to 3	0.44	39.36	-0.0015*avg. QDR + 3.9346	0.9950
3 to 2	0.75	26.24	-0.0020*avg. QDR + 5.0041	0.9807
4 to 2	1	26.24	-0.0019*avg. QDR + 4.7155	0.9245
2 to 1	2	23.62	-0.0023*avg. QDR + 5.3146	0.9913
3 to 1	3	26.24	-0.0041*avg. QDR + 7.7741	0.9937
4 to 1	4	39.36	-0.0022*avg. QDR + 4.7177	0.9694

Table 2-5: VISSIM Driving Behavior Parameter Guidance (Source: Yeom et al. 2016)

Parameter	VISSIM Default	Recommended WZ Setting
<i>Car Following Parameters</i>		
CC0 (ft)	4.92	Default
CC1 (s)	0.90	Work Zone Configuration Specific
CC2 (ft)	13.12	Work Zone Configuration Specific
CC3 (s)	-8.00	Default
CC4 (ft/s)	-0.35	Default
CC5 (ft/s)	0.35	Default
CC6	11.44	Default
CC7 (ft/s ²)	0.82	Default
CC8 (ft/s ²)	11.48	Default
CC9 (ft/s ²)	4.92	Default
<i>Lane-Changing Parameters</i>		
Lane-Changing Distance (ft)	656.20	> 656.20
Necessary lane change, 1 ft/s ² per distance (ft)	200.00	100.00
Maximum Deceleration for Cooperative Braking (ft/s ²)	-9.84	-20.00

CORSIM Case Study

Lastly, a study by Heaslip et al. in 2009 used CORSIM to develop analytical models for estimating freeway work zone capacity (Heaslip et al. 2009). The authors felt that the methodology found in the 2000 edition of the HCM did not adequately address all factors that affect work zone capacity due to the limitations of field measurement and noted that simulation is a viable alternative. Their research objectives were: (1) develop analytical models for 2-1, 3-2, and 3-1 lane closures using the results of CORSIM simulation runs, (2) calibrate and refine these models using field data from a work zone in Jacksonville, Florida, and (3) compare the results to the HCM 2000 methodology.

In developing the simulation model, the following independent variables were initially considered: lane closure configuration, work zone length, lane closure side, work intensity,

volume distribution among lanes, distance of first warning sign upstream of the closure, and percentage of trucks. Pilot simulation runs revealed that CORSIM results were not sensitive to work zone length or lane closure side, so these variables were ultimately eliminated. However, the authors did comment that this is a limitation of CORSIM and that past research has indicated that these factors may indeed be significant to work zone capacity. As such, they recommended that future research re-examine these variables. The dependent variables gathered from each simulation run were: speeds by lane, vehicle lane distributions, time headways, and maximum throughput under congested conditions.

A diagram of the simulated network is given in Figure 2-6. Links (3,4) and (6,7) were varied depending on the distance of the first upstream warning sign to the lane closure, where the former was adjusted to ensure that the overall length of the network remained the same for all simulation runs. Links (2,3) and (4,5) were used to verify headway values upstream of the closure and ensure that erratic driving behavior was not occurring. The lane closure itself was modeled as an incident because this feature in CORSIM allows for the specification of a rubbernecking factor, which the authors used to model work intensity.

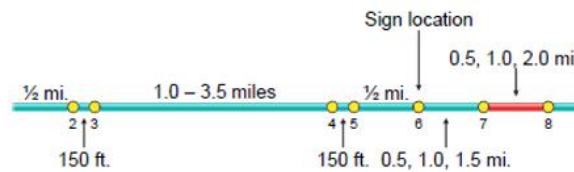


Figure 2-5: Diagram of Simulated Network (Source: Heaslip et al. 2009)

The results of the study yielded three analytical models, one for each of the studied lane closure configurations, which the authors found to predict capacity to within 1% of field-measurements. Using field data from the Jacksonville, Florida site and literature, further

adjustments were recommended to account for variation in lighting conditions, weather, and driver population, all of which could not be modeled in CORSIM. The analytical models are presented in Figure 2-7, but the reader is directed to Heaslip et al. for the full procedure.




Lane Closure Type	CAPACITY MODEL FOR OPERATIONAL PROCEDURE
2 TO 1	 <p>$R^2 = 0.915$</p> $C_{unadj}^{2-to-1} = 1855 - 693 * SignDist + 191 * f_{HV,F} - 12.3 * Rubber\% - 467 * DistrLan1(6,7) + 829 * DistrLan1(6,7) * SignDist + 7.43 * SpeedLan1(6,7)_{adj} * SignDist$
3 TO 2	 <p>$R^2 = 0.932$</p> $C_{unadj}^{3-to-2} = 917 + 461 * SignDist + 854 * f_{HV,F} - 20.4 * Rubber\% - 611 * DistrLan1(6,7) * SignDist - 4.03 * SpeedLan1(5,6)_{adj} * SignDist$
3 TO 1	 <p>$R^2 = 0.895$</p> $C_{unadj}^{3-to-1} = 1177 + 550 * f_{HV,F} - 14.5 * Rubber\% + 157 * DistrLan3(6,7)$
ALL	$C_{adj} = f_l * f_d * f_r * (C_{unadj} - v_R)$

Figure 2-6: Analytical Models by Lane Configuration (Source: Heaslip et al. 2009)

Despite the seemingly promising results, several caveats of the research were presented. For example, it was noted that CORSIM constrained the simulation effort due to its lack of versatility in accounting for the effects of variables such as work zone length, lane closure side, and lane width. Furthermore, this study only used a single 3-2 lane closure in Florida to calibrate the simulation model, which brings the results for other lane configurations into question. Thus, the authors recommended that future research apply a larger field dataset and that CORSIM algorithms be modified to aid in work zone simulation modeling.

2.7 SUMMARY

In summary, an expansive literature review was undertaken to assess the state of the practice in defining, measuring, and modeling freeway work zone capacity and motivate the

objectives of this thesis. On a broad level, it is evident that researchers still cannot agree on the most appropriate measure of freeway work zone capacity. While the most recent HCM methodology points to QDR as the most reliable and conservative measure of capacity at freeway work zones, research and agency practice strongly suggests that breakdown and queue formation be considered to drive work zone design and operations decisions. Since variability in instantaneous driving behavior and conditions in the work zone environment lead to variations in breakdown flow and QDR, there may be advantages to describing each with probability distributions rather than a single value.

The most accurate model of real traffic conditions comes from field data collection, which was the focus of most early freeway work zone capacity studies. However, these efforts require substantial time and money, and the extent of observations necessary to provide adequate data for constructing breakdown probability models is immense. Fortunately, recent research has suggested that simulation models may be a viable alternative to obtaining a large sample of capacity data under various work zone configurations. The focus of most of this work has been to provide practitioners with guidance in developing and calibrating such simulation models so that they may be applied to individual, localized work zones. That said, many agencies may not have the time or resources to generate these models, and might prefer to lean on deterministic methods, charts, or look-up tables when making work zone scheduling decisions. Therefore, past literature has revealed the need for full-scale work zone simulation models that provide data for practice-ready application.

CHAPTER THREE: METHODOLOGY

3.1 INTRODUCTION

The methods by which findings from the literature review were used to drive field data collection efforts, VISSIM model development, and final experiment design are discussed in this chapter. The first section provides an overview of the study work zone near Tuscaloosa, Alabama from which sequential speed, length, volume, and headway data were collected, screened, and processed. Next, VISSIM network coding and calibration are described in significant detail, as the validity of the results depended most strongly on the model development process. Lastly, the design of the factorial experiment used to generate breakdown probability models under various freeway work zone conditions is presented.

3.2 SITE OVERVIEW AND DATA COLLECTION PLAN

One of the primary objectives of this thesis was to produce realistic, generalizable results that could be transformed into a tool to be used by agencies and practitioners for rural freeways. As such, it was critical that simulation model outputs were validated using field-collected data. The research team coordinated with the Alabama Department of Transportation (ALDOT) to identify potential study work zones and ultimately selected a 2-1 lane closure on Interstate 59/Interstate 20 (I-59/I-20) just south of Tuscaloosa, Alabama. A map of the site is provided in Figure 3-1 along with the location of key pieces of temporary traffic control (TTC), as these TTC devices

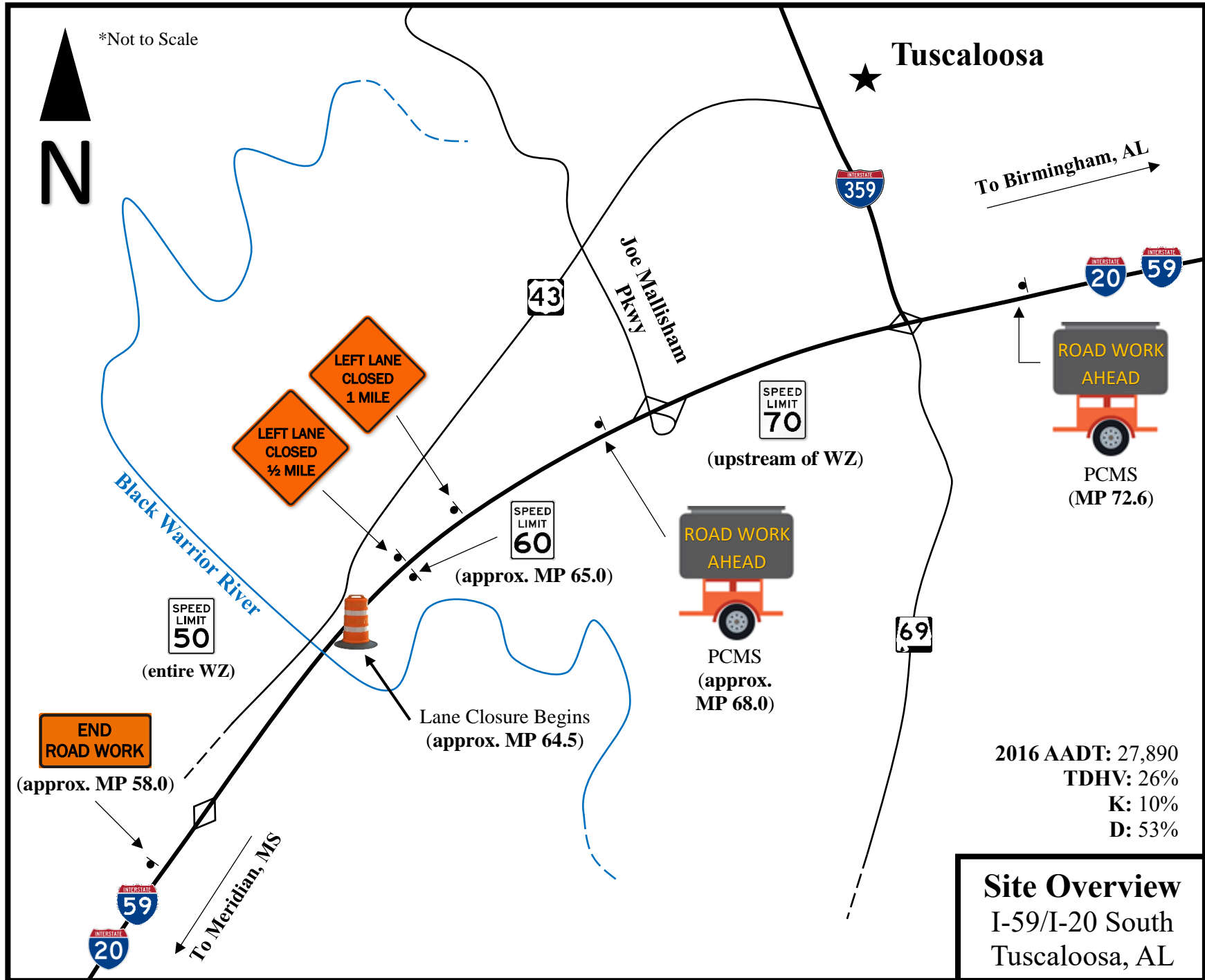


Figure 3-1: Map of Study Work Zone (Traffic Data Source: ALDOT GIS)

were influential in coding the final VISSIM model. Specifically, simulated lane-changing behavior and vehicle speed distributions were determined in large part by the location of warning signage and reduced speed limits throughout the work zone. Note that in the figure, AADT and TDHV refer to annual average daily traffic and proportion of trucks in the traffic stream during the design hour, respectively. Likewise, K and D represent the proportion of daily traffic occurring during the peak hour and in the peak direction, respectively. It should be noted that this data was obtained from the nearest ALDOT permanent counting station and may or may not reflect exact conditions at the study work zone.

Data was collected during the 14-day period from October 3rd, 2016 to October 16th, 2016 using a total of nine traffic sensors, deployed as shown in Figure 3-2. The NC350 BlueStar Portable Traffic Analyzer, manufactured by M.H. Corbin, was the chosen sensor for the study. Each sensor had the capability to collect speed, volume, length, and headway data at one-second intervals for up to 300,000 vehicles or 21 days, whichever occurred first. The product information specifies that each sensor is also accurate to within 4 mph for vehicle speeds, 4 feet for vehicle lengths, and 1% for vehicle counts (MH Corbin 2016).

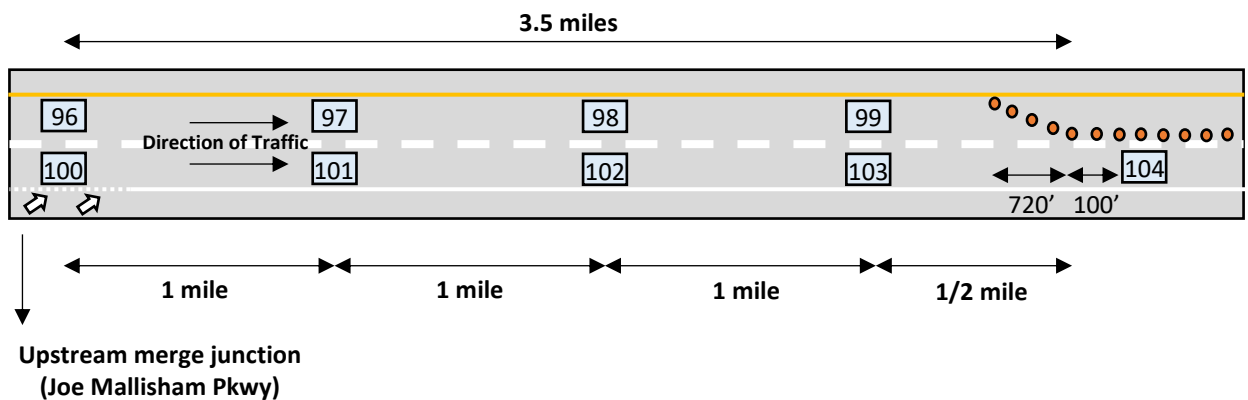


Figure 3-2: Traffic Sensor Deployment Scheme (drawing not to scale)

The sensor deployment scheme shown in Figure 3-2 was developed based on findings from the literature review suggesting that there are three primary locations at which data should be collected: well upstream of the lane closure, between a quarter and half mile upstream of the lane closure, and just downstream of the lane closure. It should be noted that the labels given to each sensor in Figure 3-2 correspond to the last two or three digits of their respective serial numbers, which will be used throughout the remainder of this thesis for brevity. Sensors 96, 97, 98, 100, 101, and 102 were placed with the intent to collect vehicle speeds in locations not influenced by downstream congestion due to the bottleneck; such speeds were ultimately used to develop free flow speed distributions in VISSIM for the non-work zone segment of the network. Sensors 99 and 103 were placed one half mile upstream of the bottleneck to observe queue propagation and dissipation due to breakdown events and to study lane distributions within the advance warning area. Lastly, sensor 104 was installed approximately 100 feet downstream of the beginning of the full lane closure to build desired speed distributions in VISSIM for the work zone segment of the network, identify breakdown events, and measure queue discharge flow rates.

Despite the relatively high accuracy of the NC350 traffic sensors, there were limitations to the data collection effort. Sensor 103 stopped collecting data before the end of the study period, the cause of which was determined to be a firmware issue after discussions with M.H. Corbin staff. In addition, the research team moved sensor 104 from the right lane to the left lane on October 6th, 2016 around 4:30PM because resurfacing operations were scheduled to shift to the right lane. Since the traffic switch did not actually occur until 7:00AM on October 8th, 2016, the number of available days to observe breakdown events was reduced. Finally, a comparison of the 14-day traffic volumes observed at each data collection location revealed significantly lower

vehicle counts at sensors 96 and 100, most likely due to their proximity to the on-ramp at Joe Mallisham Parkway. Consequently, these records were used exclusively for free flow speed data and VISSIM volume inputs were obtained from other upstream sensors.

3.3 DATA SCREENING AND PROCESSING

Even the most accurate sensors will occasionally produce erroneous measurements, so data screening was an especially vital component of this research. A combination of threshold- and traffic flow theory-based screening methods as proposed by Turochy and Smith were initially explored to identify obvious errors in the sensor data (Turochy and Smith 2000). Quick inspection of the dataset revealed that there were numerous vehicle records for which the speed or length was measured as zero or as an exceptionally high value. Further discussions with M.H. Corbin led to the discovery that the NC350 traffic sensors tend to measure unrealistic vehicle speeds and lengths during congestion, when prevailing speeds may be less than the equipment's stated minimum of 5 mph. As a result, the first threshold set was a minimum speed of 5 mph, although other speed thresholds would later be considered.

Regarding traffic flow theory-based methods, the observed values of headway (in seconds, from front bumper to front bumper) were often found to be inconsistent with the speed differential between successive vehicles. For instance, a headway of 1 second or less was frequently measured for two vehicles whose speeds differed by as much as 50 mph, suggesting that at least one of these records were erroneous. However, headway-based screening methods were ultimately abandoned for two reasons: (1) it was discovered that headway values were all rounded down to the nearest second, meaning that a value of 1 second could pertain to any headway between 1 and 1.99 seconds; (2) discarding records using other screening methods would invalidate the headway value for a given record. Therefore, several threshold- and

statistical-based screening methods were applied to the dataset as will be discussed in the following sections.

3.3.1 Vehicle Lengths

The first detailed screening effort that took place pertained to the distribution of vehicle lengths at the study work zone. For a VISSIM model to accurately replicate field conditions, it is crucial that simulated traffic is composed of the correct percentage of each vehicle class and that such vehicles are represented by their true lengths. While it was expected that there would be inconsequential variation among sensors with regards to vehicle lengths and that a prevailing distribution would be easily identified, this was not the case. Figure 3-3 provides an example of this discrepancy for sensors 101 and 102. The figure shows that sensor 101 consistently measured longer passenger cars and trucks than sensor 102 and supports the decision to pursue a statistical means of developing accurate length distributions.

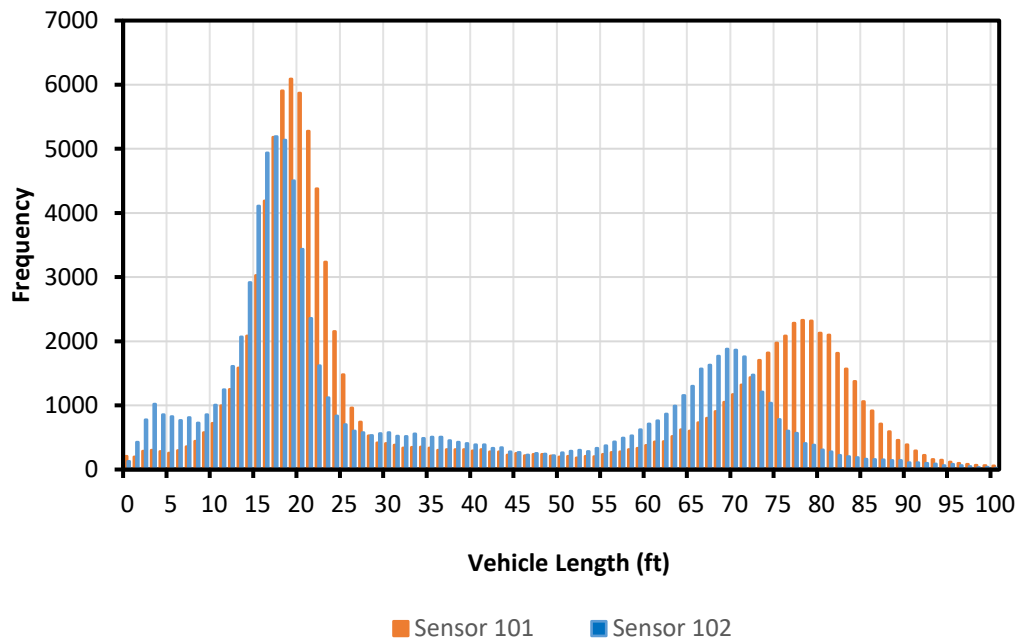


Figure 3-3: Vehicle Length Distributions for Sensors 101 and 102

The disagreement between sensors 101 and 102 was common among other sensors—the mean length for passenger cars was as small as 15 feet and as large as 20 feet, while the mean length for trucks varied between 63 feet and 82 feet. To address this issue, a multi-step procedure was utilized to address sensor error and estimate the true distribution of vehicle lengths:

1. Common vehicle lengths were identified from literature (AASHTO 2011) to gain an idea of how lengths should be distributed for each vehicle class, and extreme values were discarded.
2. The mean frequency of each observed vehicle length among the nine sensors was found to generate an average distribution.
3. The bounds for a normal distribution were approximated for each vehicle class and the mean and standard deviation calculated.
4. Upper and lower bounds for each vehicle class were set at two standard deviations away from the mean for each distribution.

The frequency distribution representing the combination of all nine sensors is given in Figure 3-4, where the average frequency of each length was calculated by dividing its total number of occurrences by nine. The disparity in vehicle length measurements for heavy trucks is underscored by the bimodal distribution found between 50 and 100 feet. However, the dotted line drawn to approximate a unimodal distribution has a peak between 73 and 75 feet, which is close to the 73.5-foot length of a WB-67 interstate semitrailer, a vehicle class composing 65% of all truck-miles in the United States (Harwood et al. 2003).

Of more interest during the screening process, however, was defining upper and lower bounds beyond which vehicles would be declassified and not considered in determining overall

proportions of each vehicle class in the traffic stream. The results of the process outlined above are presented in Table 3-1, where the absolute upper and lower lengths for passenger cars and

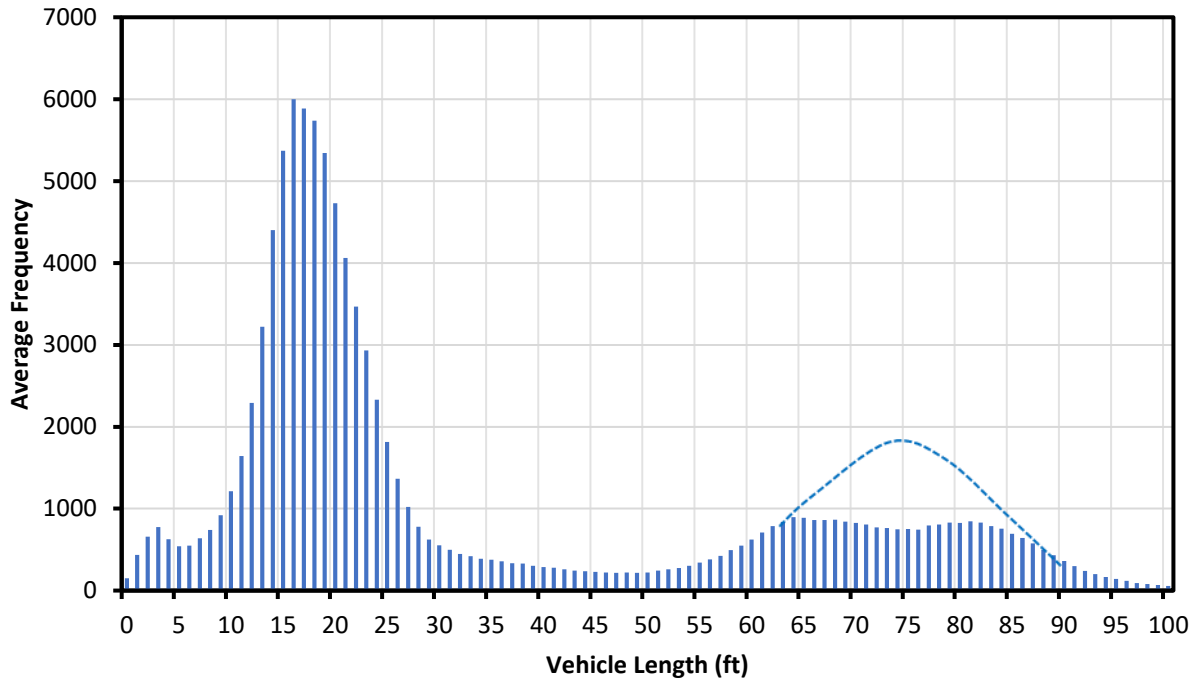


Figure 3-4: Volume-Weighted Vehicle Length Frequency Distribution

heavy trucks are defined. Single unit trucks will later be accounted for in coding the VISSIM model but were not significant to the data screening process. To account for sensor error and eliminate the possibility of falsely rejecting accurate values, the upper and lower bound lengths were conservatively defined as 99 feet and 5 feet, respectively. All records with values of length outside of these bounds were discarded for subsequent analyses not involving raw vehicle volumes. For example, when calculating free flow speed distributions, even vehicles with reasonable values of speed were not considered if their length was unreasonable.

Table 3-1: Vehicle Classification Bounds

	Mean (ft)	Standard Deviation (ft)	Lower Bound (ft)	Upper Bound (ft)
Passenger Cars	18.92	6.57	5.79	32.06
Heavy Trucks	72.57	11.14	50.29	94.85

3.3.2 Vehicle Speeds

The second data screening process that took place was the validation and filtering of vehicle speeds to be used in constructing free flow speed distributions. Like the screening of vehicle lengths, a multi-step procedure was performed to ensure that only valid speeds were included in the non-work zone and work zone desired speed distributions to be coded in VISSIM.

Specifically, three types of tests were used to eliminate erroneous records or those occurring under non-free flow conditions:

1. Threshold Screening: Given the sensor manufacturer’s specifications and site conditions, the upper and lower bound speeds were defined as 99 mph and 5 mph, respectively.
2. Statistical Screening: Speeds outside of two standard deviations from the mean speed for each 5-minute interval were discarded.
3. Density Screening: Only speed records occurring during intervals with a density of less than or equal to 11 passenger cars per mile per lane (pc/mi/ln; equivalent to LOS “A”) were considered. While not erroneous, these records were not applicable to modeling free flow speeds.

The number of records eliminated during each screening procedure are summarized in Table 3-2. The threshold and statistical tests left most of the data intact, eliminating only 14% of the records, and would be applied for other portions of VISSIM model development such as the construction of time headway distributions. Density screening eliminated an additional 27% of

all speed records, primarily from sensors 99, 103, and 104, where queueing was frequently observed and traffic flow was constrained even during marginal flow rates due to the presence of the lane closure. The speed-flow diagram for sensor 104 revealed a that there were still a few unusually low speeds remaining during periods of low flow and density, but these were found to minimally affect cumulative distribution curves and were retained.

Table 3-2: Vehicle Speed Screening Results

Sensor Group	Raw Data	After Threshold Screening		After Statistical Screening		After Density Screening	
	Records	Records Retained	Cumulative % Removed	Records Retained	Cumulative % Removed	Records Retained	Cumulative % Removed
96, 100 (3.5 Miles)	179,194	163,594	8.7%	155,099	13.4%	149,994	16.3%
97, 101 (2.5 Miles)	187,845	179,339	4.5%	170,747	9.1%	150,632	20%
98, 102 (1.5 Miles)	188,440	170,639	9.4%	162,914	13.5%	120,975	36%
99, 103 (0.5 Miles)	161,573	146,346	9.4%	117,132	27.5%	87,808	46%
104 (Lane Closure)	163,598	158,767	3.0%	151,773	7.2%	22,118	86%
<i>Total</i>	<i>880,650</i>	<i>818,685</i>	<i>7.0%</i>	<i>757,665</i>	<i>14.2%</i>	<i>531,527</i>	<i>41%</i>

Once only valid free flow speeds remained, desired speed distributions could be built and later applied in the VISSIM model. Given differences in driving behavior and vehicle performance, separate distributions were necessary for heavy trucks and passenger cars. However, single unit trucks were assumed to account for a negligible proportion of the traffic stream and follow the same speed distribution as passenger cars. Since each sensor was found to measure different truck length distributions, the lower bound length defining the cutoff between passenger cars/single unit trucks and heavy trucks was calculated independently for each, as summarized in Table 3-3.

Table 3-3: Vehicle Length Cutoff Values

Sensor	Mean Truck Length (ft)	Std. Dev. (ft)	Lower Bound Length (ft)
96	68	7	55
97	65	9	48
98	81	9	64
99	79	9	61
100	82	9	64
101	76	8	59
102	69	8	54
103	76	7	62
104	63	7	50
Weighted Average	73	11	50

Using these thresholds, a total of 18 speed distributions (nine sensors x two vehicle types) were constructed with the intent to use the weighted average of the eight upstream sensors for the non-work zone segment of the model and utilize the downstream sensor for the work zone segment. That said, observation of the lane-specific speeds upstream of the closure taper revealed that the mean speed of vehicles traveling in the left lane was much lower than that of those traveling in the right lane—a counterintuitive relationship. These findings are highlighted in Table 3-4, which shows this to be the case for the sensors 2.5 and 3.5 miles upstream of the lane closure. It was hypothesized that the portable changeable message signs shown in Figure 3-1 may have been responsible for higher-speed traffic merging into the right lane well ahead of the closure, but this theory could not be confirmed. As such, free flow speeds at sensors 98, 102, 99, and 103 were assumed to be most representative of speed behavior upstream of the lane closure and were adopted in VISSIM. These distributions are shown in Figure 3-5 and Figure 3-6. For brevity, the free flow speed distribution for sensor 104 will not be shown here, but will be described in section 3.4.

Table 3-4: Summary of Lane-Specific Mean Free Flow Speeds

Location	Vehicle Class	Sensor	Eligible Volume	Mean Speed (mph)
3.5 Miles Upstream	Passenger Cars	96	53924	71
		100	54738	81
	Trucks	96	6523	67
		100	34808	75
2.5 Miles Upstream	Passenger Cars	97	53851	64
		101	54102	72
	Trucks	97	8705	60
		101	33973	69
1.5 Miles Upstream	Passenger Cars	98	52797	79
		102	36452	63
	Trucks	98	12715	73
		102	19011	59
1/2 Mile Upstream	Passenger Cars	99	44730	78
		103	19278	72
	Trucks	99	13605	71
		103	10195	67
Downstream of Taper	Passenger Cars	104	13505	51
	Trucks	104	8613	48

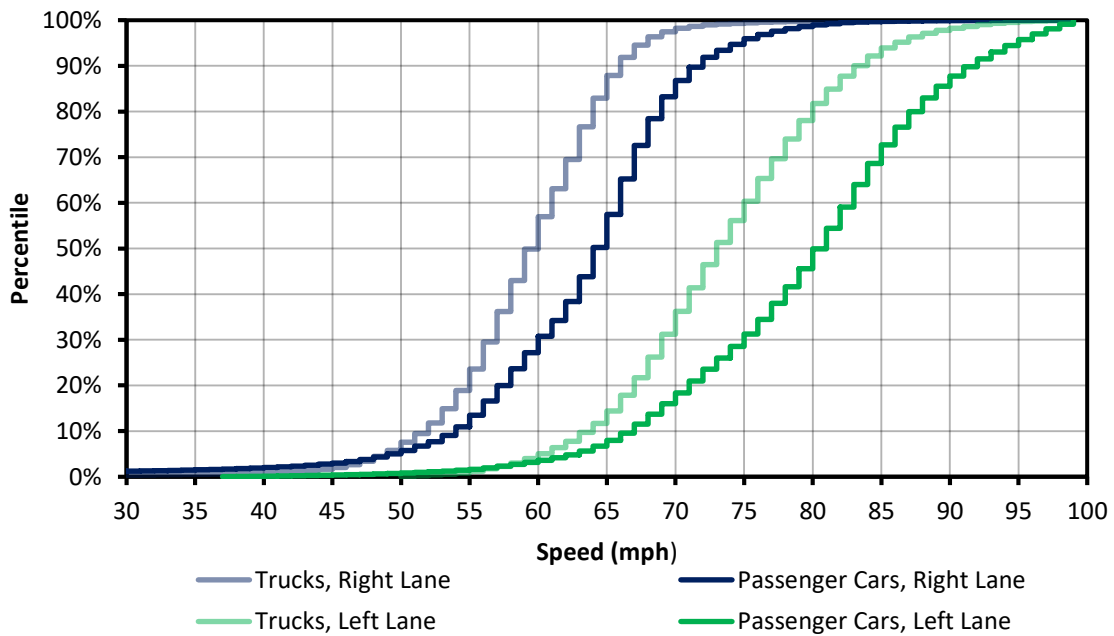


Figure 3-5: Upstream Free Flow Speed Distributions

The figure highlights a significant difference in speed by lane and vehicle type, reinforcing the need to include separate desired speed distributions for passenger cars and trucks and for the right and left lanes. Though a single, volume-weighted distribution could have been applied to both lanes in VISSIM, it was determined that the use of two distinct distributions would more accurately distribute fast- and slow-moving vehicles in the model. This conclusion was drawn based on the assumption that upstream lane distributions in the field reflected the desire of aggressive, fast-moving vehicles to travel in the left lane, while most heavy vehicles and slow-moving passenger cars traveled in the right lane.

3.3.3 Exploration of Field Data

Prior to developing and evaluating the VISSIM model, field data was examined so that typical traffic conditions could be characterized and understood. Since this research focused on studying the breakdown phenomenon at rural freeway work zones, time intervals just prior to and during congestion were of the most interest. Over the course of the data collection period, 12 major breakdown events were observed using a breakdown identification algorithm that required average speeds to be below 35 mph for at least 15 minutes. This algorithm was selected based on suggestions from the literature and the definition of breakdown in the HCM, which requires that speeds be maintained at least 25% below the free flow speed for at least 15 minutes.

The declaration of breakdown and recovery from breakdown both occasionally required the use of engineering judgement, particularly when prevailing speeds prior to sustained periods of congestion hovered near the threshold for several time intervals. A complete summary of every breakdown event at 5- and 15-minute aggregation intervals is provided in Appendix A, but an abbreviated synopsis is given in Table 3-5 to show the range of variation in PBC, QDR, and truck percentage for each congested period. From this point forward, a PCE of 2.0 (the default

for level terrain in the 6th edition of the HCM) was used in all volume conversions unless stated otherwise.

Table 3-5: Summary of Breakdown Events at Study Work Zone

	Maximum Pre-Breakdown Flow Rate (pcphpl)		Breakdown Flow Rate (pcphpl)		Average QDR (pcphpl)		% Trucks
	<i>15-Minute Intervals</i>	<i>5-Minute Intervals</i>	<i>15-Minute Intervals</i>	<i>5-Minute Intervals</i>	<i>15-Minute Intervals</i>	<i>5-Minute Intervals</i>	
	All	1161	1324	1115	1169	1049	
Left Side Closure	1125	1309	1065	1140	1035	1045	27%
Right Side Closure	1206	1342	1178	1205	1066	1060	22%
Minimum	1071	1256	989	802	936	990	16%
Maximum	1270	1392	1270	1338	1256	1256	32%

The table above was organized so that differences in traffic conditions could be highlighted for varying lane closure side, truck percentage, and aggregation interval. Several interesting findings were made that would ultimately drive subsequent decisions during model development and data analysis. For example, despite the study site having a TDHV of 26%, the proportion of heavy trucks in the traffic stream varied between 16% and 32% during the two hours prior to each breakdown event and throughout the duration of queue discharge. This can partially be explained by the fact that work zones are a source of non-recurring congestion and may cause queueing at any point throughout the day, during which truck percentage varies greatly. That said, one should still expect the truck percentage for the same hour to vary by a relatively large amount from day to day, so this finding was not surprising. Nonetheless, care was taken to ensure that an appropriate range of truck percentages were observable in VISSIM, even with static inputs for vehicle compositions, so that field conditions could be accurately replicated.

Regarding lane closure side, a stark difference in all three measures of throughput was observed between the right- and left-side closure. The maximum pre-breakdown flow rate, breakdown flow rate, and QDR were 7.2%, 10.6%, and 2.9% higher, respectively, when the right lane was closed if measured using 15-minute aggregation intervals. Figures 3-6 and 3-7 give another visualization of this trend by showing the approximate flow vs. density curve for each lane closure configuration, where the flow rate and density at capacity are both higher for the right-side lane closure. The fitted curves shown in the figure were developed based on Greenshields's model, which assumes the relationship between flow and density is parabolic. Even though small sample size made it difficult to discern how much of this difference was due to chance or exogenous factors, this finding helped reaffirm the decision to include lane closure side as a variable of interest in the final experiment.

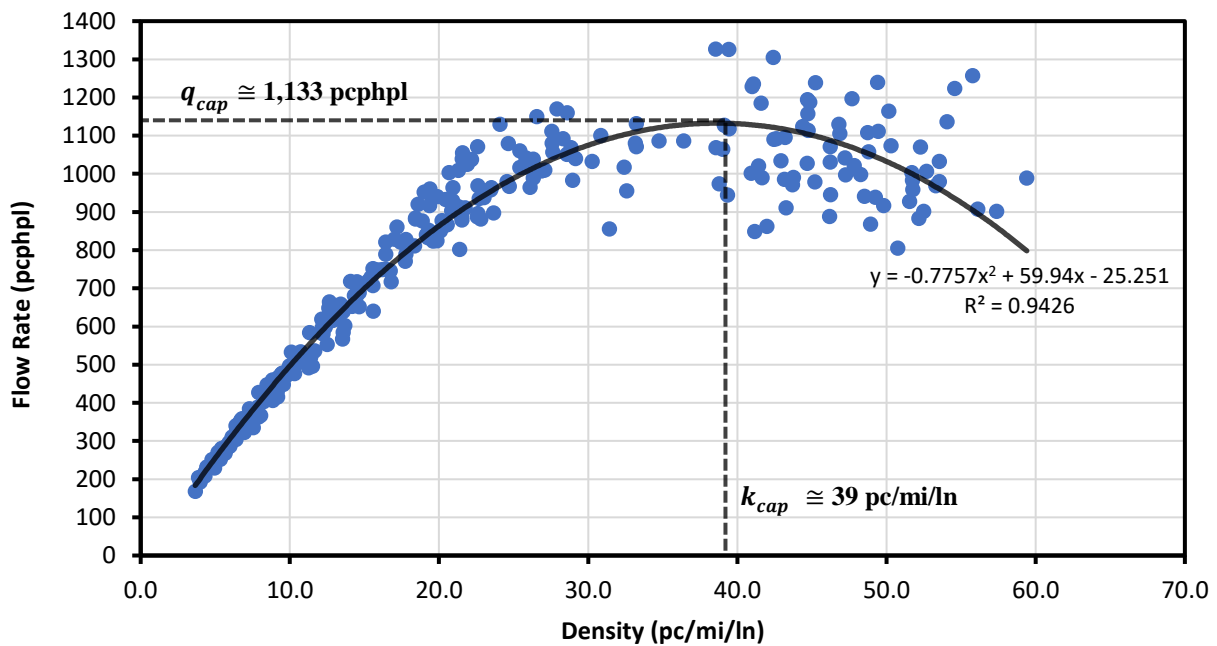


Figure 3-6: Flow vs. Density Curve (Left-Side Closure)

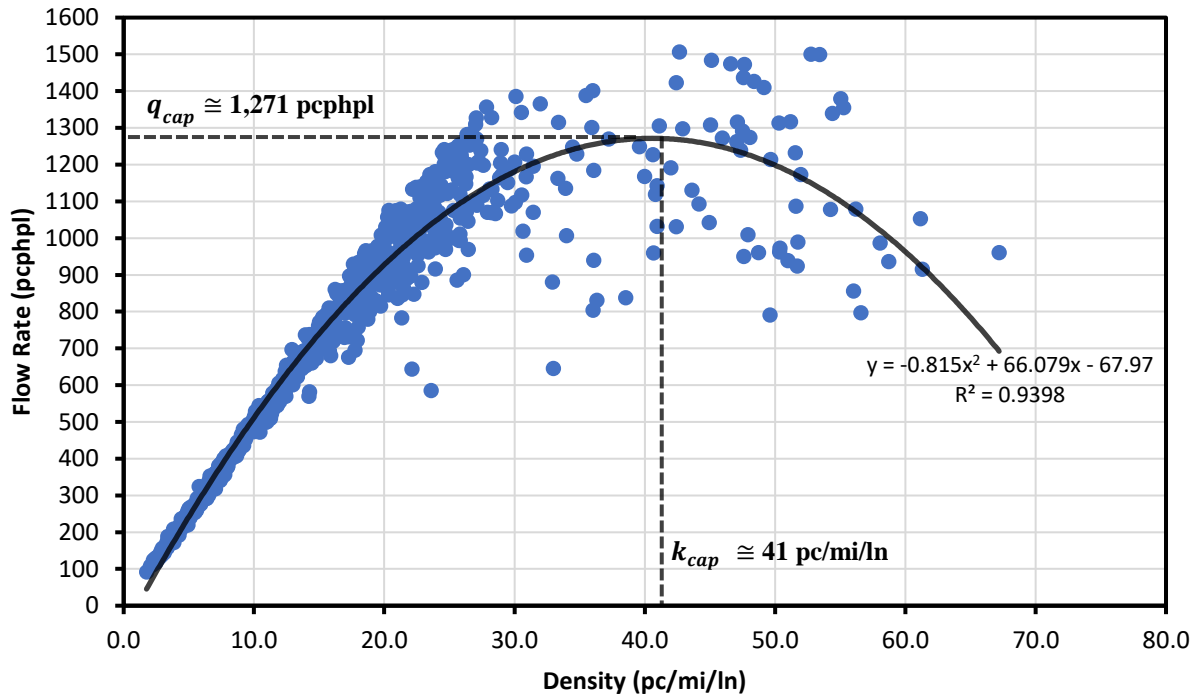


Figure 3-7: Flow vs. Density Curve (Right-Side Closure)

Lastly, it was found that the choice of aggregation interval had a significant effect on flow rates measured prior to breakdown, while queue discharge flow rates were relatively consistent between the two. This coincides well with findings from the literature review, where several authors noted that aggregation intervals smaller than 15 minutes will capture abrupt oscillations in traffic volume, which often consist of high flow rates sustained over short periods of time. Since traffic flow generally stabilizes in the presence of a queue, it is intuitive that there is less variation among 5-minute flow rates in these situations and that such volumes are approximately equivalent to their corresponding 15-minute flow rates. When formulating the factorial experiment in VISSIM, an aggregation interval needed to be selected, so a dilemma arose: from a research perspective, the use of 5-minute aggregation intervals would allow for more precision when declaring breakdown events and thus most accurately account for the effect

of the studied variables on work zone capacity. However, from a practical standpoint, agencies are most likely to have 15-minute volumes on hand, and such flow rates would more conservatively estimate breakdown probability distributions. Given the benefits of both options, it was decided that 5- and 15-minute aggregation intervals would both be explored and compared, as will be discussed in Chapter Four.

3.4 VISSIM MODEL DEVELOPMENT

After screening, processing, and aggregating the field data, the traffic inputs for a base VISSIM model could be developed. In addition to the sources cited within the literature review previously, microsimulation guidelines from several state DOTs including Florida, Oregon, Washington, and Virginia were utilized to help inform coding and calibration decisions (Dowling et al. 2004; Florida Department of Transportation 2014; Park and Won 2006; Washington State Department of Transportation 2014). Though the guidance provided by past work zone simulation case studies and sensitivity analyses provided a starting point from which to work, characteristics of the work zone used to calibrate the model in this study required many of the software's default parameters to be adjusted manually. This section will discuss setup of basic VISSIM network geometry, selection of volume inputs, fine-tuning of desired speed distributions, modification of key truck characteristics, and construction of time headway distributions.

3.4.1 Basic Network Coding

The first step in generating the work zone simulation network was coding basic geometric elements such as links, connectors, and their respective lengths and widths. Using the Bing Maps interface within VISSIM, it was possible to draw the entire network to scale with a high degree

of accuracy. Once drawn, the network was inspected to make sure that link lengths and lane widths matched those measured in the field and that other key components such as static routing decisions, desired speed decisions, and data collection points were at their ideal locations. It should be noted that despite having data from field sensors at 3.5 miles upstream of the lane closure, the VISSIM network began 2.5 miles upstream, primarily due to the volume measurement error for sensors 96 and 100 mentioned in Section 3.2. A simple drawing of the network is provided in Figure 3-8, which was sketched outside of the VISSIM software and does not include representation of the horizontal curvature found in the field.

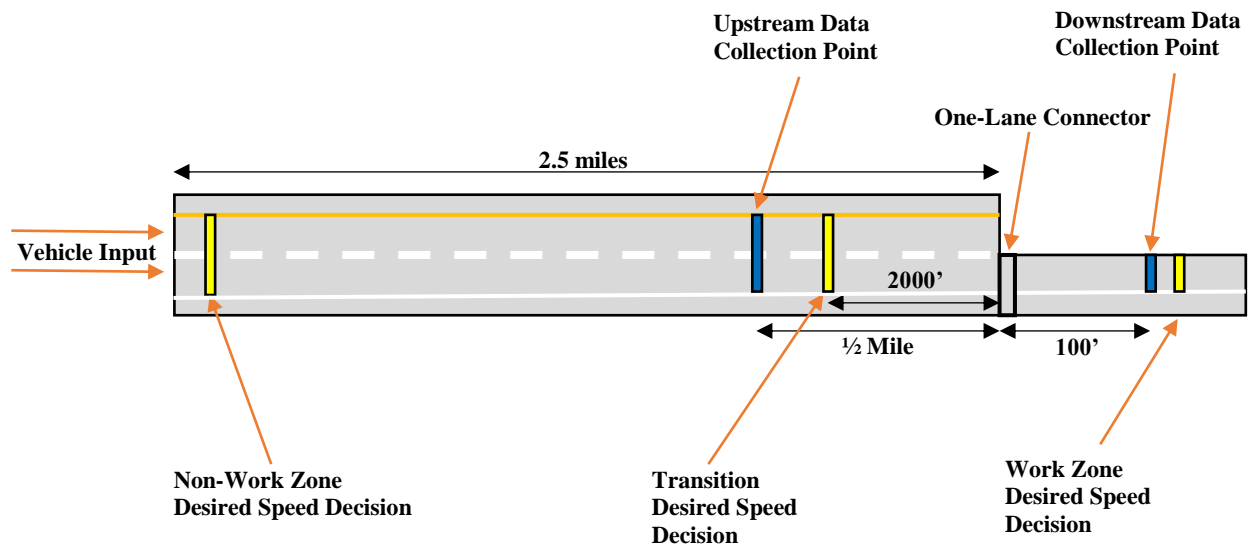


Figure 3-8: Diagram of VISSIM Network (drawing not to scale)

As noted previously, the location of TTC devices in the field played a key role in the network setup process. Referring to Figure 3-1, the “transition” desired speed decision point pictured above was included so that the model could replicate the effects of the drop from a speed limit of 70 mph to a speed limit of 60 mph 2000 feet upstream of the lane closure. The “___ Lane Closed 1/2 Mile” sign in the field also motivated the decision to set the lane-changing distance upstream of the one-lane connector to 3000 feet, where it was anticipated that drivers could first visualize this sign. The last notable component of the diagram is the placement of data

collection points at ½ mile upstream and 100 feet downstream of the lane closure. The former would be used in the calibration process to verify upstream speeds and queue propagation, while the latter would be used to detect breakdown events, measure queue discharge flow rates, and gather average vehicle speeds within the work zone during each simulation run. Each of these components will be discussed in greater detail in the sections that follow, as extensive thought was involved in most model development decisions.

3.4.2 Volume Inputs and Traffic Stream Composition

The breakdown events summarized in Table 3-5 revealed a high amount of variability in the field data, so it was desired to develop a calibrated VISSIM model from a day representing typical conditions at the study work zone. After examining the full dataset, it was determined that traffic characteristics on October 3rd were the most representative, so volume inputs and relative vehicle class proportions were extracted from that day's data. Figure 3-9 provides a plot of 15-minute average speed and flow versus time on October 3rd and shows that a significant breakdown event was observed from approximately 1:45PM to 6:30PM. Available microsimulation guidance suggests that periods of congestion should be modeled with uncongested time intervals at the beginning and end of the study period to produce realistic results, so the model was coded to run from 11:45AM to 8:00PM. An additional 15 minutes from 11:45AM to 12:00PM was included despite not having field data for these intervals as a warm-up period to allow the model to reach equilibrium. Since literature has shown that freeway segments change state from stable flow to breakdown in brief time increments (Elefteriadou et al. 1995), 5-minute input volumes were coded in VISSIM to capture the same oscillations in traffic demand that were observed in the field.

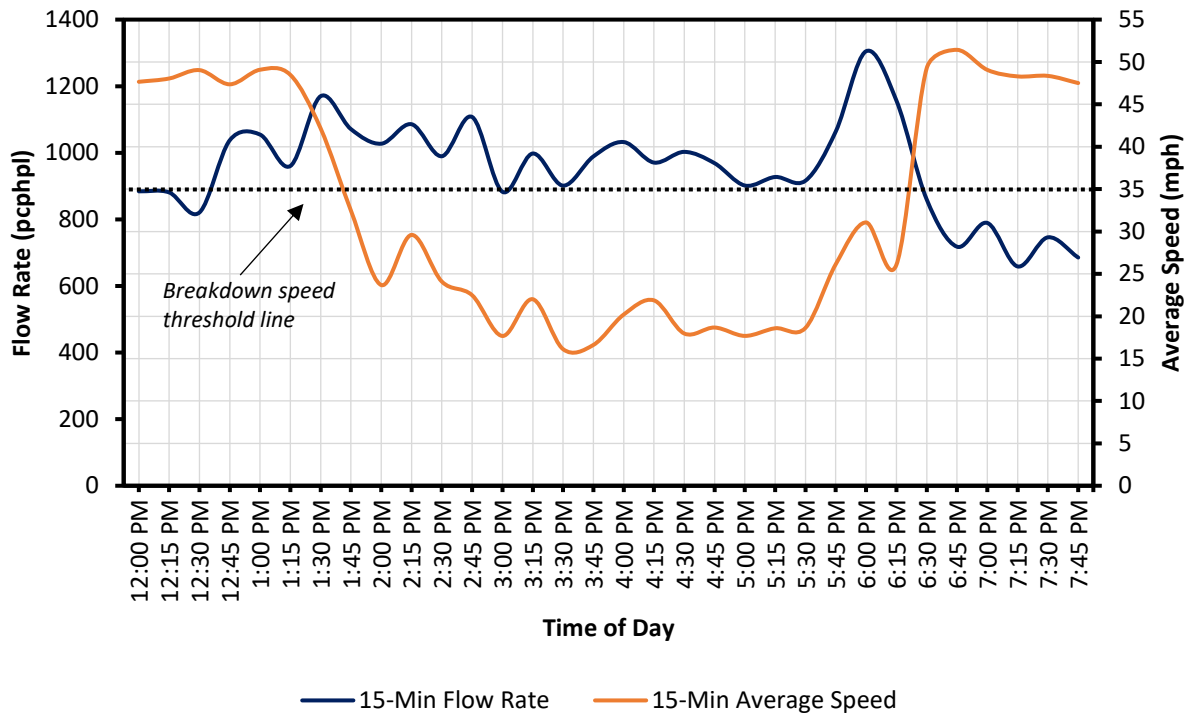


Figure 3-9: Speed and Flow vs. Time on October 3rd, 2016

As discussed earlier, the proportion of each vehicle class in the traffic stream was crucial for replicating field conditions, since heavy vehicles perform differently than passenger cars and queue length is sensitive to vehicle lengths. To account for sensor error and capture the actual percentage of heavy vehicles measured in the field during each time interval, the screening thresholds set in Section 3.3.1 were adopted to reduce the full set of raw vehicle records to a set of “classified” records from which proportions of vehicle classes would be determined. The number of trucks in each time interval were counted using the lower bound lengths of each sensor as defined in Table 3-3, then divided by the “classified” volume to calculate a best estimate of the truck percentage during each 5-minute interval. Finally, this percentage was multiplied by the raw volume of vehicles observed to obtain an adjusted truck volume for use in calculating passenger car equivalent flow rates. The same process was applied for 15-minute

interval data, as these flow rates would eventually be used as a measure of calibration. The results of this process are exemplified in Table 3-6.

Table 3-6: Example of Adjusted Truck Volumes

Time	Raw Volume	Raw Truck Volume	Classified Volume	% Trucks	Adjusted Truck Volume	Adjusted Flow Rate (pcphpl)
1:30:00 PM	75	19	69	28%	21	1148
1:35:00 PM	65	16	61	26%	17	985
1:40:00 PM	94	20	90	22%	21	1379
1:45:00 PM	71	6	68	9%	6	927
1:50:00 PM	73	14	70	20%	15	1051
1:55:00 PM	80	22	77	29%	23	1234
2:00:00 PM	67	13	60	22%	15	978
2:05:00 PM	61	17	58	29%	18	947
2:10:00 PM	83	13	80	16%	13	1158
2:15:00 PM	63	14	63	22%	14	924
2:20:00 PM	81	23	80	29%	23	1251
2:25:00 PM	78	12	77	16%	12	1082
2:30:00 PM	63	8	61	13%	8	855

The percentage of single unit trucks for each time interval was calculated using a similar procedure, where the length bounds for such vehicles were determined from the upper bound passenger car lengths and lower bound truck lengths for each individual sensor. The reader may refer to Table 3-3 and to Appendix A to see how these values were determined, but in general, single unit trucks were classified as vehicles 25-50 feet in length. The relative proportion of each vehicle class is given in Table 3-7, along with the static, rounded length assigned to each. It was assumed that defining multiple classes of vehicles within passenger cars, trucks, and single unit trucks to account for a finer distribution of lengths was not necessary, and those included in the table were believed to produce nearly identical results in the model.

Table 3-7: Base VISSIM Model Vehicle Composition Input

Vehicle Class	Relative Proportion of Traffic Stream			Length (ft)
	Right Lane	Left Lane	Total	
Passenger Cars	54%	71%	62%	16
Heavy Trucks	37%	12%	26%	74
Single Unit Trucks	9%	17%	12%	32

3.4.3 *Desired Speed Distributions*

The desired speed decision points pictured in Figure 3-9 were initially coded to match field-calculated distributions, such as those shown in Figures 3-5 and 3-6. In fact, the “transition” speed decision was omitted at first, and two desired speed distributions were applied—non-work zone and work zone. However, pilot simulation runs conducted at low input volumes revealed that speeds measured at the downstream data collector were approximately 10-20 mph higher than indicated by the field data under free flow conditions. As mentioned earlier, inspection of project traffic control reports revealed that there was a 60-mph reduced speed limit in place upstream of the closure for the duration of the work, so an additional desired speed decision point was added at this location. Since none of the sensors measured speeds between the speed limit change and the beginning of the lane closure, a representative speed distribution was built with a mean of 62 mph and standard deviation equal to that of upstream conditions. Trial and error in VISSIM revealed that these specifications produced speeds closest to those observed in the field at the bottleneck. Each of the three distributions were coded in VISSIM using the 10th, 25th, 35th, 50th, 75th, 85th, and 95th percentile speeds and are presented in Table 3-8.

Table 3-8: VISSIM Desired Speed Distributions

Speed Distribution	Vehicle Class	Mean Speed (mph)	Percentile						
			10 th	25 th	35 th	50 th	75 th	85 th	95 th
Non-Work Zone (Right Lane)	Passenger Cars	65	59	65	68	71	76	78	83
	Trucks	60	57	61	63	65	69	70	74
Non-Work Zone (Left Lane)	Passenger Cars	79	65	73	76	80	88	91	97
	Trucks	72	62	66	69	72	77	80	86
Transition (All Lanes)	All	62	53	57	60	62	67	68	73
Work Zone (All Lanes)	Passenger Cars	51	42	46	48	51	55	59	64
	Trucks	48	42	44	46	47	51	53	55

The complete free flow speed distributions for every sensor are provided in Appendix A, where one will note that the percentile values for the non-work zone distributions do not match those for any one sensor. Instead, the desired speed distribution upstream of the work zone was calculated from a weighted average of sensors 98, 99, 101, and 102. Additionally, the right-lane non-work zone speed distribution percentiles each had to be increased by 5 mph to replicate field-measured speeds in VISSIM. Even with such adjustments, it will be seen in a later section that the model could not be calibrated to match speeds perfectly, which literature has cited as a limitation of VISSIM (Kan et al. 2014). Nonetheless, the distributions above were deemed adequate since the results of this study were intended to be generalizable and prevailing speeds will vary between work zone sites.

3.4.4 Modification of Key Truck Characteristics

The components detailed in the previous three sections were combined with default driving behavior parameters in VISSIM and the initial performance of the model was evaluated. After further research, it was found that the default power, weight, and acceleration distributions for heavy trucks in VISSIM are not representative of the U.S. truck fleet, but rather of the lighter and

faster trucks found in Europe (Edara and Chatterjee 2010; Harwood et al. 2003; PTV Group 2017). By modifying truck acceleration capabilities to reflect those of the U.S. fleet, it was found that congestion could be modeled at much more reasonable values of other calibration parameters, so assigning proper truck characteristics warranted further investigation.

First, potential sources of accurate truck weight distributions were explored. Fortunately, a past study by Turochy, Timm, and Mai applying weigh-in motion (WIM) data from ALDOT infrastructure revealed that there is a WIM station (ID 918) on I-59/I-20 at MP 100.0, just 30 miles north of the study work zone (Turochy et al. 2015). Data from this station was imported into Microsoft Access, where a weight distribution was calculated and exported to VISSIM. The power distribution for U.S. trucks was generated by assuming an average value of 328 horsepower, which matches that provided in NCHRP Report 505 for interstates in the eastern United States (Harwood et al. 2003). Table 3-9 compares the default weight and power distributions for heavy trucks in VISSIM to those applicable to the southeastern U.S. truck fleet and shows only a slight difference between the two. However, since truck power-to-weight ratios define maximum truck acceleration in VISSIM, they are critical to accurately modeling scenarios with a high percentage of trucks in the traffic stream.

Table 3-9: Comparison of Truck Power and Weight in VISSIM

Percentile	Weight (lb), Default	Weight (lb), Adjusted	Power (kW), Default	Power (kW), Adjusted
0 th	6,174	13,402	150	168
5 th	10,275	29,831	163	171
25 th	26,681	41,890	213	208
35 th	34,883	47,483	238	221
50 th	47,187	57,620	275	256
75 th	67,694	70,203	338	282
85 th	75,896	72,825	363	303
95 th	84,099	76,146	388	387
100 th	88,200	115,819	400	406

Conversely, there is a dramatic difference between the default truck acceleration curve in VISSIM and that of typical U.S. interstate semitrailers. Researchers at TTI found this to be the case in a 2006 study, but chose not to modify default values in VISSIM due to a lack of recent truck performance data (Middleton et al. 2006). A 2016 study of truck standstill acceleration at ramp meters in Florida, however, contended that the acceleration capabilities of heavy trucks in the U.S. have not improved much over time and provided detailed, updated curves for trucks with various weight-to-power ratios (Yang et al. 2016). To further justify the modification of these values in VISSIM, the truck acceleration curves in CORSIM were checked and found to align with those in the literature, as shown in Figure 3-10. Specifically, the acceleration curves for medium-loaded and fully-loaded tractor-trailers is represented by performance indices 5 and 6 (PI 5 and PI 6), where acceleration values from a standstill are just above 2 ft/s².

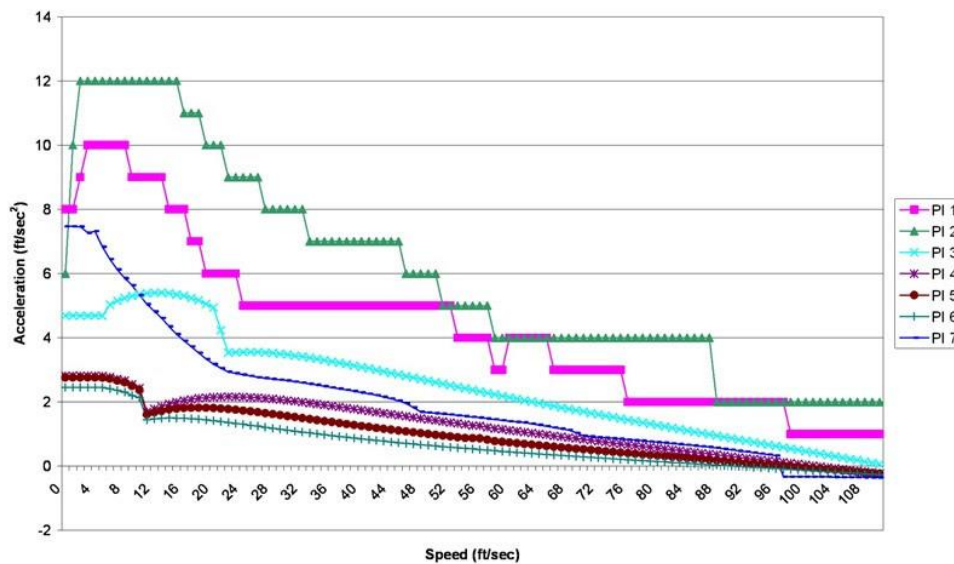


Figure 3-10: CORSIM Vehicle Acceleration Curves (Source: FHWA)

In VISSIM, the acceleration curve for trucks starts at 8.2 ft/s², which is nearly equivalent to that used for buses in CORSIM. Therefore, starting acceleration values between 2 and 3 ft/s², followed by a decreasing function similar to that in Figure 3-10, were evaluated in VISSIM through trial and error until the most appropriate distribution was settled on. Figure 3-11 compares the default desired acceleration function in VISSIM with that developed from literature review and calibration to illustrate the disparity between the two.

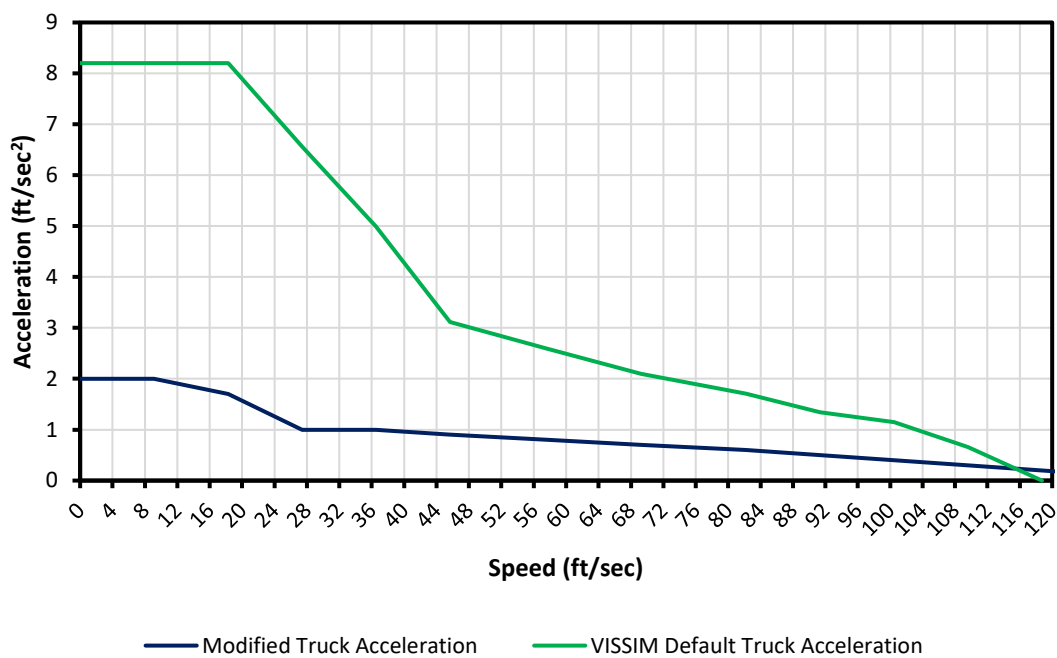


Figure 3-11: VISSIM Default vs. Calibrated Truck Acceleration

When comparing Figure 3-10 and Figure 3-11, it may be noted that the modified truck acceleration curve used in VISSIM is slightly more conservative than that used in CORSIM. Review of the VISSIM User’s Manual led to the finding that minimum and maximum acceleration values can be set at each speed, where the power-to-weight ratio of the heavy vehicle determines the exact value modeled (PTV Group 2017). Therefore, while the graph reflects only the mean acceleration at each speed value, maximum values were set that match

more closely to the values in Figure 3-10. Furthermore, acceleration curves closer to the default in VISSIM were initially tested but determined not to replicate field speeds and flow rates without modifying other driving behavior parameters beyond reason. Lastly, the aforementioned work by Yang et al. in 2016 yielded a mean and 85th percentile standstill acceleration of 1.93 ft/s² and 2.24 ft/s², respectively, for heavy trucks. Since this was found to be the most recent vehicle performance study conducted to date, the values applied in VISSIM were thought to be reasonable and accurate.

3.4.5 Time Headway Distributions

Finally, the parameter found most critical to model development was desired time headway. Given that headway is the inverse of traffic flow, it is not surprising that sensitivity analyses have typically concluded that the corresponding value of CC1 in VISSIM is the most influential in determining modeled throughput. Despite this, literature review of calibration methodology showed that many analysts select candidate values of time headway and other driving behavior parameters at random, then simply choose the values that best replicate field conditions. While this may produce valid data for a specific site and time period, it does not adequately capture the randomness of traffic flow and inherent variability that would be observed at a single site over time. Dong et al. noted this issue in a 2015 report and proposed that time headway parameters in microsimulation models be set based on field distributions if available (Dong et al. 2015). Such methodology would eliminate combinations of model parameters that may reproduce field conditions only with infeasible values of time headway, while also potentially reducing the time required for calibration.

The same study measured vehicle class-separated time headway and standstill distance on Iowa highways and found that both values depend on vehicle following pairs. Specifically,

passenger cars were found to maintain shorter headways in general than heavy vehicles, but also maintained longer headways when following tractor-trailers. Several other studies have been conducted in the past and drawn similar conclusions, suggesting that traffic flow can be modeled more accurately if separate headway distributions are constructed for passenger cars and heavy vehicles (Houchin 2015). Despite the validity of these claims, field-calculated headway distributions could not be modeled in VISSIM prior to version 9, as the value of CC1 was static. Consequently, this thesis is believed to be one of the first work zone simulation studies to apply stochastic, vehicle class-specific headway distributions measured from field data.

Like the calculation of speed distributions, constructing time headway distributions required significant filtering of the data. Unlike for speed data, however, headway calculations were only valid if the order of vehicle records was maintained. To ensure that this condition was not violated, the data was not sorted or deleted during the entire process. Rather, several indicator columns were populated to designate whether a specific following pair was to be considered in developing headway distributions. Using traffic flow theory principles and the data screening procedure detailed in Section 3.3, three screening tests were created to determine if a given headway value was valid:

1. *Speed Screening*: Only following pairs where the speed of both vehicles was greater than 5 mph, less than 100 mph, and within two standard deviations of the average speed for a given 5-minute time interval were considered.
2. *Length Screening*: Both vehicles in a following pair were required to have lengths greater than 5 ft and less than 100 ft.

3. Flow Screening: To ensure that a following vehicle's choice of speed was constrained by a leading vehicle, only time intervals with flow rates greater than or equal to 1,000 pcphpl were examined.

This procedure was executed only for data from sensor 104, as it was expected that driving behavior within the work zone would be different from that upstream due to the changes in roadway environment. After applying the three tests listed above, approximately 65,000 vehicle following pairs remained and were used to calculate time headway distributions for each vehicle class. Initially, however, it was discovered that large headways greater than 6 seconds were unusually common at low following speeds. Further investigation led to the hypothesis that longer headways were measured for trucks when following passenger cars due to differences in vehicle acceleration capabilities. Thus, vehicles with speeds less than 35 mph (the speed threshold later used to determine the onset of breakdown) were ultimately excluded from headway analysis to eliminate this potential scenario.

Histograms of time headway for passenger cars and trucks at the study work zone are provided in Figures 3-12 and 3-13, where a clear difference may be observed between the two distributions. Interpretation of these graphs and the final VISSIM input require understanding of two main ideas: (1) the sequential data collected by sensors in this study measured the arrival time of vehicles to the nearest whole second, so analysis at finer increments was not possible; (2) the CC1 parameter in VISSIM is a portion of the desired safety distance between a lead and following vehicle, which is measured from front bumper to rear bumper, rather than front bumper to front bumper. As shown in Figure 3-14, this value is also shortened by the value of the standstill distance, CC0. That said, it was assumed that the distributions shown in the figures would need to be reduced by several tenths of a second to accurately reproduce field conditions.

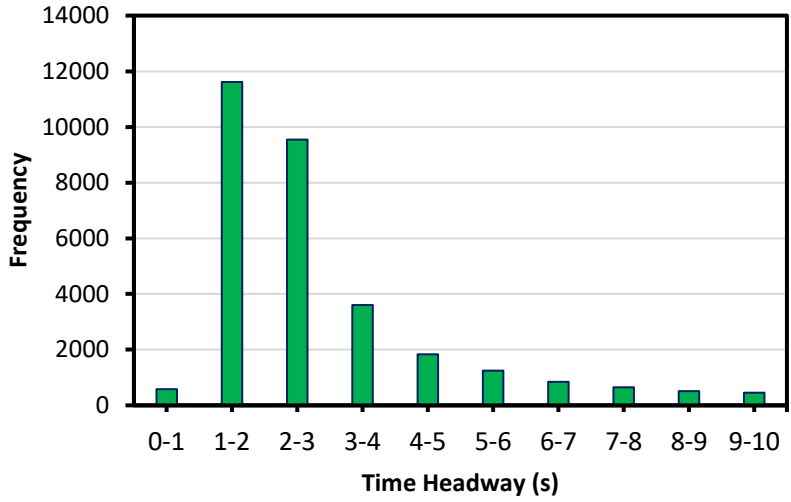


Figure 3-12: Field Headway Distribution (Passenger Cars)

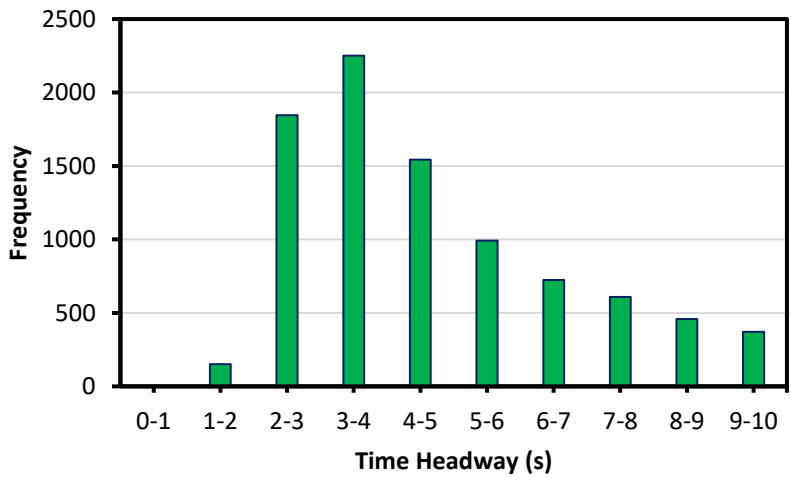


Figure 3-13: Field Headway Distribution (Trucks)

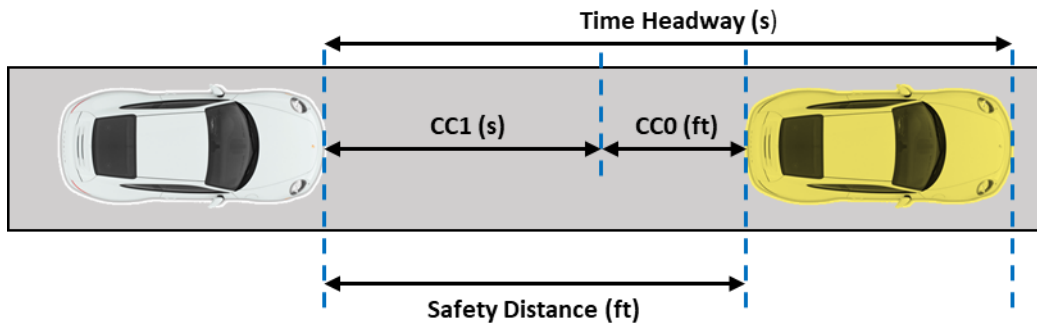


Figure 3-14: Desired Safety Distance in VISSIM

The last step in developing appropriate headway input for VISSIM was reducing the distributions shown in the figures to a set of reasonable values. For example, even at high flow rates, a headway of 10 seconds between two vehicles is likely due to circumstances beyond the selection of such a distance by drivers. Although literature has suggested typical maximum desired headways of 4-6 seconds, the field data was further scrutinized to set this threshold. For both passenger cars and trucks, the difference between successive headway intervals was plotted to observe the point at which no meaningful change in frequency occurred. These graphs are given in Figures 3-15 and 3-16.

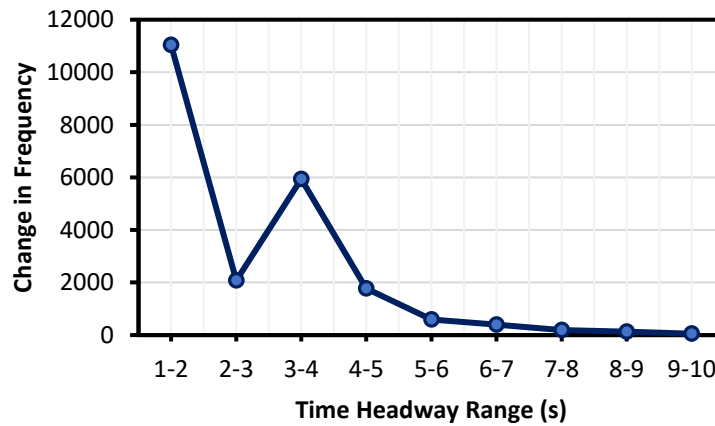


Figure 3-15: Change in Headway Frequency (Passenger Cars)

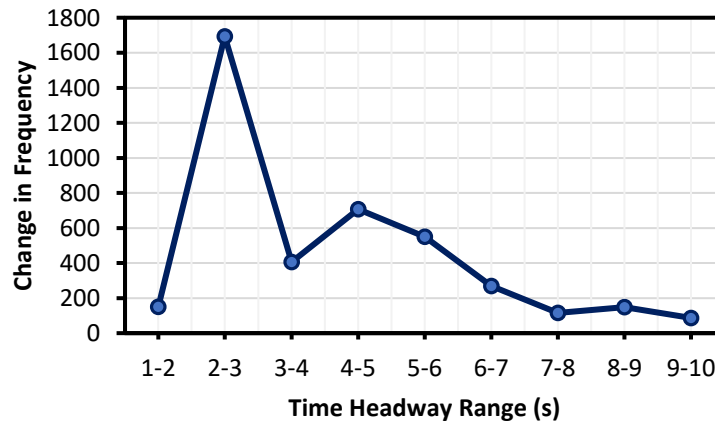


Figure 3-16: Change in Headway Frequency (Trucks)

Based on the figures, the maximum desired headway ranges used in VISSIM were 5-6 seconds and 6-7 seconds for passenger cars and trucks, respectively. In model calibration, each point on these distributions was reduced uniformly to consider the portion of desired safety distance accounted for by vehicle length and standstill distance. It was determined that doing so would change measures of central tendency without changing the variances of the distributions. Table 3-10 summarizes the initial headway distributions applied in VISSIM for the CC1 parameter, while calibrated values will be discussed in the next section.

Table 3-10: VISSIM Input Desired Headway Distributions

Headway (s)	Passenger Cars		Trucks	
	Frequency Below	% Below	Frequency Below	% Below
1	577	1%	0	0%
2	11618	43%	151	2%
3	9545	76%	1845	27%
4	3607	89%	2251	57%
5	1835	96%	1543	77%
6	1246	100%	993	90%
7	--	--	724	100%

3.5 CALIBRATION AND VALIDATION

Even when field geometry, volume, and speed data are carefully entered, simulation models may not acceptably replicate field conditions if default vehicle characteristics and driving behavior parameters are used. Accordingly, these parameters must be iteratively modified until the model is deemed to be reasonably calibrated. After achieving calibration, it is common practice to validate a simulation model using independent data from the same site to test its predictive abilities. While this process is often the most time-consuming part of developing microsimulation models, it is paramount to producing realistic outputs and drawing meaningful conclusions. This section describes the procedure used to evaluate the base VISSIM model

described in Section 3.4, define and modify significant input parameters, and validate the calibrated parameter set against field-collected measures of effectiveness (MOEs).

3.5.1 Calibration Methodology

Since the end users of a potential tool developed from this thesis are agencies and practitioners, guidance was taken from typical reference material prepared by and for these groups. As mentioned in the previous section, these sources included the FHWA Traffic Analysis Toolbox, reference manuals from state DOTs, and literature specific to freeway work zones (Dowling et al. 2004; Florida Department of Transportation 2014; Park and Won 2006; Washington State Department of Transportation 2014). Such methodology involves generating a reasonable number of calibration parameter combinations and choosing the set of values that best matches to field-collected MOEs. However, the time required for calibration can quickly balloon if parameters are not selected carefully and objectives are not well-defined.

To maximize efficiency, the literature generally suggests that the following steps be followed when calibrating microsimulation models:

1. Define calibration objectives: Select at least two MOEs (e.g. throughput, travel time, speed) that may be used to compare simulation outputs to field data. Define an acceptable amount of deviation from field data using statistical measures such as root mean square normalized error (RMNSE) or mean absolute percentage error (MAPE).
2. Perform multiple simulation runs with the default parameter set: Verify that the model is not adequately calibrated with default parameters.
3. Select Calibration Parameters: Determine which parameters are most significant to the calibration objectives. The number of remaining parameters should be minimized.

4. Determine Feasible Range of Values: Use pilot simulation runs to determine the range of values that should be explored for each parameter.
5. Search for Optimal Parameter Set: Iterate with each parameter set, collect MOEs, and choose the combination that best reproduces field data.
6. Fine-Tune: Visually inspect the simulation animation and make minor changes as necessary to ensure realistic driving behavior and best match outputs to field conditions.

The six steps listed above were adhered to throughout calibration to minimize the effort necessary to achieve a satisfactory model. Based on the variability observed in the field data, sensor error, and past practice in literature, modest calibration objectives were set. Since most analyses performed by researchers and practitioners are conducted for facilities with recurring sources of congestion, it was expected that calibrating to a non-recurring source of congestion such as a work zone would be challenging. Therefore, the objectives summarized in Table 3-11 were found acceptable for this research.

Table 3-11: Calibration Objectives

Measure of Effectiveness	Measurement Location	Calibration Metric(s)
15-Minute Average Speed (mph)	Lane Closure (Sensor 104)	RMSNE < 0.20 MAPE < 20%
Mean Queue Discharge Rate (pcphpl)	Lane Closure (Sensor 104)	Within 10% of Field Value
Queue Propagation and Dissipation	1/2 Mile Upstream (Sensors 99, 103)	Qualitative

The findings from the literature and early experimentation in VISSIM indicated that the most significant parameters to replicating the congested conditions observed in the field were CC0, CC1, CC2, SRF, lane-changing distance, and desired acceleration for heavy vehicles (the reader may refer to Chapter Two for definitions of these parameters). As such, the calibration effort focused on modifying these six variables until model performance was acceptable.

However, even six changeable parameters were thought to be excessive, so strategies were developed to reduce the number of candidate variables and the ranges of their values. First, though many have found the CC2 parameter to be influential to modeled throughput, guidance from literature and pilot simulation runs suggested that more realistic driving behavior could be observed by holding this value at its default of 13.12 feet (Washington State Department of Transportation 2014). Second, the SRF is highly dependent on the value of the lane-changing distance, which was held constant at 3000 feet, so this value was also held static at its default value of 0.60.

This logic reduced the final set of calibration parameters to CC0, CC1, and desired truck acceleration. Though the latter two parameters were initially modified as outlined in Sections 3.4.4 and 3.4.5, it was expected that additional changes would be necessary before reaching calibration. For example, it was noted earlier that the time headways calculated from field data would likely need to be reduced since a portion of time headway in VISSIM is accounted for by the standstill distance and following variation parameters. For desired truck acceleration, six candidate distributions were developed based on literature review and intended to bracket typical values with mean standstill acceleration between 2 and 3 ft/s². Finally, the range for CC0 was based on anecdotal experience and field-measured values from a study in Iowa (Dong et al. 2015; Houchin 2015). Table 3-12 shows the ranges and search increments explored for each parameter, where the empirical distribution referenced for CC1 corresponds to the values found in Table 3-10.

Table 3-12: Calibration Parameter Ranges

Parameter	Default	Feasible Range (Literature)	Explored Range	Increment
CC0 (ft)	4.92	> 4.92	8 - 16	2
CC1 (s)	0.9 ^b	0.9 - 4.0 ^b	Empirical distribution reduced by 0.1 – 0.7	0.1
Desired Truck Acceleration (ft/s ²) ^a	8.2	< 8.2	2.0 - 3.0	0.2

^aMean acceleration from a standing start

^bStatic values

3.5.2 Calibration Results

If every possible combination of the three parameters in Table 3-12 was checked, the result would be 210 unique cases (five values of CC0 x seven time headway distributions x six desired truck acceleration distributions), which would require extensive effort. Fortunately, since each parameter is potentially correlated with the others, several extreme scenarios could be eliminated. For example, high values of CC0 and low values of desired truck acceleration were not necessary for the model to produce congestion like that observed in the field when paired with longer time headways. Conversely, if smaller values of CC0 or larger values of desired truck acceleration were used, longer time headways could be applied. Initially, five simulation runs were conducted for each candidate parameter set to identify a shorter list of combinations that should be examined further. Once the list had been narrowed, it was necessary to calculate the number of simulation runs required to be statistically confident in model outputs using equation 3-1 (Washington State Department of Transportation 2014).

$$N = \left(\frac{2 * t_{1-\frac{\alpha}{2}, N-1} * S}{CI_{1-\alpha\%}} \right)^2 \quad (3-1)$$

Where:

N = number of required repetitions

$t_{1-\alpha/2, N-1}$ = t-statistic at a confidence level of $1-\alpha$ and $N-1$ degrees of freedom

s = standard deviation of model outputs

$CI_{1-\alpha\%}$ = *confidence interval for the true mean of a given parameter*

For the purposes of calibration, the mean QDR was chosen as the determining metric for calculating the required number of repetitions. Multiple simulation runs yielded a sample standard deviation of 70 pcphpl, so at a 95% confidence level, a minimum of 10 runs was required to estimate the mean QDR to within 10% of the field data. Other metrics were not examined as carefully because it was hypothesized that traffic flow is too variable to expect a high degree of precision and consistency in modeled speeds and queue lengths. Nonetheless, to best capture fluctuations in the onset of breakdown between simulation runs, the number of repetitions was increased to 20.

The final parameter set is presented in Table 3-13, and plots of speed vs. time for the field data, default VISSIM model, and calibrated VISSIM model are compared in Figure 3-17. The slight difference between the calibrated model outputs and field measurements supports the theory proposed previously, as it was not possible to match queue duration and speeds more so than what is shown in the figure. Particularly, the sharp drop in speed signaling the onset of breakdown was consistently observed too soon in the model, suggesting that simulated traffic may not be able to absorb brief spikes in volume as real traffic does in the field. That said,

observation of speed differentials showed that the greatest discrepancy actually existed later in the simulation period. Since traffic flow characteristics well after the occurrence of breakdown were not relevant to research objectives, only average speed and QDR data from 12:00PM to 3:30PM were required to meet calibration objectives. A similar truncated time window would be examined for data from October 6th during the validation phase for the purposes of consistency.

Table 3-13: Calibrated Driving Behavior Parameters

Parameter	Description	Default Value	Calibrated Value
<i>Car-Following Parameters</i>			
CC0	desired standstill distance	4.92 ft	10 ft
CC1	desired time headway	0.9 s	Empirical Distribution with 0.35 s subtracted ^a
CC2	additional distance over desired safety distance	13.12 ft	Default
CC3 - CC9	--	--	Default
<i>Lane-Changing Parameters</i>			
Lane-Changing Distance	distance upstream of a required lane change that drivers will begin looking for gaps to merge	656.2 ft	3000 ft
SRF	safety distance reduction factor	0.6	Default
Cooperative Braking	check box (yes or no)	No	Yes
Maximum Deceleration for Cooperative Braking	maximum accepted deceleration when braking cooperatively	-9.84 ft/s ²	-20 ft/s ²
Waiting Time Before Diffusion	maximum waiting time before vehicle removed from network	60 s	200 s
All others	--	--	Default

^aSee Table 3-10 for original empirical distribution

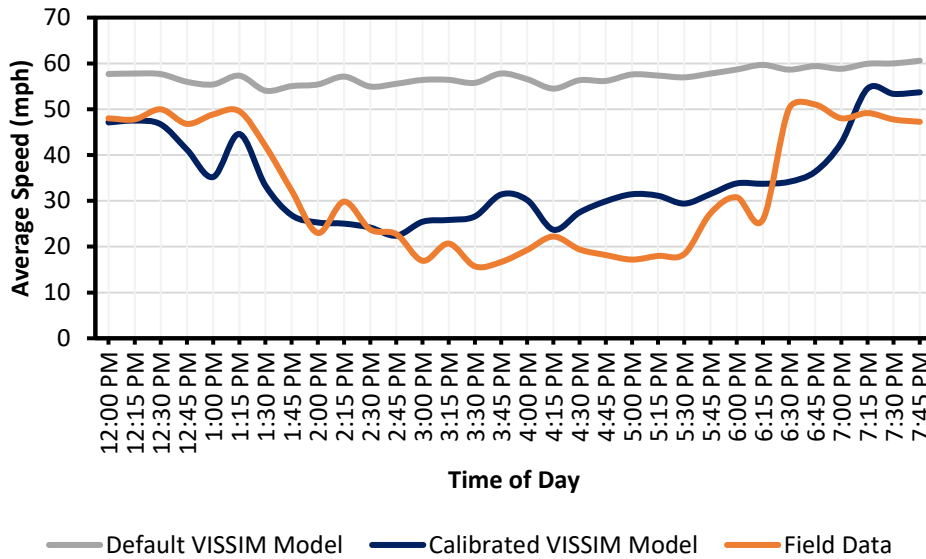


Figure 3-17: Field, Default VISSIM, and Calibrated VISSIM Speed Profile Comparisons

In Table 3-13, the adjusted empirical distribution for time headway involved subtracting 0.35 seconds from each entry in Table 3-10, resulting in values of 0, 0.65, 1.65, 2.65, 3.65, etc. in the final input distribution. Though increments of 0.1 seconds were originally explored, smaller increments of 0.05 seconds were necessary during the fine-tuning stage for the final model to meet calibration objectives. These objectives are summarized in Table 3-14 and Figure 3-18 for 15-minute average speeds and mean QDR.

Despite slight discrepancies in speed profiles, both the RMSNE and MAPE were well within calibration objectives for the period from 12:00PM to 3:30PM on October 3rd and considered adequate. The mean QDR in VISSIM was only 2% higher than that measured in the field, and an overlay of the flow rate histograms shows that the variance of the two distributions are somewhat similar. The most notable difference between the field data and simulation outputs shown in Figure 3-18 is that the highest and lowest queue discharge flow rates were

unobservable in the model. This finding substantiates the claim that the variability of real-world driving behavior cannot be fully replicated using microsimulation.

Table 3-14: Calibration Summary (October 3rd, 2016)

Time	VISSIM Speed (mph)	Field Speed (mph)	RMSNE	MAPE
12:00:00 PM	47.1	48.0	0.000	2%
12:15:00 PM	47.5	47.8	0.000	1%
12:30:00 PM	46.7	50.0	0.004	7%
12:45:00 PM	41.2	46.8	0.015	12%
1:00:00 PM	35.2	48.9	0.078	28%
1:15:00 PM	44.6	49.6	0.010	10%
1:30:00 PM	33.3	41.9	0.042	21%
1:45:00 PM	26.9	32.2	0.028	17%
2:00:00 PM	25.3	23.0	0.010	10%
2:15:00 PM	25.0	29.8	0.026	16%
2:30:00 PM	24.2	23.8	0.000	2%
2:45:00 PM	22.4	22.7	0.000	1%
3:00:00 PM	25.4	16.9	0.253	50%
3:15:00 PM	25.8	20.7	0.062	25%
Total			0.194	14%

<i>Mean QDR (pcphpl)</i>		
Calibrated VISSIM Model	Field	Error
1032	1016	2%

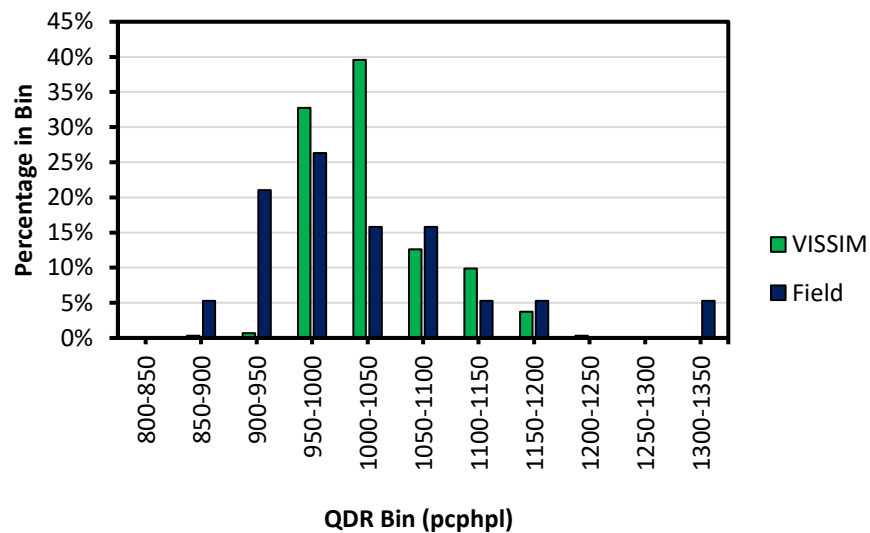


Figure 3-18: QDR Distribution Comparison (October 3rd, 2016)

3.5.3 Model Validation

While the results from the calibrated model were promising, they only applied to data from October 3rd and needed to be validated using input from a different day. Data from October 6th, 2016 was ultimately selected because congestion was observed during off-peak hours, providing a unique set of traffic volume characteristics to be modeled. Field data showed a continuous period of congestion beginning at approximately 9:45AM, so VISSIM was coded to run from 7:45AM to 11:30AM, which included a 15-minute warm-up period and 3.5 hours of independent volumes and vehicle compositions. A comparison of the speed profiles generated in VISSIM and observed in the field is provided in Figure 3-19.

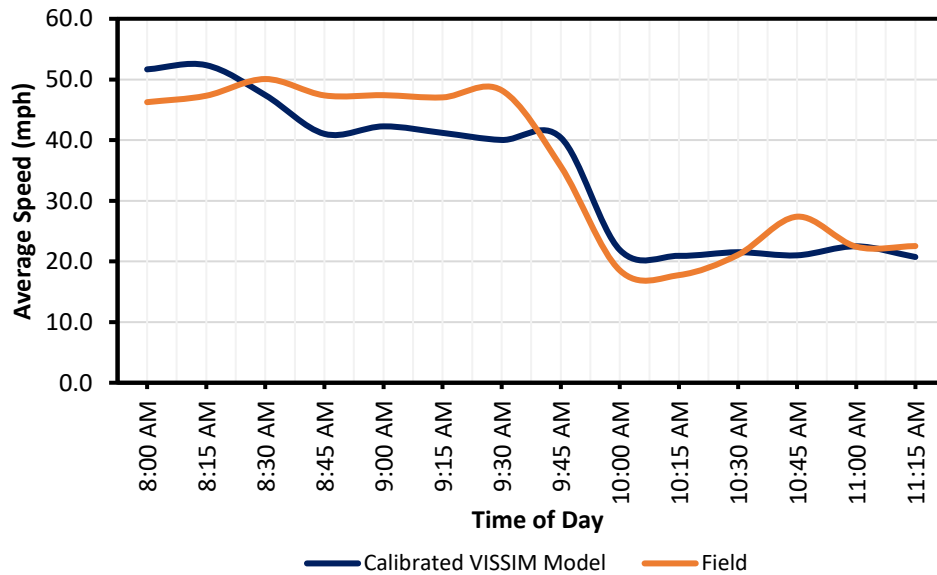


Figure 3-19: Field and Validated VISSIM Speed Profile Comparisons

The graph shows that speeds in VISSIM dropped slightly below those observed in the field approximately 45 minutes into the simulation, but generally matched field speeds otherwise. In fact, the validated model adhered to objectives even more closely than those for October 3rd, further increasing confidence in the validity of the model. The same number of

simulation runs (20) were conducted to achieve statistical confidence in the validation results presented in Table 3-15, as the standard deviation of the QDR was nearly identical to that observed during the calibration process. Following the table, Figure 3-20 provides another overlay of QDR histograms to show that the simulated distribution contains most of the field distribution. Like for October 3rd, VISSIM was unable to capture flow rates near the lower and upper bounds of the distribution, emphasizing the assertion that simulation models cannot mimic the variability of real-world traffic. Nonetheless, the model was deemed successfully validated.

Table 3-15: Validation Summary (October 6th, 2016)

Time	VISSIM Speed (mph)	Field Speed (mph)	RMSNE	MAPE
8:00:00 AM	51.7	46.3	0.014	12%
8:15:00 AM	52.3	47.3	0.011	11%
8:30:00 AM	47.4	50.1	0.003	5%
8:45:00 AM	41.0	47.4	0.018	13%
9:00:00 AM	42.3	47.4	0.012	11%
9:15:00 AM	41.2	47.0	0.015	12%
9:30:00 AM	40.0	48.2	0.029	17%
9:45:00 AM	40.4	35.7	0.018	13%
10:00:00 AM	21.9	18.5	0.033	18%
10:15:00 AM	20.9	17.7	0.032	18%
10:30:00 AM	21.5	21.1	0.000	2%
10:45:00 AM	21.0	27.4	0.054	23%
11:00:00 AM	22.5	22.4	0.000	0%
11:15:00 AM	20.7	22.5	0.006	8%
Total			0.132	12%
<i>Mean QDR (pcphpl)</i>				
Validated VISSIM Model	Field		Error	
1024	1053		3%	

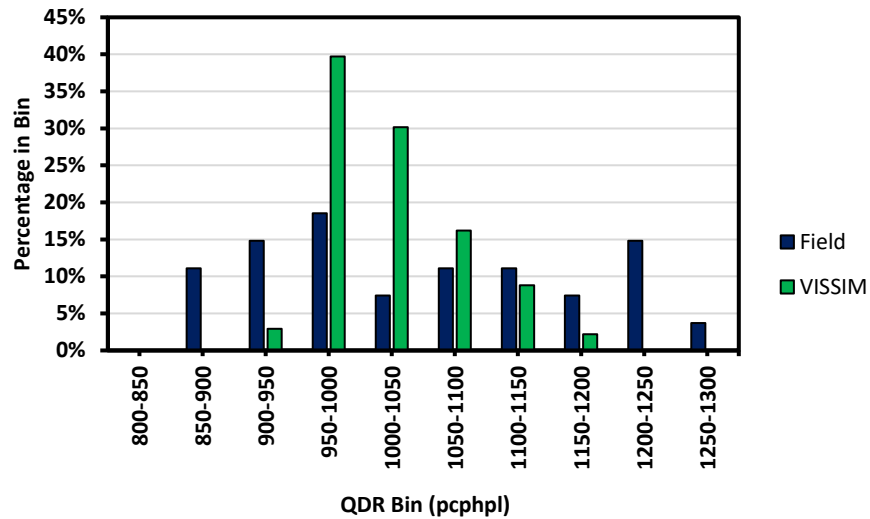


Figure 3-20: QDR Distribution Comparison (October 6th, 2016)

3.6 EXPERIMENT DESIGN

This concluding section of Chapter Three outlines the design of the VISSIM experiment conducted to generate breakdown probability models for rural freeway work zones. Based on findings from the literature, it was concluded that the following modellable factors may have a significant effect on the probability of breakdown and subsequent queueing at freeway work zones: traffic volume, upstream lane distributions, free flow speed, speed variance, truck percentage, and lane closure configuration. Since field data was only available for a single site with a 2-1 lane closure, scenarios involving other lane closure configurations and traffic characteristics were not considered for this thesis but may be a topic for future research. Instead, only traffic volume, truck percentage, and lane closure side were included as explanatory variables and expected to be sufficient for capturing the same variability in breakdown flow rates that would be observed at comparable sites in the southeastern United States.

Recalling that the primary objective of this thesis is to lay the groundwork for developing a complete rural freeway work zone analysis tool for practitioners, the methodology described herein and the results of an analysis for 2-1 lane closures may easily be extended to other contexts after future field data collection efforts. The following subsections cover the characterization of typical traffic conditions on rural freeway facilities and application of these conditions to VISSIM input parameters.

3.6.1 Characterization of Typical Traffic Conditions

Section 3.3.3 underscored the importance of fully exploring field data from the study site before setting calibration and validation objectives for the VISSIM model. That discussion centered on flow rates immediately prior to breakdown and during congestion, but it was equally vital to the experiment design phase to understand the natural rise and fall of volumes and truck percentages from hour-to-hour and day-to-day. All key pieces of literature related to studying breakdown at freeway facilities emphasized the need to collect field data for up to one year if possible (Kondyli et al. 2013; Lorenz and Elefteriadou 2001), during which a myriad of traffic conditions may be observed. Since such an extensive data collection period is not feasible for most work zones, simulation was utilized to accomplish this task, but necessitated that a diverse set of traffic volumes and truck percentages be accounted for. Table 3-16 contains daily and peak hour volumes for the two weeks of field data collection conducted as part of this research, and shows that conditions vary greatly even over a short period.

Table 3-16: Study Work Zone Volume Summary

Day	Total Daily Volume (vehicles)	Peak Hour Volume (vehicles)	K Factor (%)	Trucks During Peak Hour (%)
Monday, October 3, 2016	7,614 ^b	891	--	26
Tuesday, October 4, 2016	12,615	828	6.6	36
Wednesday, October 5, 2016	13,340	915	6.9	39
Thursday, October 6, 2016	14,153	922	6.5	30
Friday, October 7, 2016	16,693	1,244	7.5	19
Saturday, October 8, 2016	13,762	984	7.2	23
Sunday, October 9, 2016	13,330	1,105	8.3	16
Monday, October 10, 2016	12,714	1,000	7.9	13
Tuesday, October 11, 2016	12,500	968	7.7	37
Wednesday, October 12, 2016	13,041	866	6.6	36
Thursday, October 13, 2016	13,703	948	6.9	22
Friday, October 14, 2016	16,792	1,224	7.3	21
Saturday, October 15, 2016	13,871	1,030	7.4	21
Sunday, October 16, 2016	13,717	1,105	8.1	18
Averages	13,864	1,002	7.3	25

^bTraffic data was collected for only 12 hours on this day

The table was created using demand volumes from sensors 97 and 101, 2.5 miles upstream of the lane closure at the study site, and revealed several interesting trends. First, both total and peak hour volumes were substantially higher on the weekends, especially Fridays, while truck percentages were greater on weekdays. Second, the values in the table do not coincide with those calculated using the AADT, K factor, and D factor given in Figure 3-1 at the beginning of this chapter. The nearest permanent counting station maintained by ALDOT had a 2016 AADT of 27,890 vehicles, K factor of 10%, and D factor of 53%, suggesting that the peak directional hourly volume at the study work zone should be more than 1,300 vehicles, even if I-59/I-20 southbound is not the peak direction. Sensor data contradicted these calculations and

showed an average peak hour volume of 1,002 vehicles, which would require a K and D factors of approximately 7.3% and 50%, respectively, using an AADT of 27,890 vehicles. Given that there was only one minor interchange between the study work zone and counting station in question, it is unclear why such large discrepancies were observed. Nonetheless, this finding stresses the need for practitioners to verify traffic conditions at work zones of interest.

Finally, the data show that a site averaging 25% trucks during the peak hour may produce as few as 10% or as many as 40% trucks during an individual peak period. Accordingly, this window was selected as the minimum that needed to be explored to ensure that VISSIM output captured the full range of site conditions that would be observed from several weeks or months of data collection. Trial simulation runs were found to produce comparable variance in truck percentage by time interval even when a single value was used as input, ultimately motivating the use of several static percentages to represent sites with different average truck volumes. Likewise, a range of target peak hour volumes would be applied so that fluctuations of up to several hundred vehicles per hour between hours of the day and days of the week could be accounted for.

To best mimic real-world traffic conditions, it would also be necessary to gradually increase modeled demand volumes in the same pattern observed in the field. Since this thesis asserts that capacity is not a static value, simulated traffic needed to be exposed to lower volumes to allow for opportunities for breakdown at flow rates less than the expected average capacity. Conversely, the construction of breakdown probability models also required that ample uncongested, or censored, flow rates be observed at these lower volumes. Lastly, just as microsimulation models are typically coded with initialization periods, a similar extended period of steady volume increase would allow the model to reach equilibrium and ensure realistic

outputs. To inform volume inputs, demand profiles for each day of data at the study work zone were examined and assumed to be representative of other four-lane rural freeways across the southeastern United States. Figure 3-21 provides an example of traffic volumes throughout the day on October 4th, 2016.

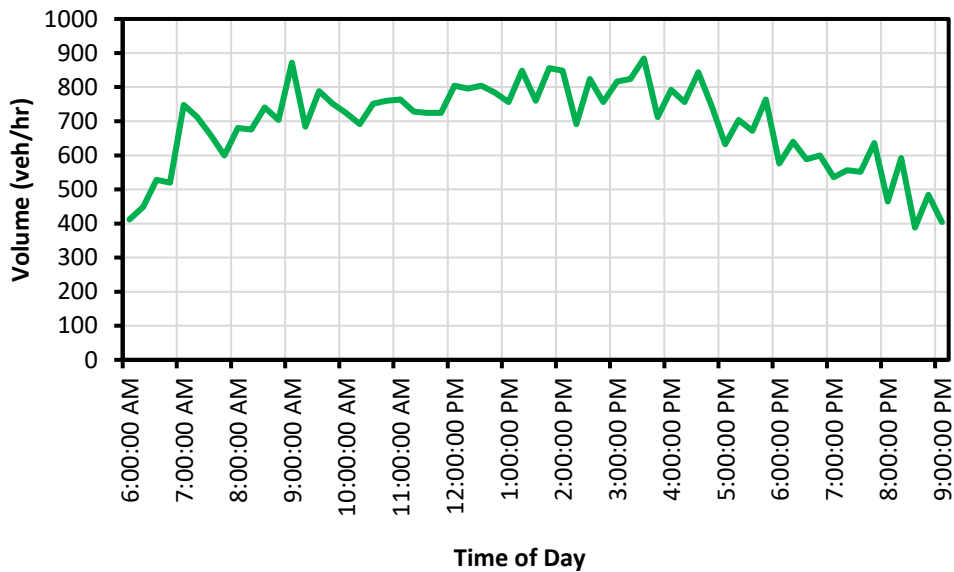


Figure 3-21: Traffic Demand Profile (October 4th, 2016)

Aside from local maxima and minima, the graph generally shows that volumes increased steadily throughout the day, then plateaued for several hours during the afternoon before retreating during the evening. Observations from other days yielded similar findings, although volumes on Saturday and Sunday typically peaked several hours before those on weekdays. While flow rates during the morning and evening hours may be 20-30% below the eventual peak hour volume, truck percentages are higher and capacity likely reduced during these time periods. These characteristics separate rural freeways from their urban counterparts in that the peak hour is not the only period of interest. Therefore, volume input schemes in VISSIM were designed to reflect a volume profile similar to that observed at the study site.

3.6.2 Experiment Input Parameters

Final Case Selection

The following factors and levels were selected as part of the final experiment design:

- Truck Percentage: 5%, 10%, 20%, 30%, 40%
- Demand Volume (vph): 700, 800, 900, 1000, 1100, 1200, 1300, 1400
- Lane Closure Side: Right, Left

Values for truck percentage were intended to include those that would realistically be observed at rural freeway sites across the United States. For example, it is unlikely that a rural freeway facility would carry less than 5% trucks, and if so, volumes would likely be well below capacity. Likewise, a truck percentage of greater than 40% would presumably only occur during off-peak periods where overall volumes are suppressed. Based on the discussion in the previous subsection, it was decided that target peak volumes would be varied between 700 vph and 1400 vph in 100 vph increments to encompass the full range of volumes observed at the study site and those that would be required to cause breakdown events at higher or lower truck percentages. Note that all volumes described in this section are given in units of vehicles per hour, as only a single lane is open through the simulated work zone. Finally, all combinations of truck percentage and input volume were run for both right- and left-side lane closures.

A full factorial experiment would consist of 80 unique cases, each of which would require multiple simulation runs. For practical reasons, the size of the VISSIM experiment was minimized by eliminating scenarios where a specific truck percentage and target volume would not be necessary to achieve congestion. For example, a volume of 700 vph would be highly unlikely to consistently produce congestion with only 5% trucks in the traffic stream. Pilot

simulation runs were used to determine these cutoffs and reduce the experiment to 20 unique cases per lane closure side, as displayed in Table 3-17.

Table 3-17: Final Volume and Truck Percentage Inputs

Input Flow Rates (vph)	Truck Percentages				
	5%	10%	20%	30%	40%
700					✓
800				✓	✓
900			✓	✓	✓
1000		✓	✓	✓	✓
1100	✓	✓	✓	✓	
1200	✓	✓	✓		
1300	✓	✓			
1400	✓				

Traffic Input Schemes

It was stated earlier that producing variable volumes and truck percentages during each simulation run was significant to the validity of the model results. Since VISSIM operates stochastically, even static traffic inputs will generate a wide range of outputs, and this variability increases as input time intervals become coarser. In the calibration and validation phase, 5-minute time intervals were used to achieve consistency in the onset of breakdown and replicate exact field conditions. For the development of breakdown probability models, variability in breakdown volumes was desired, so 15-minute time intervals were used instead. Indeed, it was found that a 15-minute equivalent hourly input flow rate of 1000 vph could produce 15-minute flow rates of greater than 1000 vph during undersaturated conditions. Most importantly, equivalent flow rates at shorter time intervals (e.g. 1-minute output intervals) were even more diverse, allowing for brief spikes in volume that would be typical in the field. Similarly, a single

average truck percentage was used for the entire simulation period for all cases to maximize fluctuations in traffic stream composition.

The VISSIM model for each of the 40 cases included as part of the experiment design were coded to run for 18,900 seconds—900 seconds of initialization and 18,000 seconds of data collection—or a total of 5 hours and 15 minutes. The first two hours of the data collection period were used to linearly increase volumes from 65% to 100% of the target peak volume, allowing for observation of undersaturated conditions and breakdown events at low flow rates. Then, mimicking a field-measured peak hour factor (PHF) of 0.95, 98% to 105% of the target peak volume was met for the next two hours of simulation to allow for measurement of queue discharge flow rates. Finally, volumes were gradually decreased again for the final hour of modeling to allow for potential recovery from breakdown. A visual depiction of this volume input strategy is provided in Figure 3-22.

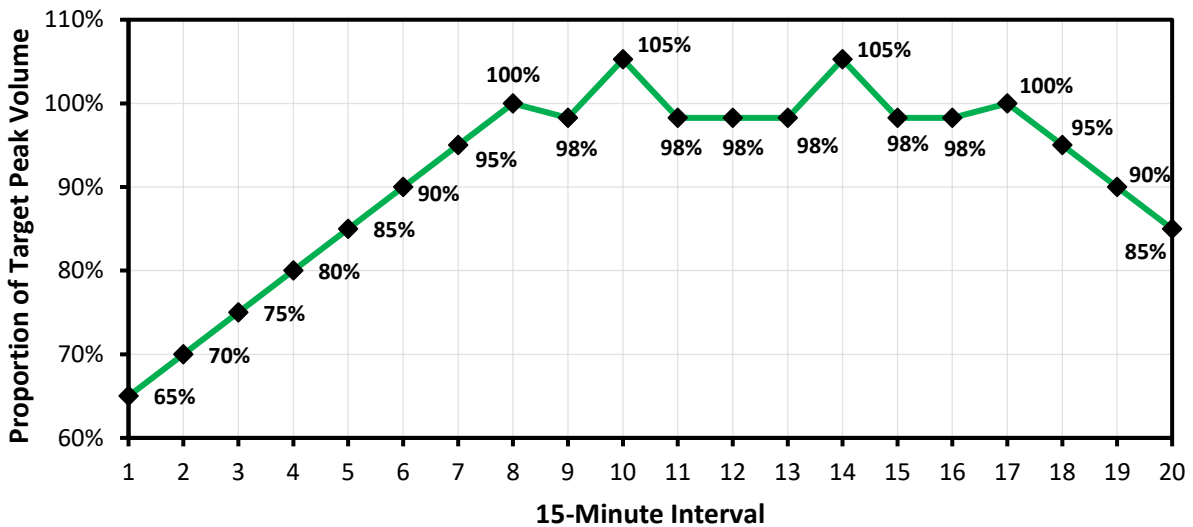


Figure 3-22: Experiment Volume Input Scheme

Once raw volumes had been established, upstream input lane distributions needed to be set. Though not included as an explanatory variable in determining breakdown probability, the

number of passenger cars and trucks in each lane and their designated desired speed distributions were considered vital components of an accurate model. To decide how to distribute vehicles among lanes, the field data was again referenced and a common theme was discovered. On average, approximately 75% of tractor-trailers and 60% of all vehicles traveled in the right lane upstream of the work zone. Thus, these proportions were preserved to best replicate typical conditions at rural four-lane freeways. Single unit trucks were observed to account for about 10% of the traffic stream throughout the data collection period at the study work zone, so this number was used regardless of the tractor-trailer percentage applied for a given case. Table 3-18 gives the lane-specific distributions for traffic upstream of the work zone.

Table 3-18: Upstream Lane Distributions

	Truck Percentage	Proportion in Right Lane	Proportion in Left Lane
Trucks	5%	6.3%	3.1%
	10%	12.5%	6.3%
	20%	25.0%	12.5%
	30%	37.5%	18.8%
	40%	50.0%	25.0%
Single Unit Trucks		8.3%	12.5%
All Traffic		60.0%	40.0%

Required Number of Breakdown Events

Work by Elefteriadou, Roess, and McShane suggested that the required sample size to validate an estimated probability of breakdown to a specified degree of confidence can be calculated using the normal approximation to the binomial distribution, provided in Equation 3-2 (Elefteriadou et al. 1995):

$$N = \frac{z^2 p(1 - p)}{h^2}$$

p = true probability of breakdown

(3-2)

$z = \text{standard normal distribution parameter}$

$h = \text{precision requirement}$

Since literature has typically recommended that capacity values obtained from the PLM be equivalent to a probability of breakdown between 10% and 20%, p was assumed to be 15%. The magnitudes of breakdown flow rates were expected to range from 700 vphpl to 1400 vphpl, so deviation of approximately 50 vphpl was deemed acceptable, and h was set at 5%. So, to estimate the flow rate corresponding to a 15% probability of breakdown with 95% confidence, the required number of breakdown events was:

$$N = \frac{1.645^2 * 0.15(1 - 0.15)}{0.05^2} = 139 \text{ breakdown events}$$

To avoid redundant simulation runs, 50 runs per case was initially determined to be sufficient and would be increased as necessary. With five truck percentages modeled at four input volumes for each lane closure side, this led to a preliminary total of 2,000 planned simulations. After executing the experiment for each of the volume inputs at 5% trucks, a total of 152 breakdown events were observed at 15-minute aggregation intervals, so the size of the experiment was not modified. Completion of the remaining cases yielded an average of approximately 150 breakdown events across all aggregation intervals, confirming that statistical confidence in the validity of probability estimates could be met as described above.

3.7 SUMMARY

To summarize, Chapter Three began by outlining the field data collection effort that was ultimately used to inform model development. Data collected from a 2-1 freeway lane closure near Tuscaloosa, Alabama in October 2016 was screened and analyzed to produce volume inputs, vehicle compositions, desired speed distributions, and time headway distributions in

VISSIM. Then, the model was calibrated and validated by manually adjusting key driving behavior and vehicle performance parameters until simulated speed profiles and queue discharge rates replicated field observed values to the specified degree of accuracy. Ultimately, modeled speeds and queue discharge rates produced error within acceptable ranges using data from two different days, so the model was deemed suitable for analysis.

Finally, a partial factorial experiment was designed to study the probability of queue formation at rural freeway work zones as a function of traffic volume, truck percentage, and lane closure side. The total number of cases was reduced by eliminating combinations of truck percentage and demand volume that would not be necessary to capture the full range of traffic conditions capable of producing breakdown events. Then, volume input schemes and upstream lane distributions were created based on trends observed in the field data. Lastly, the number of simulation runs required per case was determined by calculating the number of breakdown events required to validate the data point corresponding to a probability of breakdown of 15% on a cumulative probability distribution.

CHAPTER FOUR: ANALYSIS AND RESULTS

4.1 INTRODUCTION

The penultimate chapter of this thesis describes how results from the experiment outlined in Chapter Three led to a series of breakdown probability models, collectively forming the first component of a rural freeway work zone lane closure analysis tool. First, the cleaning and aggregation of the simulated dataset will be chronicled, with emphasis on the choice of breakdown identification algorithms used to separate undersaturated and oversaturated flow records. Next, the iterative process of fitting cumulative Weibull distributions to empirical data obtained from simulation runs will be discussed. To facilitate this discussion, Kaplan-Meier survival analysis will be explained in more detail than in the literature review, and existing methodology in the 6th edition of the HCM will be briefly covered. Finally, the main findings of this research will be presented along with the beta version of a practical tool developed as a composite of the results.

4.2 AGGREGATION OF SIMULATED DATA

To allow for the most flexibility in analysis of the results, the number and speed of passenger cars and trucks were initially collected from each simulation run in 1-minute aggregation intervals. Unfortunately, the simulated sample size was such that 1-minute data was incapable of producing breakdown probabilities high enough to generate meaningful cumulative distributions, so only 5- and 15-minute data were retained. Since the application of breakdown probability

models to rural freeway work zones is unlikely to include scenarios where an agency may make decisions based on 1-minute flow rates, let alone that such data would be available, the remaining cases were found sufficient. As stated in Chapter Three, the transition from stable flow to congestion has been found to occur suddenly, so 5-minute aggregation intervals were anticipated to shed more light on the underlying relationship between traffic flow, truck percentage, and the probability of queue formation. Conversely, 15-minute intervals were expected to be less precise in capturing the breakdown phenomenon but necessary to ensure that agencies and practitioners could apply readily available traffic data to the lane closure analysis tool developed.

Once the simulated data was appropriately aggregated, individual flow records were subdivided into one of three categories: breakdown flow rates, uncongested flow rates, and queue discharge flow rates. This step was necessary because congested flow rates provided no information about the likelihood of breakdown at a given level of demand and could be disregarded. On the contrary, stable flow rates up to those immediately preceding breakdown were significant because they combined to indicate the sustainability of a given traffic volume. The reader is referred to Chapter Two of this thesis or external sources for further discussion on the issue of capacity measurement at freeway facilities (Elefteriadou 2014; Lorenz and Elefteriadou 2001; Roess and Prassas 2016).

Classification of records into the bins mentioned above was accomplished using three distinct breakdown identification algorithms, one for each aggregation interval. In all cases, a 35-mph speed threshold was applied based on the definition of breakdown in the 6th edition of the HCM, which specifies “a sudden drop in speed at least 25% below the free flow speed for a sustained period of at least 15 minutes” (Transportation Research Board 2016). Since the free

flow speed at the lane closure bottleneck was approximately 50 mph, a reduction to at least 37.5 mph would be required to meet this definition. For simplicity, this value was rounded down to 35 mph. While the 15-minute period of sustained congestion cited by the HCM was adhered to for 5-minute data, it was found that too many false breakdown events were identified at 15-minute aggregation intervals when such criteria were used. To prevent this occurrence, it was required that speeds be maintained below 35 mph for 2 consecutive intervals, or 30 minutes, in the latter case. Similarly, recovery from breakdown was signaled by an increase in speeds above 35 mph for the same number of consecutive time intervals. Computing time was minimized by utilizing a 30-line code written in Microsoft Visual Basic, which is included in Appendix B for reference. Table 4-1 provides an example of the Excel output generated after executing the breakdown identification algorithm for a set of 5-minute simulated data.

Table 4-1: Example Breakdown Identification

Simulation Run	5-Minute Average Speed (mph)	5-Minute Flow Rate (vphpl)	Breakdown Flow Rate (1 = Yes)	Queue Discharge Flow Rate (1 = Yes)
1	51.2	1032	0	0
1	52.1	936	0	0
1	46.0	1056	0	0
1	50.4	912	0	0
1	44.9	1104	0	0
1	49.3	996	0	0
1	47.2	1092	1	0
1	22.6	1032	0	1
1	22.0	1116	0	1
1	20.5	1104	0	1
1	23.7	1200	0	1
1	24.2	1140	0	1
1	21.0	1116	0	1
1	20.4	1032	0	1
1	19.7	1056	0	1

The sample data in the table confirms that the breakdown identification algorithm successfully identified the flow rate immediately prior to the sudden drop in speed from 47 mph

to 23 mph, then classified all subsequent flow records as congested. If the table were to continue vertically, a “1” would be recorded in the last column until average speeds recovered above 35 mph for at least three consecutive 5-minute intervals (thereby indicating queue clearance and a return to uncongested flow) or data from the second simulation run began, whichever occurred first. The example shown in Table 4-1 indicates that the breakdown flow rate did not coincide with the highest flow rate observed prior to congestion, confirming one of the fundamental concepts of traffic flow theory from the literature. Namely, capacity is stochastic and may be represented by a wide range of flow rates even under identical prevailing conditions.

4.3 SURVIVAL ANALYSIS

4.3.1 Methodology

Aggregated, classified simulation data was evaluated using Kaplan-Meier survival analysis, also known as the product-limit method. This statistical methodology uses data on the lifetime of individuals to determine the approximate probability of reaching a terminal state at a given point in time. Here, “individuals” refer to traffic flow records, and the “terminal state” is the onset of breakdown. Theoretical aspects of this approach are explained in Chapter Two of this thesis, but the focus of this section will be on its practical application to simulated data. Construction of breakdown probability models using the product-limit method was accomplished by following the steps below, each referencing Table 4-2 (as an example for cases with 10% trucks).

1. Simulated data was aggregated by time interval and classified by one of three flow regimes: breakdown, uncongested, or congested.
2. After discarding congested flow rates, breakdown and uncongested flow rates were summed at each observed volume (**Columns A, B, and C**).

3. Flow rates at all volumes were summed to obtain the total risk set, or number of flow rates which had the potential to be followed by a breakdown event (**Column D, row 1**).
4. In each subsequent row of the table, the remaining risk set was determined using equation 4-1 (**Column D, rows 2 through end**):

$$Risk\ Set_i = Risk\ Set_{i-1} - Breakdowns_{i-1} - Uncongested_{i-1} \quad (4-1)$$

5. Cumulative survival and breakdown probabilities were calculated using equations 4-2, 4-3, and 4-4 (**Columns E, F, and G**):

$$Factor = \frac{Breakdowns_i}{Risk\ Set_i} \quad (4-2)$$

$$Probability\ of\ Survival = (1 - Factor_i) * Probability\ of\ Survival_{i-1} \quad (4-3)$$

$$Probability\ of\ Breakdown_i = 1 - Probability\ of\ Survival_i \quad (4-4)$$

Table 4-2: Survival Analysis Table (10% Trucks, 5-Minute Aggregation Interval, Left-Side Lane Closure)

A	B	C	D	E	F	G
<i>Volume (vphpl)</i>	<i># Breakdown Flow Rates at Volume</i>	<i># Uncongested Flow Rates at Volume</i>	<i>Risk Set</i>	<i>Factor</i>	<i>Probability of Survival</i>	<i>Probability of Breakdown</i>
708	1	47	6584	0.000152	100.0%	0.0%
780	1	103	6070	0.000165	100.0%	0.0%
816	1	139	5744	0.000174	100.0%	0.0%
900	5	160	4718	0.00106	99.8%	0.2%
912	5	156	4553	0.001098	99.6%	0.4%
924	6	182	4392	0.001366	99.5%	0.5%
936	8	212	4204	0.001903	99.3%	0.7%
--	--	--	--	--	--	--
1140	10	92	981	0.010194	92.3%	7.7%
1152	7	66	879	0.007964	91.6%	8.4%
1164	5	61	806	0.006203	91.0%	9.0%
1176	5	39	740	0.006757	90.4%	9.6%

-- Table abbreviated to allow higher breakdown probabilities to be visible

A single empirical breakdown probability distribution was built for each truck percentage by combining the data gathered from each corresponding input volume. For example, Table 4-2 was developed from the simulated data for a left-side lane closure with 10% trucks, aggregated into 5-minute time intervals. Since this combination was simulated at input volumes of 1000, 1100, 1200, and 1300 vph, four sets of flow data were used to complete the table. The distribution associated with this table is given in Figure 4-1, and reflects trends observed for data aggregated into 15-minute time intervals.

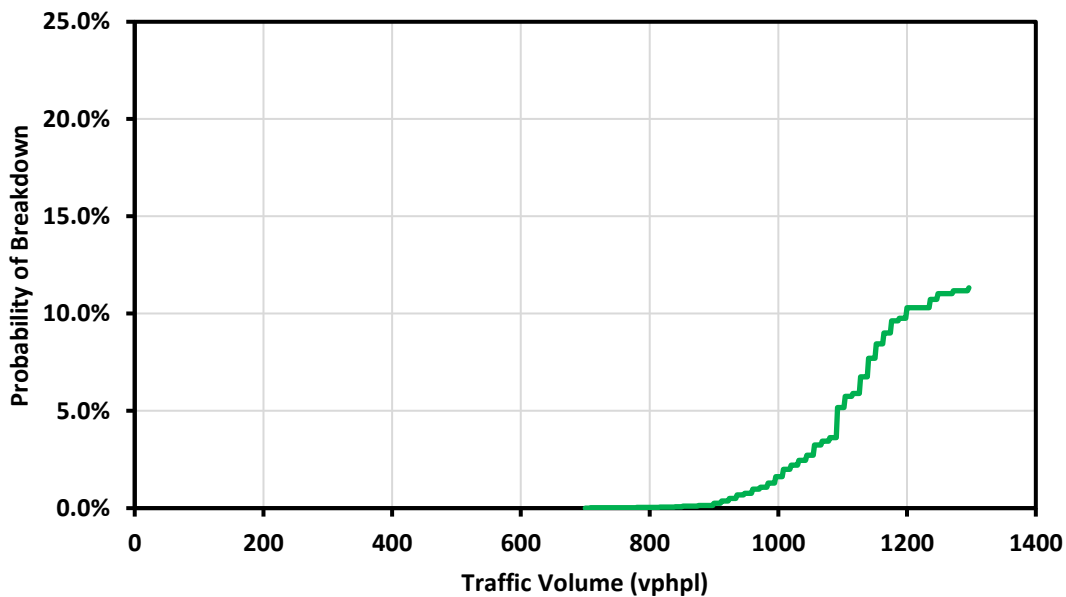


Figure 4-1: Empirical Breakdown Probability Distribution (10% Trucks, 5-Minute Aggregation Interval, Left-Side Lane Closure)

The most evident feature of the figure is the fact that the probability distribution terminates at just above 10% on the y-axis. This is common even for distributions built from substantially larger datasets. For instance, the methodology provided in the supplemental volume of the HCM is demonstrated using over 23,000 flow rate observations, yet the associated empirical distribution still truncates around a 40% probability of breakdown (Transportation

Research Board 2016). A plot of this dataset was recreated to emphasize this point and is given in Figure 4-2. In the figure, β and γ are the scale and shape parameters of the best-fit Weibull distribution, respectively.

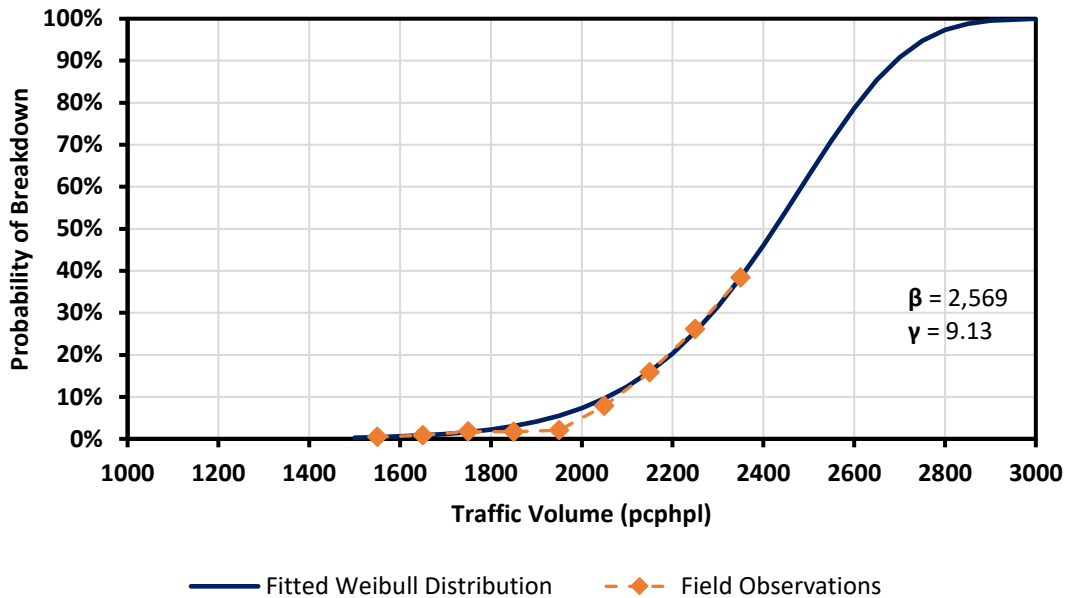


Figure 4-2: Example Fitted Weibull Distribution (Source: TRB 2016)

The figure demonstrates the enormous data requirements for developing breakdown probability models, but also the quality of fit achieved by assuming a Weibull distribution. Based on this observation and findings from past research, it was assumed that the empirical distributions in this study could be sufficiently extrapolated using best-fit Weibull distributions. There are two caveats associated with Figure 4-2 and the methodology found in the HCM, however. First, field-measured volumes were binned into 100 pcphpl increments, reducing the number of data points available for curve fitting. Second, breakdown probabilities were calculated for each bin by dividing the number of breakdown flow rates by the total number of observed flow rates. Since this calculation occurs independently for each bin, the effect of previously observed flow rates is unaccounted for. As documented in literature, this leads to an

overly conservative (low) estimate of capacity (Asgharzadeh and Kondyli 2018). For these reasons, the product-limit method was deemed the more appropriate technique for use in this research. Curves like the one shown in Figure 4-1 were constructed for each combination of truck percentage and lane closure side, with flow rates aggregated into 5- and 15-minute intervals.

4.3.2 Curve Fitting

Once all survival analysis tables and empirical probability distributions were completed, simulated data points were fitted to Weibull distributions to develop complete cumulative distribution functions. The Weibull cumulative distribution function is given in equation 4-5, where λ is the probability of breakdown, q is the flow rate in vphpl, β is the scale parameter, and γ is the shape parameter. Solving this expression for q yields equation 4-6, which was ultimately used to calculate goodness of fit statistics.

$$\lambda = 1 - e^{-\left(\frac{q}{\beta}\right)^\gamma} \quad (4-5)$$

$$q = \beta * \sqrt[\gamma]{-\ln(1 - \lambda)} \quad (4-6)$$

To simplify the analysis, basic curve fitting with Excel's Solver function was applied in lieu of maximum likelihood estimation, the methodology typically used in literature. In this case, instead of maximizing the log-likelihood value, the MAPE between simulated data points and those on the best-fit Weibull curve was minimized. This statistic was calculated using equation 4-7.

$$MAPE = \frac{1}{n} * \sum_{i=1}^n \left(\frac{|Flow Rate_{weibull,i} - Flow Rate_{simulated,i}|}{Flow Rate_{simulated,i}} \right) \quad (4-7)$$

Here, the empirical flow rate corresponding to a known probability of breakdown was compared to the flow rate calculated for the same probability of breakdown on a cumulative Weibull distribution with given shape and scale parameters. This process was iterated by Excel's Solver add-in until the smallest MAPE was achieved, typically at a value of less than 2%. The results of these calculations for a simulated work zone with 10% trucks, a left-side lane closure, and 5-minute aggregation intervals are shown as an example in Figure 4-3.

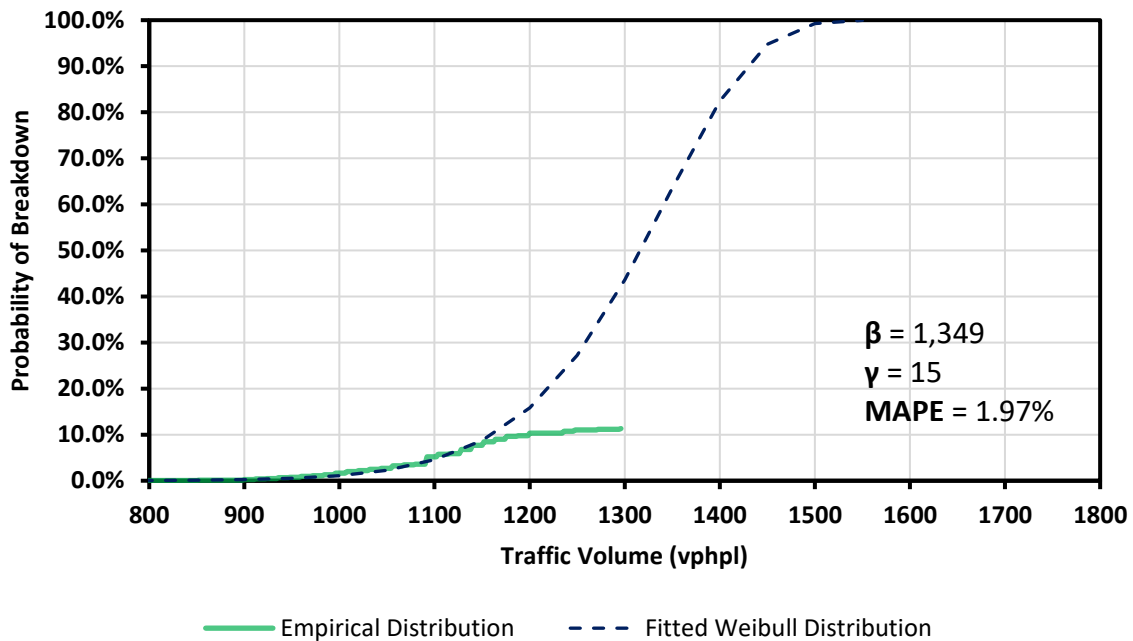


Figure 4-3: Curve Fitting Example (10% Trucks, Left-Side Lane Closure, 5-Minute Aggregation Intervals)

In the figure, the dashed Weibull distribution diverges from the truncated survival curve approximately midway between volumes of 1100 and 1200 vphpl, illustrating a key component of the curve fitting process. That is, because the simulated sample size was too small to create true cumulative distributions, survival curves typically flattened out near their maximum value. To avoid misleading results, data points corresponding to flow rates at or above which breakdown was seldom observed were excluded from MAPE calculations. Such points were

identified by binning flow rates into 50 vphpl increments, where bins with fewer than 50 observations were generally excepted from curve fitting. It should be noted that the quality of fit for each Weibull distribution was inflated by the number of censored data points present at lower flow rates. For example, 6,390 of the 6,584 data points (97%) used to generate Figure 4-3 were censored, with 56% of such records occurring at flow rates of less than 1,000 vphpl. Similar trends were also observed for data aggregated into 15-minute intervals.

Tables summarizing the best-fit Weibull distribution parameters for all 20 combinations of truck percentage, lane closure side, and aggregation interval (five truck percentages x two lane closure sides two aggregation intervals) are provided in Appendix B but omitted here for brevity. In the next section, the culmination of the results as a preliminary 2-1 lane closure analysis tool for rural freeway work zones will be presented. Supplemental findings will also be discussed, including the effect of explanatory variables on breakdown probability and calculation of capacity-based passenger car equivalents specific to rural freeway work zones.

4.4 RESULTS

4.4.1 Effect of Explanatory Variables on Breakdown Probability

Prior to compilation of the results as a single breakdown probability model, the effect of the studied independent variables on rural freeway work zone capacity was explored. This step was necessary to determine which variables should be provided as user inputs when developing a final spreadsheet tool. That said, the number and extent of explanatory variables included here are not all those expected to influence rural freeway work zone capacity, and further research will be necessary before finalizing the parent project that this thesis supports. Nonetheless, the

effect of truck percentage and lane closure side were analyzed to determine the magnitude and significance of their influence on the probability of queue formation.

First, fitted Weibull distributions for left- and right-side lane closures at 5- and 15-minute aggregation intervals were plotted on the same set of axes to make any differences apparent. These graphs are included in Figures 4-4 and 4-5 for each truck percentage modeled, where the solid lines and dashed lines correspond to left-side and right-side lane closures, respectively. The plots reveal several interesting trends that appear to be consistent regardless of aggregation interval. For example, lane closure side seems to influence modeled throughput for a 2-1 lane closure, but this difference is likely not practically significant. In fact, for 30% and 40% trucks, the dashed lines plot almost directly on top of the solid lines, indicating no observable difference in the probability of queue formation. On the contrary, there is a noticeable rightward shift in the breakdown probability distributions for right-side closures when compared to left-side closures as truck percentage decreases, particularly for higher probability values. This is potentially because relatively faster-moving traffic in the right lane allows for slightly higher flow rates to be realized, and these higher flow rates tend to occur with a greater probability of breakdown.

Even so, this difference is almost negligible until the probability of breakdown exceeds 50%, which is expected to be higher than any reasonable threshold set by an agency in a risk-based approach to establishing freeway work zone capacity. For these reasons, lane closure side was not included as an influential variable in developing the first version of a lane closure analysis tool, but will be considered for other lane closure configurations in the future.

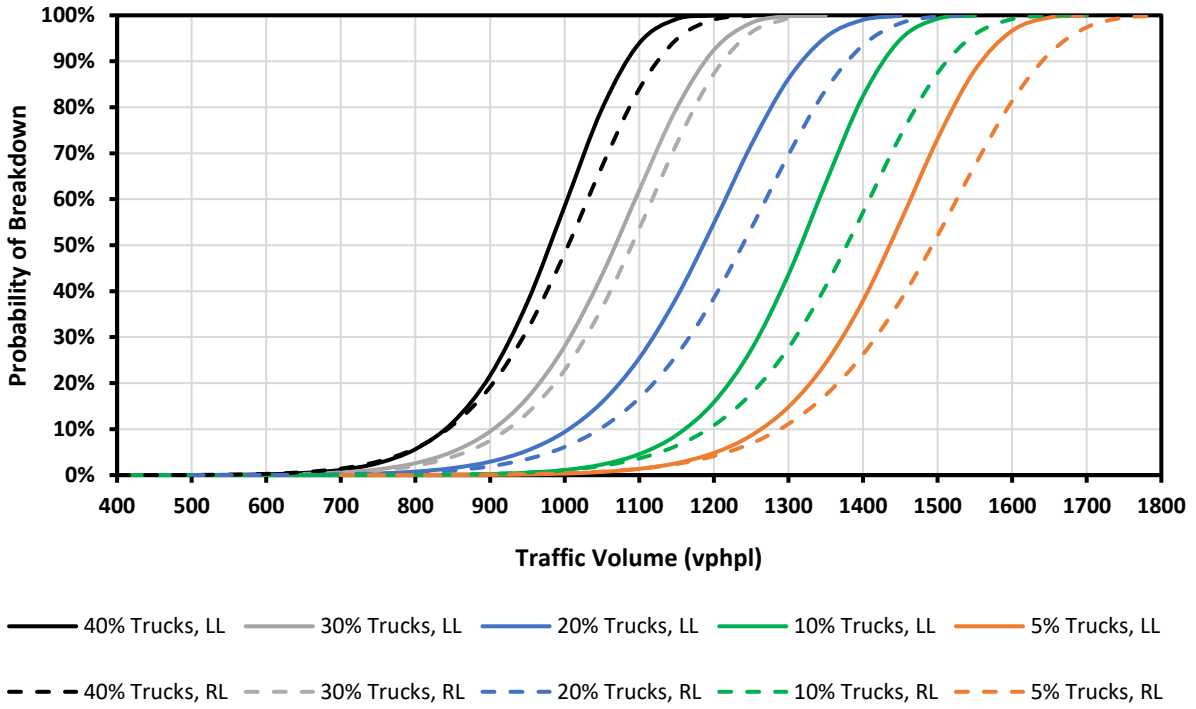


Figure 4-4: Breakdown Probability vs. Lane Closure Side (5-Minute Intervals)

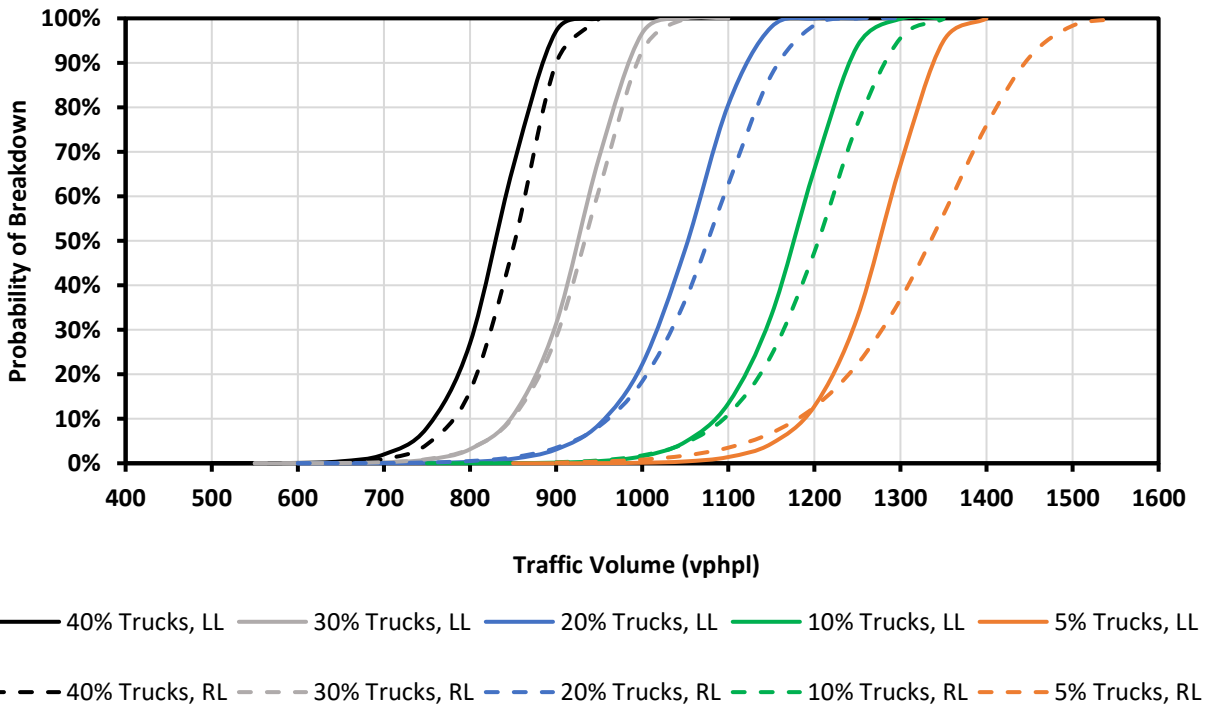


Figure 4-5: Breakdown Probability vs. Lane Closure Side (15-Minute Intervals)

Second, the use of 5-minute aggregation intervals captured much more variability in breakdown flow rates than 15-minute aggregation intervals. As stated previously, differences in flow rates at 5- and 15-minute time intervals may be attributed to increases in breakdown probability as larger flow rates are sustained for longer periods of time. For instance, with 20% trucks in the traffic stream and the left lane closed, the flow rate corresponding to a 10% probability of breakdown is approximately 1000 vphpl and 950 vphpl when 5- and 15-minute intervals are used, respectively. During a single 15-minute period with an equivalent hourly flow rate of 1000 vphpl, it is possible that a set of three 5-minute intervals would observe stable flow rates of greater than or equal to this value multiple times, thus deflating the overall breakdown probability at this flow rate.

That said, since breakdown typically occurs immediately following brief spikes in demand, it would be reasonable to assume that the use of shorter time intervals would define breakdown flow rates more accurately. By the same token, the use of larger time intervals may create false data points that include vehicle records occurring both prior to and after breakdown. Despite this finding, it was anticipated that the distributions created from 15-minute time intervals would reflect realistic trends and be applicable in the absence of more precise traffic data.

Lastly, using the same charts, one can infer that there is a strong, negative correlation between truck percentage and the probability of breakdown. Given that heavy vehicles are typically accounted for with passenger car equivalents due to their substantial impact on capacity, this finding is not surprising. However, though the HCM recommends default PCEs based on terrain, these were not developed for work zones and literature has debated whether

alternative values should be used in such cases. As such, the choice of PCE values is not a trivial task, so this burden was eliminated by reporting all flow rates in terms of raw vehicles.

4.4.2 Calculation of Capacity-Based Passenger Car Equivalents

Considering that capacity values are often reported in units of PCEs, quantification of the effect of heavy vehicles was explored further. The findings in this subsection were motivated in part by Sarasua and Geistefeldt, who have each published research questioning the use of static PCE values regardless of site conditions (Geistefeldt 2009; Sarasua et al. 2006). Specifically, they have calculated values ranging from 1.3 to 2.6, varying based on prevailing speeds, terrain, and the number of lanes. These two studies were particularly relevant because Sarasua focused on determining PCEs for freeway work zones, while Geistefeldt compared stochastic estimates of capacity at different truck percentages.

Sarasua's work included data from 35 freeway work zones in South Carolina, where headway values from time intervals containing only passenger cars were compared to those from intervals with a sizeable proportion of heavy vehicles. Geistefeldt constructed probabilistic capacity models for sites with various lane configurations and solved for the PCE value that minimized the variance of breakdown flow rates. Since the latter approach was more applicable to the experiment methodology used in this thesis, it was adopted here.

To perform the analysis, two measures of stochastic capacity were considered: (1) the flow rate corresponding to a probability of breakdown of 15%, and (2) the flow rate which maximized the sustained flow index (SFI). The former of these two was chosen to coincide with guidance in the 6th edition of the HCM recommending that a probability of breakdown of 15% be used to estimate capacity from BPMs. The latter was developed by Shojaat and Geistefeldt and is

a sustainability measure calculated by taking the product of each flow rate and its corresponding survival probability. These volumes were calculated using Equations 4-7 and 4-8, and a composite standard deviation computed using Equation 4-9 (Transportation Research Board 2016; Shojaat et al. 2016).

$$Flow Rate_{15\%} = \beta * \sqrt[\gamma]{-\ln(1 - 0.15)} \quad (4-7)$$

$$SFI_{Max} = \beta * \left(\frac{1}{\gamma}\right)^{\frac{1}{\gamma}} = \text{Max}(Flow Rate * (1 - Probability of Breakdown)) \quad (4-8)$$

$$\sigma_{composite} = \frac{\sigma_{15\%} + \sigma_{SFI}}{2} \quad (4-9)$$

Both measures of capacity were considered because variability between the fitted Weibull distributions increased with probability of breakdown, and the y-value that maximized the SFI was typically around 5%. Thus, it was expected that using a 15% probability of breakdown alone may overestimate the optimum PCE value. The composite standard deviation referenced in Equation 4-9 was calculated by averaging the standard deviation of the flow rates at capacity for each truck percentage at both 5- and 15-minute aggregation intervals. Finally, the ideal PCE was found by minimizing the composite standard deviation, as shown in Tables 4-3 and 4-4.

Table 4-3: PCE Calculation Summary (15-Minute Intervals)

Truck %	Flow Rate _{15%} (vph)	Flow Rate at SFI _{Max} (vph)	Flow Rate _{15%} (pcphpl)	Flow Rate at SFI _{Max} (pcphpl)
5	1190	1130	1291	1225
10	1120	1053	1309	1231
20	980	919	1311	1230
30	870	818	1311	1233
40	770	726	1290	1217
Standard Deviation			10.30	6.00
Composite Standard Deviation			8.15	
Optimum PCE			2.69	

Table 4-4: PCE Calculation Summary (5-Minute Intervals)

Truck %	Flow Rate_{15%} (vph)	Flow Rate at SFI_{Max} (vph)	Flow Rate_{15%} (pcphpl)	Flow Rate at SFI_{Max} (pcphpl)
5	1290	1216	1386	1307
10	1210	1144	1390	1314
20	1040	984	1350	1277
30	940	887	1360	1283
40	870	826	1388	1318
Standard Deviation			16.57	16.70
Composite Standard Deviation			16.63	
Optimum PCE			2.49	

The PCE that minimized variation between equivalent flow rates at capacity were 2.69 and 2.49 for 15-minute and 5-minute volumes, respectively. These are both substantially higher than the default value of 2.0 recommended in the HCM for level terrain, which the study work zone site exhibited. This finding suggests that the impact of trucks is much higher at freeway work zones than basic freeway segments, and aligns well with findings from the field data used to develop the VISSIM model. Recalling the time headway distributions from Chapter Three, the mean headway for trucks was 3 seconds, while that for passenger cars was just below 2 seconds, a multiplicative difference of 1.5. Given that these headways were often measured during queue discharge conditions, it is likely that the acceleration and deceleration characteristics of heavy vehicles are primarily to blame. Such an assertion would coincide well with Sarasua’s findings, that PCEs increase as average speed decreases, with a maximum value of 2.47 observed at speeds less than 15 mph. Likewise, Geistefeldt concluded that fewer and narrower lanes lead to larger capacity-based PCEs, conditions that are both reflected in the presence of a 2-1 freeway work zone lane closure.

Based on these results, a PCE of 2.0 is not recommended for use with the data obtained from this study, and analyses involving sites with varying lane configurations, lateral clearance, terrain, and work intensity should convert flow rates with caution. Moreover, future study should

be considered to develop a set of PCE values applicable to work zones based on prevailing site characteristics. Accordingly, the models presented in the next section should be applied as-is in units of vehicles per hour.

4.4.3 Development of a Freeway Work Zone Lane Closure Analysis Tool

The culmination of this thesis was the development of the first component of a full-scale lane closure analysis tool for rural freeway work zones. When complete, practitioners will have access to a spreadsheet tool that defines work zone capacity based on the probability of queue formation, rather than a static pre-breakdown or queue discharge flow rate. The advantages of this approach are twofold, as the model accounts for the stochastic nature of capacity while giving users the ability to define their tolerance for risk when selecting a volume threshold. Since differences in breakdown probability observed between right- and left-side lane closures fell within the margin of error of probability estimates, only the left-side models were used in developing tools for 5-minute and 15-minute flow rates. It is anticipated that most users will be able to obtain 15-minute volume data from AADT values, K factors, D factors, and a peak hour factor, but finding 5-minute data may prove more difficult. As a result, only the 15-minute product will be presented in the body of this thesis, but a 5-minute model was developed as well and will be made available to users.

For the final model to be useful to agencies and practitioners, it will need to account for a wide range of truck percentages since lane closures may be in place at any hour of the day. Accordingly, the experiment was designed to capture the practical range of values that may be observed at a rural freeway work zone when overall volumes are high enough that there is a risk of queueing. However, even with Weibull distributions for 5%, 10%, 20%, 30%, and 40% trucks, one may ask: “What would the capacity of a facility be if there were 25% trucks?” Any

number of intermediate truck percentages could be addressed in the previous question, so a methodology for developing fully flexible probabilistic capacity distributions was sought after. Knowing that any Weibull distribution can be constructed if the scale and shape parameters, β and γ , are known, these values were investigated to determine if any noticeable trends occurred as the percentage of trucks changed. Table 4-5 contains these parameters for each case at 15-minute aggregation intervals.

Table 4-5: Summary of Weibull Shape and Scale Parameters (Left-Side Closure, 15-Minute Intervals)

Truck %	Scale	Δ Scale	Shape	Δ Shape
5	1294.91	--	26.16	--
10	1196.04	98.87	23.15	3.01
20	1072.78	123.27	19.68	3.47
30	943.21	129.56	20.90	-1.22
40	846.36	96.85	20.59	0.32
Average	1070.66	112.14	22.10	1.39

The table shows that the scale parameter decreases steadily with increasing truck percentage, while the shape parameter is only slightly variable. This is intuitive, as the scale parameter associated with a Weibull distribution is always equal to the x-value corresponding to a cumulative probability of 63.2%. Thus, as intermediate points determining capacity (such as a 15% probability of breakdown) decrease, so does the scale parameter. On the contrary, the shape parameter determines how steeply or flatly the Weibull curve transitions from probabilities of 0% to 100%, which was not observed to change much between cases. Ultimately, regression and linear interpolation were found most appropriate for estimating the scale and shape parameters, respectively.

Considering that only five data points were used to estimate the best-fit curve for the scale parameter, Excel's trendline functionality was considered sufficient for this analysis. The

data was fit to linear, exponential, polynomial, and logarithmic functions to determine which best fit the data and followed realistic trends beyond the upper and lower bounds of the truck percentages studied. In the end, the exponential function was found to estimate the known Weibull scale parameter most closely while also providing realistic decreasing behavior beyond 40% trucks. Having said that, extreme values of truck percentage greater than 50% are not recommended for use with this tool. Figure 4-6 shows the best-fit exponential curve and equation for the Weibull scale parameter at 15-minute aggregation intervals.

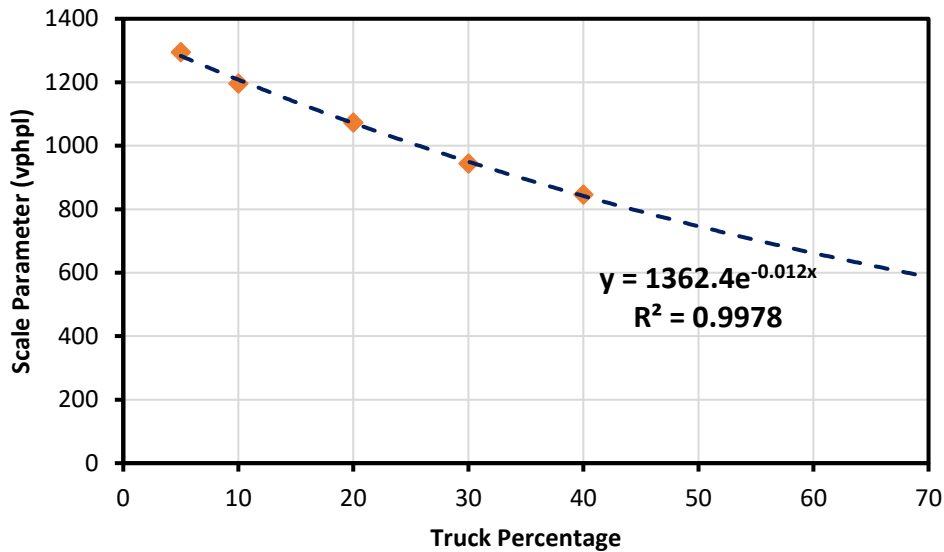


Figure 4-6: Regression on Weibull Scale Parameter (15-Minute Intervals)

Using the equation in Figure 4-6 and linear interpolation between the points in Table 4-5, the Weibull scale and shape parameters could be estimated for any input truck percentage. The validity of each estimate was verified using two criteria: (1) the estimated scale parameters did not differ greatly from that for each known truck percentage; (2) Weibull distributions at intermediate truck percentages (i.e. 7.5%, 15%, 25%, 35%, and 45%) plotted as expected between the curves for preceding and subsequent truck percentages. The first criterion was

easily satisfied, as the scale parameter differed by 1% or less and the curves all plotted virtually on top of those calculated using survival analysis. The test results for the second of these two criteria are shown in Figure 4-7, where each estimated distribution fell completely between those for neighboring truck percentages. Thus, the functions used to approximate these Weibull distributions were adopted for the preliminary lane closure analysis tool. A nearly identical procedure was followed for 5-minute aggregation intervals and led to similar findings.

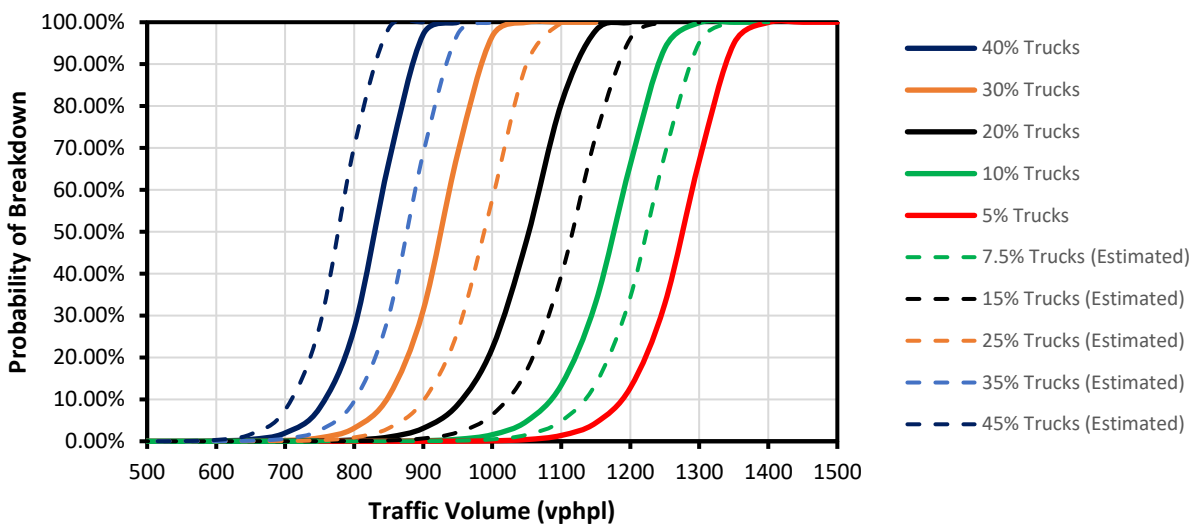


Figure 4-7: Composite Breakdown Probability Model Verification (15-Minute Intervals)

Finally, a beta version of a user interface was developed in Microsoft Excel to demonstrate application of the final model by decision makers. It should be noted that the scope of this thesis did not include examination of additional factors that would be necessary to developing a complete, robust work zone capacity tool. For this reason, the number of input parameters is small and adjustments to any capacity estimates would likely be necessary. That said, after selecting a truck percentage and desired level of risk, the user could apply supplemental multiplicative factors to account for variables such as work type and intensity,

terrain, and lateral clearance if desired. For guidance on the selection of these factors, the reader should refer to outside sources such as the HCM or material provided by their governing state agency. A screenshot from the first version of a capacity analysis spreadsheet tool for 2-1 rural freeway work zones is presented in Figure 4-8.

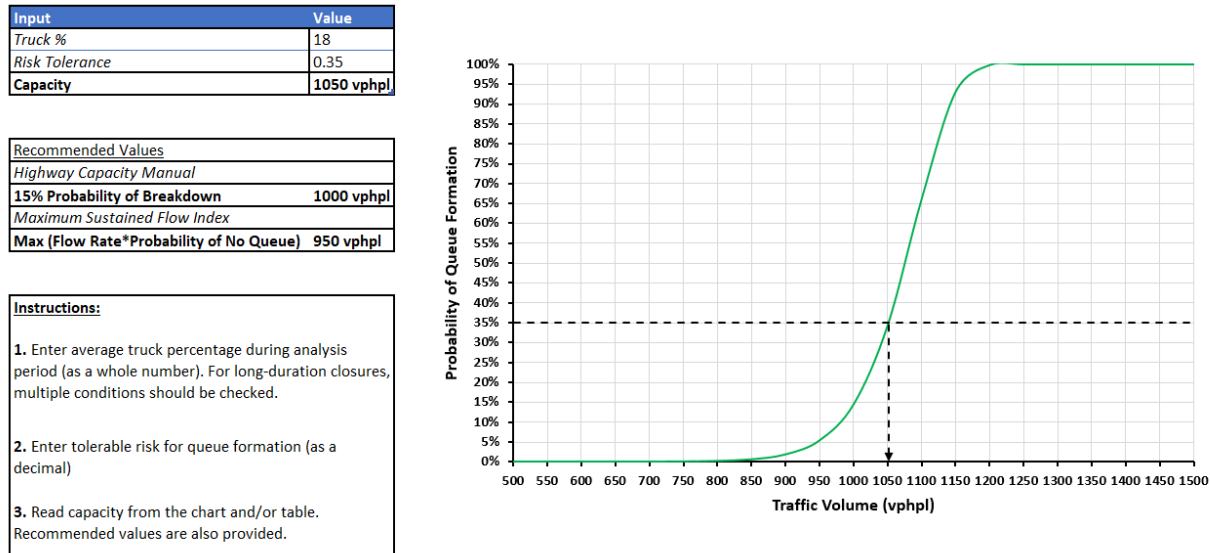


Figure 4-8: Beta Version of Rural Freeway Work Zone Capacity Analysis Tool

The figure provides an example for a 2-1 rural freeway work zone lane closure with an average prevailing truck percentage of 18% and a queue risk tolerance of 35%. Volume characteristics should ideally be collected at the analysis site during all hours that a lane closure may be in place so that accurate 15-minute flow rates and truck percentages are reflected in capacity estimates. However, information from nearby permanent counting stations may be used with caution to predict values like those above for time periods of interest. In this example, the specified input variables yielded a probabilistic capacity of 1,050 vphpl, with a 35% chance of queue formation. In the block below, values of 1,000 vphpl and 950 vphpl are recommended based on the HCM-specified 15% probability of breakdown and maximum sustained flow index,

respectively. The field data collected for this thesis contained several peak periods with an average truck percentage near 18% and seemed to verify most closely with guidance from the HCM. Nevertheless, this product will allow for flexibility when site conditions and tolerance for queue formation vary.

4.5 SUMMARY

In summary, Chapter Four began by describing the methodology required to clean, aggregate, and analyze simulated speed and flow data such that a series of breakdown probability distributions could be constructed. The most critical components of this methodology were: (1) the definition of breakdown identification algorithms to classify flow records as uncongested or congested; (2) the execution of survival analysis to build empirical breakdown probability curves; (3) the fitting of Weibull distributions to these truncated curves through an iterative optimization process.

Next, best-fit Weibull distributions for different truck percentages, lane closure side, and time interval were compared to determine the influence of each independent variable on breakdown probability. It was concluded that the effect of lane closure side was negligible, but truck percentage exhibited a strong, negative correlation with the probability of queue formation. To quantify the effect of heavy vehicles, capacity-based PCEs were calculated and found to be much higher than the default values recommended in the HCM. Specifically, PCEs of 2.69 and 2.49 were calculated for flow rates gathered at 15- and 5-minute intervals, respectively. Finally, the experiment data was combined to develop a preliminary capacity estimation tool for rural 2-1 freeway work zone lane closures. While this current tool is skeletal in nature, it provides flexible estimates of capacity based on truck percentage and agency-specific risk tolerance. Furthermore,

it lays the framework for future efforts incorporating additional input variables such as lane closure configuration, terrain, and work intensity.

CHAPTER FIVE: CONCLUSIONS AND RECOMMENDATIONS

5.1 INTRODUCTION

The current state of the National Highway System often necessitates that agencies interrupt normal traffic operations for maintenance and capacity improvements. With nearly 9 million lane-miles of public roadway and an economy driven by the automobile, these interruptions are inevitable, but the significant safety and mobility impacts associated with queueing at freeway work zones are mitigable. The current methodology in the 6th edition of the HCM is a vast improvement over historical work zone capacity guidance, but approaches the issue differently than research suggests agencies and practitioners should. Namely, a capacity defined by the mean queue discharge is deterministic and fails to account for the stochastic nature of traffic flow and breakdown. Rather, the frequency of rear-end crashes and high speed differentials at freeway work zones warrants that the risk of queue formation always be minimized.

Rural freeway facilities are particularly important, as they compose more than half of all interstate lane-miles in the United States and account for 30% of all interstate vehicle miles of travel (Federal Highway Administration 2016). Despite lessened exposure compared to urban facilities, rural freeway segments pose an increased safety risk because drivers are less expectant of changes to the roadway environment and given increased opportunities to travel at high speeds. In 2015, NHTSA findings substantiated this claim by finding that 43% of all fatal interstate crashes occurred in rural areas (NHTSA 2016a).

This thesis addressed these core issues by developing a methodology for obtaining probabilistic capacity estimates at rural freeway work zones using field data and simulation. The results of the analyses conducted culminated in a preliminary version of a spreadsheet tool that provides users with a suggested volume threshold based on the average site truck percentage and desired risk of queue formation. Outputs from this tool are applicable to rural freeways across the southeastern United States and provide guidance for agencies who wish to minimize the safety and mobility concerns associated with queueing at work zone lane closures.

5.2 CONCLUSIONS

This research sought to accomplish three main objectives:

1. Assess the validity of microsimulation outputs as a means to obtain probabilistic estimates of capacity at rural freeway work zone lane closures
2. Develop breakdown probability models for 2-1 lane closures with varying truck percentage and lane closure side to determine the effect of these variables on the likelihood of queue formation
3. Provide a framework for the continuation of future research, which will develop models for other lane closure configurations commonly experienced on rural and urban freeway facilities

First, field data was collected at a single-lane work zone on I-59/I-20 southbound near Tuscaloosa, Alabama for 14 days in October 2016. Site characteristics were determined to be typical of rural freeways in the southeastern United States and used to calibrate and validate a model in VISSIM. Critical components of model development included the use of time headway distributions and modified truck characteristics obtained from field observations and literature.

Comparison of simulation outputs to field-collected data matched speed profiles reasonably well and yielded differences in mean queue discharge rates of less than 2%. Based on these findings, it was determined that microsimulation was an appropriate tool for collecting large samples of data for hypothetical freeway work zones.

Second, a set of generalizable traffic conditions were developed and intended to capture the full range of variability in traffic volume and truck percentage that would be observed at rural freeway facilities similar to the one studied here. A total of 40 distinct combinations of truck percentage, lane closure side, and traffic volumes were converted to VISSIM inputs and simulated 50 times each using different random number seeds to obtain a sufficient amount of speed and flow data. Kaplan-Meier survival analysis was utilized to estimate empirical breakdown probability distributions for each case, which were then fitted to Weibull distributions. This approach was an extension of existing methodology found in the literature and the 6th edition of the *Highway Capacity Manual* for metered on ramps and other sources of recurring congestion. However, its use for freeway work zones is thought to make a unique contribution to the existing body of highway capacity research.

Comparison of these distributions showed that lane closure side has a minor but practically insignificant effect on the probability of queue formation, regardless of truck percentage. Conversely, truck percentage has a noteworthy effect on the traffic volume at which queues will form. This influence on capacity was quantified by developing freeway work-zone specific PCEs, which were found to be substantially higher than those provided as defaults in the *Highway Capacity Manual*.

Finally, subsets of the fitted Weibull distributions were combined to develop a draft version of a work zone capacity analysis tool in Microsoft Excel. The tool will allow a user to specify a

site-specific truck percentage and tolerable risk for queue formation, then return a suggested volume threshold. The outputs from this tool may be used by agencies and practitioners to make defensible lane closure scheduling decisions based on stochastic capacity estimates, rather than deterministic values or anecdotal experience alone.

5.3 RECOMMENDATIONS FOR FUTURE RESEARCH

This thesis approached the issue of work zone capacity measurement in a unique manner by producing throughput estimates based on the probability of queue formation, rather than through traditional deterministic methods. While the results of this work make a significant contribution to the existing body of literature, they only provide a framework for the completion of a larger project funded by the Southeastern Transportation Research, Innovation, Development, and Education Center (STRIDE). Other phases of this project and future research may build upon the findings of this thesis by:

1. Extending field data collection efforts
 - a. Data should be collected at rural freeway work zone sites in different states and with various lane closure configurations (e.g. 2-1, 3-2, 3-1), traffic characteristics (e.g. upstream lane distributions by vehicle type), and work types (e.g. resurfacing, bridge repair, major widening projects).
 - b. Video cameras should be used to verify driving behavior near the bottleneck location and identify atypical occurrences such as traffic incidents or the movement of construction equipment in and out of the work area.
2. Increasing the number of modeled input variables
 - a. Data collection at other sites will allow for additional variables such as lane closure configuration, work type and intensity, free flow speed, merge control

strategy, and terrain to be modeled and included as user inputs in an expanded lane closure analysis tool.

- b. Breakdown probability distributions should be combined with estimated queue discharge rates to provide approximations of queue length and delay for agencies that will tolerate a queue but wish to minimize its impacts.
3. Accounting for future changes to vehicle characteristics and travel behavior
 - a. The effect of varying levels of market penetration of automated and connected passenger cars and trucks should be incorporated in a supplemental model given that these technology advancements may soon be realized.

The methodologies, results, conclusions, and recommendations presented provide promise for future study and application of rural freeway work zone safety and mobility best practices. The decline of the structural and functional adequacy of the National Highway System suggests that work zones will become more prevalent and that careful attention to their design and operation is critical. Therefore, agencies and practitioners should make data-driven decisions based on the results of this thesis and similar research.

REFERENCES

1. AASHTO. (2011). “A Policy on Geometric Design of Highways and Streets”. Washington, D.C.
2. Abdelmohsen, A. Z., and El-Rayes, K. (2016). “Optimal Trade-Offs Between Construction Cost and Traffic Delay for Highway Work Zones.” *ASCE Journal of Construction Engineering and Management*, 142(7).
3. Al-Kaisy, A., and Hall, F. (2001). “Examination of Effect of Driver Population at Freeway Reconstruction Zones.” *Traffic Flow Theory and Highway Capacity 2001: Highway Operations, Capacity, and Traffic Control*, (1776), 35–42.
4. Al-Kaisy, A., and Hall, F. (2003). “Guidelines for Estimating Capacity at Freeway Reconstruction Zones.” *ASCE Journal of Transportation Engineering*, 129(5), 572–577.
5. Al-Kaisy, A., Hall, F. L., and Reisman, E. (2002). “Developing Passenger Car Equivalent for Heavy Vehicles on Freeways During Queue Discharge Flow.” *Transportation Research Part A: Policy and Practice*, 36A(8), 725–742.
6. Asgharzadeh, M. A., and Kondyli, A. (2018). “Comparison of Highway Capacity Estimation Methods.” *Presented at the Transportation Research Board 97th Annual Meeting*, Washington, D.C.
7. Benekohal, R. F., Kaja-Mohideen, A.-Z., and Chitturi, M. V. (2003). “Evaluation of Construction Work Zone Operational Issues: Capacity, Queue, and Delay.” *Report No. ITRC FR 00/01-4*.
8. Bham, G., Khazraee, S., and Initiative, S. (2011). “Missouri Work Zone Capacity:

- Results of Field Data Analysis.” *Report No. MATC-MST: 118*.
9. Brilon, W., Geistefeldt, J., and Regler, M. (2005). “Reliability of Freeway Traffic Flow: A Stochastic Concept of Capacity.” *Proceedings of the 16th International Symposium on Transportation and Traffic Theory*, (July), 125–144.
 10. Chatterjee, I., Edara, P., Menneni, S., and Sun, C. (2009). “Replication of Work Zone Capacity Values in a Simulation Model.” *Transportation Research Record: Journal of the Transportation Research Board*, 2130, 138–148.
 11. Chitturi, M. V, and Benekohal, R. F. (2008). “Calibration of VISSIM for Freeways.” *Presented at the Transportation Research Board 87th Annual Meeting*, Washington, D.C.
 12. Chow, A. H. F., Lu, X. Y., and Qiu, T. Z. (2009). “An Empirical Analysis of Freeway Traffic Breakdown Probability Based on Bivariate Weibull Distribution.” *Presented at the 12th IFAC Symposium on Transportation Systems*, IFAC, Redondo Beach, CA.
 13. “Comprehensive Truck Size and Weight Study.” (2000). *Report No. FHWA-PL-00-029*, FHWA, Washington, D.C.
 14. Dixon, K., Hummer, J., and Lorscheider, A. (1996). “Capacity for North Carolina Freeway Work Zones.” *Transportation Research Record: Journal of the Transportation Research Board*, 1529, 27–34.
 15. Dong, J., Houchin, A., Shafieirad, N., Lu, C., Hawkins, N., and Knicherbocker, S. (2015). “VISSIM Calibration for Urban Freeways.” *Report No. INTRANS 14-487*. Ames, IA.
 16. Dowling, R., Skabardonis, A., and Alexiadis, V. (2004). “Traffic Analysis Toolbox Volume III : Guidelines for Applying Traffic Microsimulation Modeling Software.” *Report No. FHWA-HRT-04-040*. Washington, D.C.

17. Drake, J. S., Schofer, J., and May, A. D. J. (1967). "A Statistical Analysis of Speed-Density Hypotheses." *Highway Research Record*, (154), 112–117.
18. Edara, P., and Chatterjee, I. (2010). "Multivariate Regression for Estimating Driving Behavior Parameters in Work Zone Simulation to Replicate Field Capacities." *Transportation Letters*, 2(3), 175–186.
19. Edie, L. (1961). "Car-Following and Steady-State Theory for Non-Congested Travel." *Operations Research*, 9(1), 66–76.
20. Elefteriadou, L. (2014). *An Introduction to Traffic Flow Theory*. Springer, New York.
21. Elefteriadou, L., Arguea, D., Heaslip, K., and Kondyli, A. (2007). "Impact of Trucks on Arterial LOS and Freeway Work Zone Capacity (Part B: Freeway Work Zone Capacity)." *Report No. FDOT BD-545-51*. Gainesville, FL.
22. Elefteriadou, L., Hall, F., Brilon, W., Roess, R. P., and Romana. (2006). "Revisiting the Definition and Measurement of Capacity." *Presented at the 5th International Symposium on Highway Capacity and Quality of Service*, Yokohoma, Japan.
23. Elefteriadou, L., Roess, R. P., and McShane, W. R. (1995). "Probabilistic Nature of Breakdown at Freeway Merge Junctions." *Transportation Research Record: Journal of the Transportation Research Board*, 1484, 80–89.
24. Federal Highway Administration. (2015). *Status of the Nation's Highways, Bridges, and Transit: Conditions and Performance*.
25. Federal Highway Administration. (2016). *Highway Statistics 2015*. Washington, D.C.
26. Federal Highway Administration. (2017). "Work Zone Facts and Statistics." Federal Highway Administration,
<https://ops.fhwa.dot.gov/wz/resources/facts_stats/mobility.htm> (Aug. 17, 2017).

27. Florida Department of Transportation. (2014). *Traffic Analysis Handbook: A Reference for Planning and Operations*. Tallahassee, FL.
28. Geistefeldt, J. (2009). "Estimation of Passenger Car Equivalents Based on Capacity Variability." *Transportation Research Record: Journal of the Transportation Research Board*, 2130, 1–6.
29. Gomes, G., May, A., and Horowitz, R. (2004). "Congested Freeway Microsimulation Model Using VISSIM." *Transportation Research Record: Journal of the Transportation Research Board*, 1876, 71–81.
30. Hancher, D., and Taylor, T. (2001). "Nighttime Construction Issues." *Transportation Research Record: Journal of the Transportation Research Board*, 1761, 107–115.
31. Harwood, D. W., Torbic, D. J., Richard, K. R., Glauz, W. D., and Elefteriandou, L. (2003). *NCHRP Report 505: Review of Truck Characteristics as Factors in Roadway Design*. Washington, D.C.
32. Heaslip, K., Kondyli, A., Arguea, D., Elefteriadou, L., and Sullivan, F. (2009). "Estimation of Freeway Work Zone Capacity Through Simulation and Field Data." *Transportation Research Record: Journal of the Transportation Research Board*, 2130, 16–24.
33. Heiden, N. Von Der, and Geistefeldt, J. (2016). "Capacity of Freeway Work Zones in Germany." *Transportation Research Procedia*, Elsevier B.V., 15, 233–244.
34. "Highway Capacity Manual 6th Edition: A Guide for Multimodal Mobility Analysis." (2016). Transportation Research Board, Washington, D.C.
35. Houchin, A. J. (2015). "An Investigation of Freeway Standstill Distance , Headway , and Time Gap Data in Heterogeneous Traffic in Iowa." Iowa State University Theses and

Dissertations.

36. Hu, J., Schroeder, B. J., and Roupail, N. M. (2012). "Rationale for Incorporating Queue Discharge Flow into Highway Capacity Manual Procedure for Analysis of Freeway Facilities." *Transportation Research Record: Journal of the Transportation Research Board*, 2286, 76–83.
37. Jia, A., Williams, B. M., and Roupail, N. M. (2010). "Identification and Calibration of Site-Specific Stochastic Freeway Breakdown and Queue Discharge." *Transportation Research Record: Journal of the Transportation Research Board*, 2188, 148–155.
38. Jiang, X., and Adeli, H. (2003). "Freeway Work Zone Traffic Delay and Cost Optimization Model." *ASCE Journal of Transportation Engineering*. 129(3), 230–241.
39. Jiang, Y. (1999). "Traffic Characteristics and Estimation of Traffic Delays and User Costs at Indiana Freeway Work Zones." *Report FHWA/INDOT No. SPR-2121*.
40. Kan, X. D., Ramezani, H., and Benekohal, R. F. (2014). "Calibration of VISSIM for Freeway Work Zones with Time-Varying Capacity." *Presented at the Transportation Research Board 93rd Annual Meeting*. Washington, D.C.
41. Kaplan, E. L., and Meier, P. (1958). "Nonparametric Estimation from Incomplete Observations." *Journal of the American Statistical Association*, 53(282), 457–481.
42. Kim, T., and Lovell, D. J. (2001). "A New Methodology to Estimate Capacity for Freeway Work Zones." *Presented at the Transportation Research Board 80th Annual Meeting*.
43. Kondyli, A., Elefteriadou, L., Brilon, W., Hall, F. L., Persaud, B., and Washburn, S. (2013). "Development and Evaluation of Methods for Constructing Breakdown Probability Models." *ASCE Journal of Transportation Engineering*, 139(9), 931–940.

44. Krammes, R. A., and Lopez, G. O. (1994). "Updated Capacity Values for Short-Term Freeway Work Zone Lane Closures." *Transportation Research Record: Journal of the Transportation Research Board*, 1442, 49–56.
45. Lorenz, M., and Elefteriadou, L. (2001). "Defining Freeway Capacity as Function of Breakdown Probability." *Transportation Research Record: Journal of the Transportation Research Board*, 1776, 43–51.
46. Lownes, N. E., and Machemehl, R. B. (2006). "Sensitivity of Simulated Capacity to Modification of VISSIM Driver Behavior Parameters." *Transportation Research Record: Journal of the Transportation Research Board*, 1988, 102–110.
47. MH Corbin. (2016). "NC350 BlueStar Portable Traffic Analyzer."
<<http://www.mhcorbin.com/wp-content/uploads/bsk-pdf-manager/2016/12/NC350-v2-002.pdf>> (Jan. 15, 2018).
48. Middleton, D., Venglar, S., Quiroga, C., and Lord, D. (2006). "Strategies for Separating Trucks from Passenger Vehicles." *Report No. FHWA/TX-07/0-4663-2*. College Station, TX.
49. Minderhoud, M., Botma, H., and Bovy, P. (1997). "Assessment of Roadway Capacity Estimation Methods." *Transportation Research Record: Journal of the Transportation Research Board*, 1572, 59–67.
50. NHTSA. (2015). "Fatality Analysis Reporting System (FARS)."
<<https://www.nhtsa.gov/research-data/fatality-analysis-reporting-system-fars>> (Aug. 21, 2017).
51. NHTSA. (2016a). *Traffic Safety Facts 2015*. Washington, D.C.
52. NHTSA. (2016b). *Rural/Urban Comparison of Traffic Fatalities*. Washington, D.C.

53. Park, B. B., and Won, J. (2006). *Microscopic Simulation Model Calibration and Validation Handbook*. Charlottesville, VA.
54. Park, S.-B., Douglas, K. D., Griffith, A. S., and Haas, K. J. (2002). “Factors of Importance for Determining Daytime Versus Nighttime Operations in Oregon.” *Transportation Research Record: Journal of the Transportation Research Board*, 1813, 305–313.
55. Persaud, B., Yagar, S., and Brownlee, R. (1998). “Exploration of the Breakdown Phenomenon in Freeway Traffic.” *Transportation Research Record: Journal of the Transportation Research Board*, 1567, 64–69.
56. “PTV VISSIM 10 User Manual.” (2017). PTV Group, Karlsruhe, Germany.
57. Ramadan, O., and Sisiopiku, V. (2016). “Impact of Bottleneck Merge Control Strategies on Freeway Level of Service.” *Transportation Research Procedia*, Elsevier B.V., 15, 583–593.
58. Ramezani, H., and Benekohal, R. F. (2012). “Work Zones as a Series of Bottlenecks.” *Transportation Research Record: Journal of the Transportation Research Board*, 2272, 67–77.
59. Rebholz, F. E., Al-Kaisy, A., Nassar, K., Liu, L. Y., El-Rayes, K., and Soibelman, L. (2004). “Nighttime Construction: Evaluation of Construction Operations.” *Report No. ITRC FR 00/01-5*.
60. Roess, R. P., and Prassas, E. S. (2016). *The Highway Capacity Manual: A Conceptual and Research History*. Springer, New York.
61. Sarasua, W. A., Davis, W. J., Clarke, D. B., Kottapally, J., and Mulukutla, P. (2004). “Evaluation of Interstate Highway Capacity for Short-Term Work Zone Lane Closures.”

- Transportation Research Record: Journal of the Transportation Research Board*, 1877, 85–94.
62. Sarasua, W., Davis, W., Chowdhury, M., and Ogle, J. (2006). “Estimating Interstate Highway Capacity for Short-Term Work Zone Lane Closures: Development of Methodology.” *Transportation Research Record: Journal of the Transportation Research Board*, 1948, 45–57.
63. Schrank, D., Eisele, B., Lomax, T., and Bak, J. (2015). *2015 Urban Mobility Scorecard*. Texas A&M Transportation Institute.
64. Shojaat, S., Geistefeldt, J., Parr, S. A., Wilmot, C. G., and Wolshon, B. (2016). “Sustained Flow Index.” *Transportation Research Record: Journal of the Transportation Research Board*, 2554, 158–165.
65. Sisiopiku, V. P., and Ramadan, O. E. M. (2016). “Evaluation of Traffic Control Options in Work Zones.” *Report No. 2016-001*. Southeastern Transportation Research, Innovation, Development, and Education Center.
66. Tang, Y., and Chien, S. (2008). “Scheduling Work Zones for Highway Maintenance Projects: Considering a Discrete Time-Cost Relation.” *Transportation Research Record: Journal of the Transportation Research Board*, 2055, 21–30.
67. Trask, L., Aghdashi, B., Schroeder, B., and Roupail, N. (2015). “FREEVAL-WZ Users Guide.” North Carolina State University, Raleigh, NC.
68. Turochy, R. E., and Smith, B. L. (2000). “New Procedure for Detector Data Screening in Traffic Management Systems.” *Transportation Research Record: Journal of the Transportation Research Board*, 1727, 127–131.
69. Turochy, R. E., Timm, D. H., and Mai, D. (2015). *Development of Alabama Traffic*

Factors for Use in Mechanistic-Empirical Pavement Design. Auburn, AL.

70. Venugopal, S., and Tarko, A. (2001). “Investigation of Factors Affecting Capacity at Rural Freeway Work Zones.” *Presented at the Transportation Research Board 80th Annual Meeting*, Washington, D.C.
71. Washington State Department of Transportation. (2014). *Protocol for VISSIM Simulation*.
72. Weng, J., and Meng, Q. (2013). “Estimating Capacity and Traffic Delay in Work Zones: An Overview.” *Transportation Research Part C: Emerging Technologies*, 35, 34–45.
73. Weng, J., and Yan, X. (2016). “Probability Distribution-Based Model for Work Zone Capacity Prediction.” *Journal of Advanced Transportation*, 50(2), 165–179.
74. Weng, J., and Yang, X. (2014). “New Methodology to Determine Work zone Capacity Distribution.” *Transportation Research Record: Journal of the Transportation Research Board*, 2461, 25–31.
75. Woody, T. (2006). “Calibrating Freeway Simulation Models in VISSIM.” University of Washington Theses and Dissertations.
76. Yang, G., Xu, H., Wang, Z., and Tian, Z. (2016). “Truck Acceleration Behavior Study and Acceleration Lane Length Recommendations for Metered On-Ramps.” *International Journal of Transportation Science and Technology*, 5(2), 93–102.
77. Yeom, C., Hajbabaie, A., Schroeder J, B., Vaughan, C., Xuan, X., and Roupail M, N. (2015). “Innovative Work Zone Capacity Models from Nationwide Field and Archival Sources.” *Transportation Research Record: Journal of the Transportation Research Board*, 2485, 51–60.
78. Yeom, C., Roupail, N. M., Rasdorf, W., and Schroeder, B. J. (2016). “Simulation

Guidance for Calibration of Freeway Lane Closure Capacity.” *Transportation Research Record: Journal of the Transportation Research Board*, 2553, 82–89.

**APPENDIX A:
FIELD-COLLECTED DATA AND VISSIM INPUTS**

Table A-1: Sensor Vehicle Length Frequencies

Sensor 96		Sensor 97		Sensor 98		Sensor 99		Sensor 100		Sensor 101		Sensor 102		Sensor 103		Sensor 104	
<i>Length (ft)</i>	<i>Freq.</i>	<i>Length (ft)</i>	<i>Freq.</i>	<i>Length (ft)</i>	<i>Freq.</i>	<i>Length (ft)</i>	<i>Freq.</i>	<i>Length (ft)</i>	<i>Freq.</i>	<i>Length (ft)</i>	<i>Freq.</i>	<i>Length (ft)</i>	<i>Freq.</i>	<i>Length (ft)</i>	<i>Freq.</i>	<i>Length (ft)</i>	<i>Freq.</i>
0	65	0	152	0	248	0	130	0	68	0	206	0	125	0	163	0	171
1	461	1	469	1	596	1	684	1	481	1	199	1	427	1	260	1	359
2	541	2	454	2	676	2	900	2	1159	2	288	2	776	2	350	2	605
3	560	3	483	3	739	3	1065	3	1460	3	300	3	1021	3	427	3	709
4	393	4	446	4	527	4	792	4	1153	4	282	4	857	4	355	4	630
5	337	5	421	5	441	5	621	5	760	5	259	5	824	5	352	5	656
6	353	6	504	6	439	6	542	6	695	6	298	6	766	6	315	6	755
7	431	7	674	7	461	7	585	7	694	7	358	7	809	7	360	7	1004
8	605	8	806	8	540	8	615	8	673	8	440	8	724	8	349	8	1364
9	852	9	1064	9	669	9	623	9	575	9	574	9	858	9	376	9	1920
10	1099	10	1464	10	813	10	704	10	526	10	719	10	1003	10	444	10	2880
11	1374	11	1985	11	982	11	824	11	598	11	997	11	1243	11	502	11	4273
12	1662	12	2807	12	1234	12	1032	12	747	12	1251	12	1609	12	621	12	6434
13	2054	13	4248	13	1557	13	1374	13	879	13	1584	13	2067	13	963	13	9490
14	2996	14	5878	14	1992	14	1771	14	1079	14	2083	14	2915	14	1387	14	13056
15	4325	15	6974	15	2590	15	2404	15	1494	15	3027	15	4109	15	1996	15	14635
16	5999	16	7367	16	3876	16	3486	16	1965	16	4186	16	4937	16	3134	16	13714
17	6557	17	6238	17	4768	17	4086	17	2516	17	5179	17	5193	17	3666	17	11154
18	6675	18	4770	18	6125	18	4953	18	3312	18	5903	18	5137	18	3916	18	8608
19	6547	19	3442	19	6827	19	5601	19	4332	19	6090	19	4504	19	3855	19	5919
20	5407	20	2426	20	6720	20	6216	20	4921	20	5872	20	3433	20	3521	20	3749
21	3589	21	1581	21	6473	21	6239	21	5530	21	5275	21	2359	21	3016	21	2242
22	2323	22	1128	22	5795	22	5838	22	5744	22	4379	22	1619	22	2399	22	1526
23	1401	23	939	23	5157	23	5470	23	5504	23	3237	23	1121	23	1819	23	1146
24	867	24	775	24	3970	24	4703	24	4831	24	2154	24	838	24	1243	24	935
25	548	25	631	25	3069	25	3722	25	3829	25	1481	25	703	25	860	25	840
26	373	26	672	26	2104	26	2820	26	2931	26	962	26	601	26	598	26	723
27	291	27	610	27	1388	27	1916	27	2093	27	742	27	576	27	423	27	705

Sensor 96		Sensor 97		Sensor 98		Sensor 99		Sensor 100		Sensor 101		Sensor 102		Sensor 103		Sensor 104	
<i>Length (ft)</i>	<i>Freq.</i>	<i>Length (ft)</i>	<i>Freq.</i>	<i>Length (ft)</i>	<i>Freq.</i>	<i>Length (ft)</i>	<i>Freq.</i>	<i>Length (ft)</i>	<i>Freq.</i>	<i>Length (ft)</i>	<i>Freq.</i>	<i>Length (ft)</i>	<i>Freq.</i>	<i>Length (ft)</i>	<i>Freq.</i>	<i>Length (ft)</i>	<i>Freq.</i>
28	240	28	616	28	1016	28	1230	28	1505	28	524	28	533	28	341	28	651
29	195	29	623	29	680	29	863	29	975	29	416	29	559	29	300	29	671
30	183	30	570	30	563	30	623	30	741	30	406	30	578	30	300	30	708
31	162	31	559	31	502	31	476	31	572	31	384	31	523	31	300	31	706
32	172	32	555	32	368	32	395	32	429	32	336	32	514	32	355	32	681
33	125	33	529	33	328	33	368	33	322	33	347	33	555	33	349	33	644
34	134	34	522	34	327	34	323	34	288	34	353	34	484	34	323	34	564
35	134	35	502	35	329	35	287	35	286	35	338	35	506	35	309	35	541
36	148	36	441	36	269	36	279	36	275	36	302	36	507	36	307	36	542
37	130	37	439	37	275	37	253	37	267	37	312	37	451	37	257	37	482
38	121	38	492	38	278	38	244	38	282	38	312	38	428	38	257	38	436
39	105	39	441	39	227	39	238	39	261	39	311	39	407	39	223	39	398
40	98	40	393	40	250	40	225	40	288	40	294	40	385	40	210	40	340
41	109	41	371	41	227	41	181	41	291	41	314	41	389	41	213	41	339
42	86	42	309	42	203	42	222	42	293	42	276	42	334	42	196	42	322
43	86	43	303	43	189	43	178	43	242	43	279	43	340	43	175	43	306
44	70	44	274	44	209	44	196	44	258	44	227	44	276	44	154	44	334
45	59	45	255	45	206	45	183	45	241	45	253	45	266	45	161	45	306
46	68	46	221	46	193	46	215	46	228	46	219	46	227	46	135	46	334
47	49	47	200	47	194	47	154	47	177	47	239	47	253	47	137	47	376
48	65	48	208	48	145	48	144	48	224	48	237	48	242	48	128	48	403
49	59	49	168	49	139	49	148	49	189	49	212	49	219	49	136	49	436
50	81	50	199	50	124	50	128	50	199	50	198	50	264	50	103	50	455
51	52	51	182	51	129	51	149	51	195	51	205	51	289	51	99	51	569
52	61	52	202	52	143	52	147	52	187	52	183	52	300	52	90	52	657
53	75	53	215	53	134	53	148	53	172	53	205	53	283	53	103	53	727
54	68	54	238	54	134	54	119	54	160	54	200	54	334	54	88	54	879
55	84	55	235	55	121	55	126	55	136	55	236	55	374	55	106	55	1047
56	101	56	274	56	137	56	142	56	172	56	265	56	433	56	114	56	1133

Sensor 96		Sensor 97		Sensor 98		Sensor 99		Sensor 100		Sensor 101		Sensor 102		Sensor 103		Sensor 104	
<i>Length (ft)</i>	<i>Freq.</i>	<i>Length (ft)</i>	<i>Freq.</i>	<i>Length (ft)</i>	<i>Freq.</i>	<i>Length (ft)</i>	<i>Freq.</i>	<i>Length (ft)</i>	<i>Freq.</i>	<i>Length (ft)</i>	<i>Freq.</i>	<i>Length (ft)</i>	<i>Freq.</i>	<i>Length (ft)</i>	<i>Freq.</i>	<i>Length (ft)</i>	<i>Freq.</i>
57	111	57	293	57	111	57	141	57	190	57	275	57	489	57	104	57	1318
58	146	58	316	58	121	58	171	58	188	58	312	58	524	58	105	58	1601
59	141	59	354	59	115	59	177	59	162	59	332	59	621	59	131	59	1834
60	155	60	371	60	138	60	153	60	193	60	379	60	710	60	141	60	2109
61	160	61	441	61	156	61	162	61	166	61	432	61	760	61	166	61	2469
62	197	62	483	62	133	62	171	62	217	62	434	62	866	62	177	62	2752
63	204	63	550	63	170	63	192	63	219	63	516	63	991	63	194	63	2832
64	216	64	560	64	170	64	214	64	262	64	623	64	1153	64	246	64	2906
65	262	65	575	65	183	65	250	65	314	65	603	65	1302	65	271	65	2701
66	250	66	559	66	191	66	223	66	302	66	732	66	1567	66	284	66	2341
67	276	67	444	67	206	67	258	67	380	67	800	67	1628	67	344	67	2213
68	345	68	427	68	281	68	271	68	427	68	907	68	1767	68	365	68	1980
69	430	69	359	69	259	69	314	69	489	69	1050	69	1876	69	450	69	1597
70	432	70	324	70	295	70	337	70	530	70	1168	70	1864	70	463	70	1387
71	438	71	289	71	304	71	371	71	588	71	1320	71	1760	71	568	71	1165
72	454	72	267	72	352	72	405	72	618	72	1432	72	1472	72	594	72	980
73	435	73	222	73	370	73	471	73	705	73	1704	73	1212	73	700	73	768
74	371	74	208	74	440	74	513	74	788	74	1819	74	1035	74	795	74	589
75	299	75	162	75	497	75	571	75	900	75	1972	75	781	75	836	75	541
76	254	76	151	76	517	76	624	76	929	76	2083	76	601	76	956	76	439
77	205	77	133	77	579	77	736	77	1127	77	2281	77	567	77	1100	77	334
78	184	78	154	78	635	78	759	78	1286	78	2328	78	408	78	1121	78	288
79	121	79	121	79	685	79	876	79	1482	79	2315	79	384	79	1178	79	229
80	122	80	124	80	746	80	923	80	1655	80	2130	80	306	80	1182	80	188
81	73	81	115	81	819	81	1045	81	1875	81	2097	81	276	81	994	81	151
82	68	82	87	82	915	82	1106	82	2095	82	1814	82	224	82	830	82	128
83	55	83	94	83	928	83	1121	83	2112	83	1571	83	202	83	699	83	83
84	41	84	82	84	925	84	1033	84	2268	84	1372	84	189	84	570	84	78
85	40	85	86	85	881	85	1068	85	2168	85	1058	85	162	85	446	85	73

Sensor 96		Sensor 97		Sensor 98		Sensor 99		Sensor 100		Sensor 101		Sensor 102		Sensor 103		Sensor 104	
<i>Length (ft)</i>	<i>Freq.</i>	<i>Length (ft)</i>	<i>Freq.</i>	<i>Length (ft)</i>	<i>Freq.</i>	<i>Length (ft)</i>	<i>Freq.</i>	<i>Length (ft)</i>	<i>Freq.</i>	<i>Length (ft)</i>	<i>Freq.</i>	<i>Length (ft)</i>	<i>Freq.</i>	<i>Length (ft)</i>	<i>Freq.</i>	<i>Length (ft)</i>	<i>Freq.</i>
86	27	86	71	86	874	86	905	86	2188	86	914	86	158	86	331	86	53
87	26	87	70	87	770	87	869	87	2010	87	709	87	153	87	289	87	53
88	26	88	44	88	671	88	757	88	1754	88	590	88	142	88	209	88	44
89	19	89	50	89	653	89	618	89	1563	89	456	89	142	89	174	89	33
90	10	90	52	90	515	90	550	90	1293	90	388	90	106	90	141	90	40
91	11	91	51	91	476	91	423	91	1048	91	293	91	106	91	111	91	26
92	16	92	48	92	365	92	322	92	880	92	222	92	96	92	85	92	21
93	17	93	52	93	302	93	290	93	725	93	159	93	86	93	73	93	28
94	16	94	37	94	279	94	194	94	590	94	148	94	62	94	50	94	31
95	21	95	37	95	210	95	188	95	494	95	117	95	83	95	50	95	18
96	7	96	32	96	178	96	170	96	405	96	95	96	62	96	33	96	23
97	11	97	23	97	128	97	112	97	316	97	81	97	48	97	34	97	25
98	12	98	33	98	111	98	99	98	267	98	69	98	34	98	35	98	32
99	12	99	24	99	108	99	70	99	244	99	61	99	37	99	18	99	16

Table A-2: Vehicle Length Summary (Passenger Cars)

Sensor	Mean	Std. Dev.	Lower Bound Length (ft)	Upper Bound Length (ft)
96	17.28	4.1	9.08	25.48
97	16.97	5.62	5.72	28.21
98	20.07	5.45	9.16	30.97
99	20.69	5.65	9.39	31.99
100	21.75	4.76	12.24	31.27
101	18.84	4.57	9.71	27.98
102	17.81	5.57	6.67	28.95
103	18.63	4.5	9.63	27.63
104	15.5	3.8	7.91	23.1
<i>Weighted Average</i>	<i>18.92</i>	<i>6.57</i>	<i>5.79</i>	<i>32.06</i>

Table A-3: Vehicle Length Summary (Tractor-Trailers)

Sensor	Mean	Std. Dev.	Lower Bound Length (ft)	Upper Bound Length (ft)
96	68.3	6.7	54.9	81.8
97	65.1	8.6	47.9	82.2
98	81.1	8.7	63.8	98.5
99	79.5	9.3	61.0	98.0
100	82.0	8.9	64.2	99.7
101	75.8	8.4	58.9	92.7
102	68.9	7.7	53.5	84.2
103	76.4	7.1	62.1	90.6
104	63.3	6.8	49.7	76.9
<i>Weighted Average</i>	<i>72.6</i>	<i>11.1</i>	<i>50.3</i>	<i>94.9</i>

Table A-4: Free Flow Speed Distribution (3.5 Miles Upstream)

		Cars							
<i>Sensor</i>	<i>Free Flow Volume</i>	<i>Speed Percentile (mph)</i>							
		Mean	10th	25th	35th	50th	75th	85th	95th
96 (LL)	56733	71	63	67	69	70	74	77	83
100 (RL)	55187	81	69	76	79	82	88	91	96
<i>Weighted Avg.</i>	--	75.9	66.0	71.4	73.9	75.9	80.9	83.9	89.4

		Trucks							
<i>Sensor</i>	<i>Free Flow Volume</i>	<i>Speed Percentile (mph)</i>							
		Mean	10th	25th	35th	50th	75th	85th	95th
96 (LL)	6855	66	61	64	65	66	69	71	74
100 (RL)	37718	75	67	71	72	75	79	81	85
<i>Weighted Avg.</i>	--	73.6	66.1	69.9	70.9	73.6	77.5	79.5	83.3

Table A-5: Free Flow Speed Distribution (2.5 Miles Upstream)

		Cars							
<i>Sensor</i>	<i>Free Flow Volume</i>	<i>Speed Percentile (mph)</i>							
		Mean	10th	25th	35th	50th	75th	85th	95th
97 (LL)	59774	64	55	59	61	63	68	71	75
101 (RL)	60503	72	60	66	69	73	78	81	88
<i>Weighted Avg.</i>	--	68.0	57.5	62.5	65.0	68.0	73.0	76.0	81.5

		Trucks							
<i>Sensor</i>	<i>Free Flow Volume</i>	<i>Speed Percentile (mph)</i>							
		Mean	10th	25th	35th	50th	75th	85th	95th
97 (LL)	9686	60	53	56	58	60	63	65	70
101 (RL)	39700	68	60	64	66	68	73	75	78
<i>Weighted Avg.</i>	--	66.4	58.6	62.4	64.4	66.4	71.0	73.0	76.4

Table A-6: Free Flow Speed Distribution (1.5 Miles Upstream)

		Cars							
<i>Sensor</i>	<i>Free Flow Volume</i>	<i>Speed Percentile (mph)</i>							
		Mean	10th	25th	35th	50th	75th	85th	95th
98 (LL)	61271	79	66	73	77	81	87	90	96
102 (RL)	48794	63	53	58	61	64	68	70	75
<i>Weighted Avg.</i>	--	71.9	60.2	66.4	69.9	73.5	78.6	81.1	86.7

		Trucks							
<i>Sensor</i>	<i>Free Flow Volume</i>	<i>Speed Percentile (mph)</i>							
		Mean	10th	25th	35th	50th	75th	85th	95th
98 (LL)	16804	74	64	68	71	74	79	82	87
102 (RL)	27445	59	51	55	57	59	63	64	67
<i>Weighted Avg.</i>	--	64.7	55.9	59.9	62.3	64.7	69.1	70.8	74.6

Table A-7: Free Flow Speed Distribution (1/2 Mile Upstream)

Cars									
<i>Sensor</i>	<i>Free Flow Volume</i>	<i>Speed Percentile (mph)</i>							
		Mean	10th	25th	35th	50th	75th	85th	95th
99 (LL)	54365	79	63	72	75	79	88	92	97
103 (RL)	13711	72	59	67	69	73	80	82	87
<i>Weighted Avg.</i>	--	77.6	62.2	71.0	73.8	77.8	86.4	90.0	95.0

Trucks									
<i>Sensor</i>	<i>Free Flow Volume</i>	<i>Speed Percentile (mph)</i>							
		Mean	10th	25th	35th	50th	75th	85th	95th
99 (LL)	18915	71	60	65	68	71	76	79	85
103 (RL)	5160	66	57	63	65	67	71	73	78
<i>Weighted Avg.</i>	--	69.9	59.4	64.6	67.4	70.1	74.9	77.7	83.5

Table A-8: Free Flow Speed Distribution (Bottleneck)

Cars									
<i>Sensor</i>	<i>Free Flow Volume</i>	<i>Speed Percentile (mph)</i>							
		Mean	10th	25th	35th	50th	75th	85th	95th
104	11481	51	42	46	48	51	55	59	64

Trucks									
<i>Sensor</i>	<i>Free Flow Volume</i>	<i>Speed Percentile (mph)</i>							
		Mean	10th	25th	35th	50th	75th	85th	95th
104	7433	48	42	44	46	47	51	53	55

Table A-9: Field Volumes and VISSIM Input (October 3rd, 2016)

Time of Day	Total Volume (vph)	Total Truck Volume (vph)	VISSIM Input (vph)	
			Right Lane	Left Lane
12:00 PM	648	145	336	312
12:05 PM	900	314	120	780
12:10 PM	888	118	456	432
12:15 PM	756	215	456	300
12:20 PM	696	222	312	384
12:25 PM	780	110	480	300
12:30 PM	828	166	492	336
12:35 PM	732	202	432	300
12:40 PM	708	288	348	360
12:45 PM	948	144	480	468
12:50 PM	816	273	384	432
12:55 PM	960	237	504	456
1:00 PM	900	175	348	552
1:05 PM	960	256	408	552

Time of Day	Total Volume (vph)	Total Truck Volume (vph)	VISSIM Input (vph)	
			Right Lane	Left Lane
1:10 PM	732	122	492	240
1:15 PM	672	253	348	324
1:20 PM	792	153	468	324
1:25 PM	924	208	588	336
1:30 PM	852	293	492	360
1:35 PM	948	155	564	384
1:40 PM	1008	248	552	456
1:45 PM	876	206	552	324
1:50 PM	840	223	528	312
1:55 PM	888	289	540	348
2:00 PM	888	310	480	408
2:05 PM	984	193	636	348
2:10 PM	840	276	516	324
2:15 PM	828	269	516	312
2:20 PM	828	209	576	252
2:25 PM	912	241	492	420
2:30 PM	960	193	600	360
2:35 PM	780	201	480	300
2:40 PM	888	194	588	300
2:45 PM	1008	194	696	312
2:50 PM	756	271	420	336
2:55 PM	660	101	420	240
3:00 PM	888	232	492	396
3:05 PM	696	279	444	252
3:10 PM	984	255	504	480
3:15 PM	804	208	540	264
3:20 PM	888	268	504	384
3:25 PM	768	255	444	324
3:30 PM	960	175	600	360
3:35 PM	876	282	504	372
3:40 PM	756	208	504	252
3:45 PM	780	170	480	300
3:50 PM	828	160	576	252
3:55 PM	768	233	504	264
4:00 PM	660	211	456	204
4:05 PM	888	246	576	312
4:10 PM	804	343	420	384
4:15 PM	1092	169	648	444
4:20 PM	816	305	552	264
4:25 PM	804	206	456	348
4:30 PM	804	251	456	348
4:35 PM	876	207	480	396

Time of Day	Total Volume (vph)	Total Truck Volume (vph)	VISSIM Input (vph)	
			Right Lane	Left Lane
4:40 PM	876	160	480	396
4:45 PM	816	226	420	396
4:50 PM	756	139	492	264
4:55 PM	840	222	492	348
5:00 PM	744	282	504	240
5:05 PM	708	193	456	252
5:10 PM	780	200	420	360
5:15 PM	804	210	468	336
5:20 PM	780	181	456	324
5:25 PM	732	241	456	276
5:30 PM	852	240	516	336
5:35 PM	900	245	504	396
5:40 PM	648	192	396	252
5:45 PM	852	232	528	324
5:50 PM	744	280	372	372
5:55 PM	660	158	432	228
6:00 PM	684	250	348	336
6:05 PM	708	142	444	264
6:10 PM	540	255	300	240
6:15 PM	684	174	420	264
6:20 PM	708	201	420	288
6:25 PM	588	237	408	180
6:30 PM	648	171	444	204
6:35 PM	804	242	480	324
6:40 PM	552	214	324	228
6:45 PM	528	146	372	156
6:50 PM	456	142	324	132
6:55 PM	744	230	456	288
7:00 PM	492	276	336	156
7:05 PM	756	103	432	324
7:10 PM	444	176	276	168
7:15 PM	576	193	384	192
7:20 PM	528	230	324	204
7:25 PM	504	163	324	180
7:30 PM	492	174	336	156
7:35 PM	612	249	324	288
7:40 PM	636	126	444	192
7:45 PM	468	143	216	252
7:50 PM	612	108	336	276
7:55 PM	420	118	240	180
Average Truck %			27%	
Maximum Volume (vph)			1092	

Table A-10: Field Volumes and Average Speeds at Bottleneck (October 3rd, 2016)

Time of Day	Field Volume (vph)	Field Average Speed (mph)
12:00 PM	716	48.0
12:15 PM	720	47.8
12:30 PM	684	50.0
12:45 PM	820	46.8
1:00 PM	872	48.9
1:15 PM	740	49.6
1:30 PM	936	41.9
1:45 PM	896	32.2
2:00 PM	844	23.0
2:15 PM	888	29.8
2:30 PM	856	23.8
2:45 PM	968	22.7
3:00 PM	752	16.9
3:15 PM	816	20.7
3:30 PM	812	15.7
3:45 PM	868	16.6
4:00 PM	876	19.3
4:15 PM	844	22.2
4:30 PM	844	19.4
4:45 PM	844	18.2
5:00 PM	780	17.2
5:15 PM	768	18.0
5:30 PM	780	18.4
5:45 PM	852	27.3
6:00 PM	1028	30.8
6:15 PM	900	25.9
6:30 PM	644	50.1
6:45 PM	552	51.0
7:00 PM	592	48.0
7:15 PM	496	49.2
7:30 PM	548	47.8
7:45 PM	540	47.3
Breakdown Flow Rate (vphpl)		936
Average QDR (vphpl)		853

Table A-11: Field Volumes and VISSIM Input (October 6th, 2016)

Time of Day	Total Volume (vph)	Total Truck Volume (vph)	VISSIM Input (vph)	
			Right Lane	Left Lane
8:00 AM	672	180	396	156
8:05 AM	744	228	372	240
8:10 AM	648	204	432	288
8:15 AM	756	240	384	276
8:20 AM	696	216	372	324
8:25 AM	720	216	480	276
8:30 AM	636	204	528	264
8:35 AM	720	288	564	288
8:40 AM	660	216	492	300
8:45 AM	756	216	480	360
8:50 AM	588	216	420	216
8:55 AM	744	168	468	312
9:00 AM	648	240	504	264
9:05 AM	648	156	540	276
9:10 AM	816	216	516	336
9:15 AM	792	264	492	264
9:20 AM	828	204	516	264
9:25 AM	744	204	468	252
9:30 AM	708	252	540	228
9:35 AM	708	288	492	288
9:40 AM	1008	300	576	540
9:45 AM	840	264	576	336
9:50 AM	816	276	456	276
9:55 AM	1092	300	408	576
10:00 AM	720	240	660	228
10:05 AM	756	264	504	240
10:10 AM	768	240	528	300
10:15 AM	960	348	504	420
10:20 AM	708	204	528	216
10:25 AM	972	360	480	396
10:30 AM	960	312	468	384
10:35 AM	912	204	516	456
10:40 AM	684	288	444	276
10:45 AM	1080	312	504	420
10:50 AM	888	324	504	384
10:55 AM	876	192	504	348
11:00 AM	960	240	540	456
11:05 AM	864	228	516	336
11:10 AM	828	300	528	348
11:15 AM	816	336	552	348
11:20 AM	804	312	456	288

Time of Day	Total Volume (vph)	Total Truck Volume (vph)	VISSIM Input (vph)	
			Right Lane	Left Lane
11:25 AM	708	288	432	264
11:30 AM	780	228	552	276
11:35 AM	708	288	468	204
11:40 AM	960	264	588	456
11:45 AM	948	216	504	408
11:50 AM	912	324	636	396
11:55 AM	900	372	492	372
12:00 PM	852	300	492	300
12:05 PM	840	180	576	384
12:10 PM	804	228	516	372
12:15 PM	816	276	432	264
12:20 PM	912	252	600	444
12:25 PM	1008	336	516	420
12:30 PM	852	252	540	348
12:35 PM	1164	384	684	528
12:40 PM	792	216	540	300
12:45 PM	792	252	516	300
12:50 PM	936	288	516	360
12:55 PM	768	180	504	252
1:00 PM	732	228	444	300
1:05 PM	804	300	456	204
1:10 PM	900	216	492	384
1:15 PM	768	384	384	228
1:20 PM	948	288	480	264
1:25 PM	1008	276	612	468
1:30 PM	828	312	588	312
1:35 PM	804	264	480	288
1:40 PM	720	264	504	216
1:45 PM	756	264	468	312
1:50 PM	828	276	564	372
1:55 PM	828	228	468	336
2:00 PM	612	204	396	228
2:05 PM	876	312	492	396
2:10 PM	840	300	468	228
2:15 PM	768	180	324	180
2:20 PM	996	276	600	516
2:25 PM	864	204	504	360
2:30 PM	1068	276	684	600
2:35 PM	984	240	588	420
2:40 PM	792	228	492	324
2:45 PM	720	264	636	324
2:50 PM	732	348	456	240

Time of Day	Total Volume (vph)	Total Truck Volume (vph)	VISSIM Input (vph)	
			Right Lane	Left Lane
2:55 PM	792	228	480	324
3:00 PM	552	72	444	228
3:05 PM	720	288	264	120
3:10 PM	816	204	504	312
3:15 PM	1056	312	504	372
3:20 PM	1068	276	564	480
3:25 PM	816	300	504	324
3:30 PM	1044	300	600	408
3:35 PM	948	228	648	492
3:40 PM	732	276	300	252
3:45 PM	900	228	336	456
3:50 PM	768	84	384	504
3:55 PM	1092	264	564	588
Average Truck %		31%		
Maximum Volume (vph)		1164		

Table A-12: Field Volumes and Average Speeds at Bottleneck (October 6th, 2016)

Time of Day	Field Volume (vph)	Field Average Speed (mph)
8:00 AM	576	46.3
8:15 AM	724	47.3
8:30 AM	728	50.1
8:45 AM	768	47.4
9:00 AM	804	47.4
9:15 AM	772	47.0
9:30 AM	768	48.2
9:45 AM	912	35.7
10:00 AM	804	18.5
10:15 AM	760	17.7
10:30 AM	844	21.1
10:45 AM	968	27.4
11:00 AM	1008	22.4
11:15 AM	1012	22.5
11:30 AM	964	30.0
11:45 AM	828	19.1
12:00 PM	912	21.0
12:15 PM	900	24.1
12:30 PM	892	21.3
12:45 PM	844	22.3

Time of Day	Field Volume (vph)	Field Average Speed (mph)
1:00 PM	780	19.1
1:15 PM	952	26.5
1:30 PM	924	28.5
1:45 PM	844	18.3
2:00 PM	820	22.6
2:15 PM	888	20.5
2:30 PM	752	20.5
2:45 PM	896	21.7
3:00 PM	828	19.0
3:15 PM	780	16.2
3:30 PM	748	19.2
3:45 PM	964	25.1
4:00 PM	752	20.4
4:15 PM	820	19.4
Breakdown Flow Rate (vphpl)		912
Mean QDR (vphpl)		865

Table A-13: Detailed Summary of Breakdown Events

Breakdown Event	Lane Closure Side	Maximum Pre-Breakdown Flow Rate (pcphpl)		Breakdown Flow Rate (pcphpl)		Average QDR (pcphpl)		% Trucks
		15-Minute Aggregation Interval	5-Minute Aggregation Interval	15-Minute Aggregation Interval	5-Minute Aggregation Interval	15-Minute Aggregation Interval	5-Minute Aggregation Interval	
October 3, 2016	Left	1170	1379	1170	1234	1016	1012	20%
October 4, 2016	Left	1086	1265	1069	1069	1012	1023	30%
October 5, 2016	Left	1150	1308	989	802	936	992	32%
October 5, 2016 (2)	Left	1150	1256	1057	1256	1160	1151	30%
October 6, 2016	Left	1071	1338	1039	1338	1053	1049	24%
October 10, 2016	Right	1167	1298	1133	1089	993	991	18%
October 12, 2016	Right	1196	1392	1119	1152	1005	1005	29%
October 13, 2016	Right	1270	1295	1270	1295	1011	990	27%
October 14, 2016 (2)	Right	1189	1382	1189	1284	1256	1256	16%
Averages	All	1161	1324	1115	1169	1049	1052	25%
	Left-Side Closure	1125	1309	1065	1140	1035	1045	27%
	Right-Side Closure	1206	1342	1178	1205	1066	1060	22%
Minimum		1071	1256	989	802	936	990	16%
Maximum		1270	1392	1270	1338	1256	1256	32%

(2) Multiple breakdown events observed on date

PCE of 2.0 used to convert all flow rates

**APPENDIX B:
BREAKDOWN IDENTIFICATION ALGORITHMS AND WEIBULL
DISTRIBUTION PARAMETERS**

```

Sub breakdown_identification()

LastRow = Cells(Rows.Count, 1).End(xlUp).Row

For x = 2 To LastRow
    If Cells(x, 18) = 0 And Cells(x + 1, 19) = 15 Then

        Cells(x, 20) = 1
        Cells(x, 21) = 0

        Do Until Cells(x + 1, 19) = 0 Or Cells(x + 1, 2) <> Cells(x, 2)

            Cells(x + 1, 20) = 0
            Cells(x + 1, 21) = 1

            x = x + 1

        Loop

    Else

        Cells(x, 20) = 0
        Cells(x, 21) = 0

    End If

Next x

End Sub

```

Figure A-1: VBA Code (1-Minute Breakdown Identification)

```

Sub breakdown_identification_five()

LastRow = Cells(Rows.Count, 1).End(xlUp).Row

For x = 2 To LastRow
    If Cells(x, 12) = 0 And Cells(x + 1, 13) = 3 Then

        Cells(x, 14) = 1
        Cells(x, 15) = 0

        Do Until Cells(x + 1, 13) = 0 Or Cells(x + 1, 2) <> Cells(x, 2)

            Cells(x + 1, 14) = 0
            Cells(x + 1, 15) = 1

            x = x + 1

        Loop

    Else

        Cells(x, 14) = 0
        Cells(x, 15) = 0

    End If

Next x

End Sub

```

Figure A-2: VBA Code (5-Minute Breakdown Identification)


```

Sub breakdown_identification_fifteen()

LastRow = Cells(Rows.Count, 1).End(xlUp).Row

For x = 2 To LastRow
    If Cells(x, 12) = 0 And Cells(x + 1, 13) = 2 Then

        Cells(x, 14) = 1
        Cells(x, 15) = 0

        Do Until Cells(x + 1, 13) = 0 Or Cells(x + 1, 2) <> Cells(x, 2)

            Cells(x + 1, 14) = 0
            Cells(x + 1, 15) = 1

            x = x + 1

        Loop

    Else

        Cells(x, 14) = 0
        Cells(x, 15) = 0

    End If

Next x

End Sub

```

Figure A-3: VBA Code (15-Minute Breakdown Identification)

```

Sub breakdown_identification_fifteen()

LastRow = Cells(Rows.Count, 1).End(xlUp).Row

'Tell Excel to find the last row of the sheet.'

For x = 2 To LastRow
  If Cells(x, 12) = 0 And Cells(x + 1, 13) = 2 Then

    Cells(x, 14) = 1
    Cells(x, 15) = 0

    'For all rows from row 2 to the last row, if average speed > 35 mph (reflected as a "0" in column #12)
    and the number of subsequent consecutive rows with average speed < 35 mph is at least 2 (reflected by
    a moving two-record sum of "2" in column #13), then a breakdown event is identified by placing a "1" in
    column #14.'

    Do Until Cells(x + 1, 13) = 0 Or Cells(x + 1, 2) <> Cells(x, 2)

      Cells(x + 1, 14) = 0
      Cells(x + 1, 15) = 1

      x = x + 1

    Loop

    'Loop until speeds have recovered above 35 mph for at least 2 intervals (the moving two-record sum in
    column #13 is "0") or data from the next simulation run begins (simulation ID in column #2 = x + 1). A "1"
    will be recorded in column #15 to indicate congestion until one of these conditions is met.'

    Else

      Cells(x, 14) = 0
      Cells(x, 15) = 0

    End If

  Next x

  'When the loop ends, record a "0" in columns #14 and #15 to indicate the return to stable flow and
  proceed to the next iteration.'

End Sub

```

Figure A-4: VBA Code with Comments (15-Minute Breakdown Identification)

Table A-14: Best-Fit Weibull Distribution Parameter Summary

Aggregation Interval	Lane Closure Side	Truck %	Scale Parameter (β)	Shape Parameter (γ)
5-Minutes	Left-Side	5	1472.35	14.71
		10	1349.28	15.00
		20	1224.62	11.43
		30	1103.39	11.31
		40	1010.66	12.17
	Right-Side	5	1536.41	12.80
		10	1417.98	12.99
		20	1279.82	11.20
		30	1125.96	11.38
		40	1039.70	10.73
15-Minutes	Left-Side	5	1294.91	26.16
		10	1196.04	23.15
		20	1072.78	19.68
		30	943.21	20.90
		40	846.36	20.59
	Right-Side	5	1346.61	17.21
		10	1227.27	19.70
		20	1101.01	16.58
		30	952.26	19.55
		40	866.41	21.77